# SCIENTIFIC COMMITTEE
# SEVENTEENTH REGULAR SESSION

## ELECTRONIC MEETING

**11-19 August 2021**

---

**Stock assessment of Southwest Pacific blue shark**

---

**WCPFC-SC17-2021/SA-WP-03**

**Philipp Neubauer[1], Kath Large[1] and Stephen Brouwer[2]**

[1] **Dragonfly Data Science**

[2] **Saggitus Consulting**

# Stock assessment of Southwest Pacific blue shark

**Authors:**
Philipp Neubauer
Kath Large
Stephen Brouwer

DRAGONFLY
Data Science

SAGGITUS

## Cover Notes

To be cited as:

Neubauer, Philipp; Large, Kath; Brouwer, Stephen (2021). Stock assessment of Southwest Pacific blue shark, 66 pages. WCPFC-SC17-2021/SA-WP-03. Report to the WCPFC Scientific Committee. Seventeenth Regular Session, 13–20 August 2018.

# CONTENTS

## EXECUTIVE SUMMARY

This analysis assesses the south Pacific blue shark stock in the Western and Central Pacific Ocean (WCPO) hereafter referred to as the Southwest Pacific.

Blue shark are caught in large numbers in a range of fisheries in the Southwest Pacific. Blue shark in the Southwest Pacific are thought to make up a single stock, but an initial attempt at assessing this stock in 2016 was not successful. Here, we used a range of CPUE indices, length frequencies and predicted catch scenarios to infer stock status and trends of blue shark in this region.

The stock assessment was set up in Stock Synthesis as a three-fleet model, using an approach with fleets covering: high-latitude fisheries on juveniles and adults around New Zealand and South-Eastern Australia; the EU-Spain mid-latitude fishery that operates to the north and east of New Zealand; and, a high latitude and high seas fishery capturing adult sharks. The model was run for a 26 year period from 1995 to 2020, with the start year taken to be 1995 due to highly uncertain catches prior to this period. The catches were reconstructed from observer data and were comparable to previous analyses, albeit at lower median estimated total catches. The catch reconstruction model also produced high uncertainties in catches between the mid 1990s and early 2000s. A range of catch scenarios were applied in this assessment to reflect these uncertainties.

In addition to catches, discard rates are uncertain for all but the most recent (i.e., last 5) years in the time series, as are catches from the driftnet fisheries that operated in south Tasman and north-east Australian waters in the 1980s. Additional uncertainties pertain to individual CPUE time series from log-sheet data, as any individual time series is likely to suffer from changing degrees of under-reporting (although we attempted to address this problem by grooming out vessels with poor reporting records).

To adequately reflect uncertainties, we ran an extensive sensitivity grid with nine grid axes, covering catch, discard, CPUE and biological assumptions, totalling over 3500 models. Across the sensitivity grid, a large majority of stock trajectories showed a decline from relatively high stock levels in 1995, reflecting increasing effort during that time, followed by a steady increase in biomass as effort plateaued and discard rates increased, especially in lower latitude fisheries. The mean outcome suggested a current stock status near $SB_0$, with a range of outcomes between $0.58$ to $1.49SB_0$. Dynamic surplus production models provided additional support for the conclusion that the stock has likely recovered from low levels in the mid to late 2000s to levels close to the estimates of biomass under average recruitment.

CPUE series, although in agreement about recent increases in the stock, were in conflict with regards to stock size (average recruitment) and, consequently, were the largest drivers of differences among sensitivity runs. Removing the EU-Spain time series or removing initial years from the New Zealand index led to lower estimates of stock status and altogether lower stock trajectories, while including all indices with equal weight led to consistently higher stock status outcomes.

Although the sensitivity analysis highlighted a number of uncertainties, we found a number of consistent patterns in the outcomes:

- The most influential axes of uncertainty was the weighting and inclusion of CPUE indices; high uncertainty remains in many model outputs across the sensitivity grid.
- The stock biomass was low throughout the region through the early 2000s following the expansion of longline fishing effort in the region.

- Estimates across the uncertainty grid largely indicated that the stock has recovered from lower biomass levels.
- 90% of model runs indicate that fishing mortality at the end of the assessment period was below $F_{\text{MSY}}$ and 96% of model runs show that the biomass is above $SB_{\text{MSY}}$, with high estimated spawning biomass levels near those expected under $F = 0$ and average recruitment across model runs, and minimum estimated $SB$ of $0.3SB_0$.
- Fishing mortality has declined over the last decade and is currently relatively low. This is largely as a result of most sharks being released upon capture in the majority of longline fleets.
- Finally, considered against all conventional reference points the stock on average does not appear to be overfished and overfishing is not occurring.

Given some of the fundamental uncertainties highlighted in this assessment, we recommend:

- Increased effort to re-construct catch histories for sharks (and other bycatch species) from a range of sources. Our catch reconstruction models showed that model assumptions and formulation can have important implications for reconstructed catches. Additional data sources, such as log-sheet reported captures from reliably reporting vessels, may be incorporated into integrated catch-reconstruction models to fill gaps in observer coverage.
- Dynamic/non-equilibrium reference points, such as $SB_{F=0}$ be investigated for shark stock status, as they may be more appropriate for fisheries with uncertain early exploitation history and strong environmental influences.
- Additional tagging be carried out using satellite tags in a range of locations, especially known nursery grounds in South-East Australia and New Zealand, as well as high seas areas to the north and east of New Zealand, where catch-rates are high. Such tagging may help to resolve questions about the degree of natal homing and mixing of the stock.
- Tagging may also help to obtain better estimates of natural mortality, if carried out in sufficient numbers. This could be taken up as part of the WCPFC Shark Research Plan to assess the feasibility and scale of such an analysis.
- Additional growth studies from a range of locations could help build a better understanding of typical growth, as well as regional growth differences. Current growth data are conflicting, despite evidence that populations at locations of current tagging studies are likely connected or represent individuals from the same population.
- Genetic/genomic studies could be undertaken to augment the tagging work to help resolve these stock/sub-stock structure patterns.

# 1. INTRODUCTION

Blue sharks (*Prionace glauca*) are widely distributed throughout the world's oceans and in the Pacific Ocean they are frequently landed in longline fisheries between 50$^o$N and 50$^o$S (Brouwer and Hamer 2020). Compared to other sharks, blue sharks are relatively productive with fast growth and high fecundity (Francis and Duffy 2005; Clarke et al. 2015). In the Pacific Ocean, the Southwest Pacific blue shark stock appears separated from blue sharks in the north Pacific at the equator, with no equatorial crossings observed in tagging studies (Sippel et al. 2016, Kai and Fujinami 2020).

While blue sharks have been caught in longline fisheries since their inception in the 1950s, they have only been reported in catch records since the 1990s, but most records are from 2012 onwards (Brouwer et al. 2021). The paucity of data is a result of a lack of logsheet reporting of bycatch in general, but particularly sharks. In addition, in the past, shark species were often lumped together and reported to a generic shark code. This situation has been exacerbated by poor observer coverage for most flags in Pacific Ocean longline fisheries (Williams et al. 2020). Unknown, but potentially large number of blue sharks were caught in Southwest Pacific albacore fisheries in the late 1980s (Murray 1990, Northridge 1991, Richards 1994).

This paper reports on the 2021 stock assessment of Southwest Pacific blue sharks in the Western and Central Pacific Fisheries Commission Convention Area (WCPFC-CA). This is the second attempt at undertaking an assessment of this stock and follows on from the work of Takeuchi et al. 2016. Blue sharks in the north Pacific have been assessed and that stock has recovered from low biomass and high fishing mortality in the 1990s and is currently considered not to be overfished and overfishing is not taking place (ISC 2018).

The 2016 Southwest Pacific blue shark assessment was undertaken in MULTIFAN-CL (MFCL) which fits size-based, age- and spatially-structured population models to data from multiple sources (Takeuchi et al. 2016). That assessment, however, did not lead to reliable estimates of stock status or Maximum Sustainable Yield (MSY) based reference points due to difficulties estimating the stock recruitruitment relationship. The 12$^{th}$ Scientific Committee of the WCPFC (SC12) noted that realistic estimates of equilibrium unexploited recruitment and spawning biomass could not be obtained due to the lack of available data, conflicting CPUE time series, and uncertainty in the estimated stock recruitment relationship (WCPFC 2016).

SC12 concluded that the 2016 Southwest Pacific blue shark assessment was preliminary and considered to be a work in progress and it was not used to provide management advice, nor were definitive stock status statements agreed. In addition, SC12 noted the uncertainties in historical and contemporary longline catch and CPUE estimates, and that an improvement in the amount and quality of available biological and fishery information was required in order to develop a useful integrated stock assessment model (WCPFC 2016).

Since that time, shark data reporting within the Western and Central Pacific Fisheries Commission (WCPFC) has generally improved and we now have a longer time series of fisheries data and some data improvements have been observed compared to that available in 2016 (Brouwer & Hamer 2020). Moreover, additional biological information is also available (e.g. Joung et al. 2018). These data improvements led Brouwer and Hamer (2020) to conclude that a data rich assessment[1] could be attempted. However, they also noted the need for the development of a reliable catch history prior to undertaking the assessment.

A catch data series has been estimated and CPUE indices have been developed from multiple

[1]Fully integrated stock assessment model using multiple sources of data including catch, effort and biological information in a model such as MULTIFAN-CL, Stock Synthesis or similar.

fleets (Neubauer et al. 2021). These data along with a number of different estimates of growth, and observed length data from the population were available as inputs to this assessment. The assessment results are presented here, but as there are no agreed reference points for Western and Central Pacific Ocean (WCPO) sharks, a range of metrics are provided as recommended by Brouwer and Hamer (2020) for SC16s consideration. This report should be considered along with the data inputs (Neubauer et al. 2021) and fisheries characterisation work (Brouwer et al. 2021) that have been undertaken as part of this assessment.

# 2. METHODS

## 2.1 Stock structure and fleet assumptions

Although there is limited knowledge about migratory patterns in blue shark, available tagging data suggest that mature individuals move from New Zealand to forage at lower latitudes (Sippel et al. 2016, Elliott 2020). In addition, length composition data shows a clear signal of smaller individuals in higher latitudes, with a high proportion of mature females (Neubauer et al. 2021, West et al. 2004), suggesting that, similar to other oceans (Coelho et al. 2018), higher latitudes act as nursery areas for blue shark. Some individuals in a recent tagging study returned to nearly their exact tagging location off the coast of New Zealand after nearly a year foraging in the high seas (Elliott 2020), suggesting that there is some degree of site fidelity with individuals returning to known areas periodically.

In addition to latitudinal ontogenetic movement patterns and differences in abundance, blue sharks forage vertically which may lead to differential availability to surface longline fisheries (Elliott 2020, Vedor et al. 2021). During foraging, individuals may reside at depths of 100-600 m, especially in lower latitudes where surface waters are oligotrophic (Vedor et al. 2021). Latitudinal patterns in distribution and ocean productivity therefore structure blue shark populations spatially and result in variability in catchability by longline gear.

## 2.2 Length compositions

Length composition data show smaller individuals reside near the New Zealand and south Australia coast, with larger individuals at higher latitudes and further offshore (Figure 1). Although sampling is spatially representative of the whole area, it is temporally dominated by early samples from Australia and Japan (Figure 2). Between the late 1990s and mid-2010s most samples came from New Zealand, while recent samples are a mix of Japanese, Chinese Taipei and Chinese samples. Within target fisheries and flags, there is substantial annual variability in LF samples (Neubauer et al. 2021), suggesting potentially complex spatio-temporal movement dynamics. As we have little information about drivers of these patterns in the length frequencies (LFs), we only consider fits to aggregate LFs here, by latitudinal bands and fisheries, although the model is fitted to annual LF samples.

At high latitudes, we found large variability in LF distributions among flags (Figure 3). Australian and Japanese data from the early 1990s show a distinct peak in small individuals around 100 cm. The New Zealand data show a similar peak, but with almost flat LFs between 100 and 200 cm. Samples from the EU-Spain fleet were larger, as were samples from the Chinese Taipei fleet operating in high seas outside of the New Zealand EEZ.

Based on these findings, and inferences from Southwest Pacific and global blue shark tagging data, we structured our assessment with respect to trends in observed length frequencies by fleet, and corresponding trends in CPUE indices into three fleets (Figures 4, 5):

1. High latitude fleets catching juvenile and mature blue shark south of 35°South, mainly in New Zealand and the South Tasman Sea;
2. The EU-Spain fleet fishing at intermediate latitudes to the North-East and North-West of the New Zealand EEZ, capturing a broad size range from just mature to large individuals (>250 cm); and
3. Low latitude fleets, capturing largely mature fish, but with a notable absence of large individuals.

### 2.3 Catch assumptions

Catches were reconstructed between 1990 and 2020 using a spatial GLMM model (Neubauer et al. 2021) that included effects for oceanographic predictors as well as targeting clusters and total effort per stratum (5x5 degree grid, flag, year, month). The model produced lower estimates than in previous analyses, albeit with much higher uncertainty, especially in the late 1990s and early 2000s (Figure 6).

Catch estimates were combined with a model for annual discard rates per flag (Figure 7), which was used to produce scenarios of total fishing-induced mortalities. Due to high discard uncertainties, especially before increased observer coverage in the 2010s, we considered the possibility of high and low discards alongside the base assumption of the median discard estimate from the discard model (Figures 8, 9, 10; Table 1). Post-release mortality was included at a rate of 17% in calculations of total fishing-related mortality (Neubauer et al. 2021).

### 2.4 CPUE indices

A range of CPUE indices were available for consideration in the analysis (Neubauer et al. 2021; Figure 12). As discussed in Neubauer et al. 2021, CPUE indices from observer data suffer from representation issues meaning that they do not represent any particular area for the entirety of the time-series from 1990-2020, with the exception for New Zealand, where the observer index lines up very closely with the series derived from groomed logbook data (Figure 12). For Australia and Japan, the series shows a strong increase in the early 1990s, suggesting a strong increase in the South Tasman sea in the early 1990s following the closure of local driftnet fisheries. However, the time-series for this area effectively stops in the mid-1990s as observer coverage dropped.

The New Zealand index provides a potentially useful indicator of abundance in the southwest Pacific; the main difference between the observer time-series and logbook records is an initial peak in abundance in the early 1990s. West et al. (2004) attributed this increase to the transition from the Japanese distant water fleet, which operated in these waters until the early 1990s, and the domestic fleet which started fishing at the time. Effort and catch was markedly lower during this period, which may have allowed local abundance to recover. Nevertheless, the observer index does not show this same peak, and it is unclear whether this transitional peak represents changes in abundance or changes in the fishery. Although there were additional changes in the fleet at the introduction of blue shark into the Australia quota management system in 2004, logbook and observer CPUE line up favourably in the 2000s, suggesting that logbook CPUE may have still been a reasonable indicator of local abundance. The EU-Spain index, based on reported weight of captured blue shark, lines up closely with the Australian index if the latter is lagged by 5 years (which is consistent with the time taken for blue shark to grow to the sizes predominantly seen in the EU-Spain region).

At lower latitudes (i.e., <35°South) and the high seas, the extremely limited early observer

coverage means that it is difficult to validate early CPUE trends. Nevertheless, lower latitude logsheet CPUE from groomed datasets from the Japanese high seas fishery showed a steady decline in abundance in the 1990s and early 2000s, followed by an increase in the 2010s. A similar trend was produced by the index based on low-latitude Australian logsheet data. The recent increase in CPUE aligns with similar increases in the EU-Spain index, as well as an index based on the Chinese Taipei distant-water observer programme.

Although individual indices may not be without problems, all indices suggest a recent increase in CPUE across latitudes, and a decline in the 1990s and early 2000s in low latitudes. Whether a similar decline also occurred in higher latitudes prior to this period is unclear. However, increasing CPUE in observer series in Australian and Japanese fleets in the south Tasman, as well as initial increases in the Australian observer CPUE, suggest this may have been the case.

### 2.5 Model setup

The model used Stock Synthesis (Version V3.30.17.01; Methot Jr & Wetzel 2013), and parametrisation largely followed that of ISC (2018). We used Southwest Pacific specific parameters where possible (Clarke et al. 2015), but reverted to North Pacific parameters/analyses where necessary. CPUE data were included from 1995 (when suitable CPUE data became available) up to and including 2019, catch to 2020 (as this came from a predictive model based on effort estimates only, rather than reported catches). Models were run from 1995 to 2020, and outputs were analysed with respect to stock status in 2020.

#### 2.5.1 Growth

Growth assumptions were based on growth studies described in Manning and Francis (2005) and Joung et al. (2018). The former suggests overall smaller individuals at-age (Figure 13), with a size-at-birth of just above 40 cm. Growth described in Joung et al. (2018) suggests a size-at-birth of 53.5 cm (averaged between males and females), which is slightly above the size-at-first capture in New Zealand fisheries (some blue sharks are caught at 40-60 cm). The Manning and Francis (2005) study had a wider range of ages and sizes available to construct growth curves and is therefore taken as the reference here. However, both studies may present an unknown degree of spatial bias. Manning and Francis (2005) mainly sampled from fisheries operating near New Zealand, while Joung et al. (2018) sampled in the high seas north of New Zealand. If larger (faster growing) individuals leave New Zealand for high-seas foraging, then samples from New Zealand waters may be biased towards slow growing individuals, whereas high seas samples may over-represent fast-growing individuals. We also cannot discount the hypothesis of temporal variability in growth due to oceanic foraging conditions. For these reasons, we include both growth studies in our structural uncertainty grid.

#### 2.5.2 Reproductive output and recruitment

We followed ISC (2018) in using a low fecundity stock recruitment relationship (Taylor et al. 2013), using values employed in ISC (2018) as sensitivities for stock recruitment scenarios. The function is parametrised where survival fraction is in terms of the survival of recruits as a function of stock size (labelled **survival fraction**) and a parameter ($\beta$) dictating the amount of density dependence in the stock recruit curve. Both parameters were taken from ISC (2018), with sensitivities to investigate the impact of assumptions about the amount of compensation (density dependence; $\beta$) and juvenile survival.

The numeric values were based on simulations in Kai and Fujinami (2018), based on blue

sharks in the North Pacific. Although these estimates also employ North Pacific life-history parameters, we did not repeat the simulations here as we found that the stock recruitment relationship had limited impact on the estimated stock trajectory.

We assumed a constant reproductive output of 35 pups annually per female, which corresponds to mean values found for both the south and north Pacific (Fujinami et al. 2019, Clarke et al. 2015). Length-at-50% maturity was assumed to be 180 cm (Francis & Duffy 2005).

### 2.5.3 Selectivity

The diagnostic model was set up to initially estimate selectivities based on available length-composition data. All selectivities were assumed to be double-normal, reflecting both spatial availability to the fisheries, as well as potential for large sharks to bite off hooks for some gears (ISC 2018, Tremblay-Boyer et al. 2019). A sensitivity with logistic-like selectivity for all fleets (i.e., fixing the right-hand limb of the double-normal selectivity to one) was also performed, but was not retained for the sensitivity grid as it lead to poor LF fits, with little difference in other assessment quantities. To estimate selectivities, the LF weighting was initially set to high values (0.5 for Australia and low latitude data, 1 for the EU-Spain fleet data). Selectivities were then fixed at estimated values for remaining model runs, and LF data were weighted according to Francis 2011.

### 2.5.4 Initial fishing mortality

Equilibrium catch was set to the mean catch from the catch-reconstruction predictions for the 1990-1994 years. Initial fishing mortality corresponding to those catches was fixed by adjusting parameter values to reflect two distinct scenarios:

1. Base assumption: equilibrium F was in line with F values estimated in the base run for the second half of the 1990s. This reflects the assumption that the 1990s were a transitional period with Japanese effort declining in high latitudes in the early 1990s, with national fleets taking over in the second half of the 1990s. Overall longline effort more than doubled in the Southwest Pacific in the early 2000s, but was relatively steady during the 1990s.
2. High initial F: this assumption reflects the potential that the stock may have been fished substantially harder in the late 1980s and early 1990s before the drift-net fishery was phased out. There is evidence for local increases in CPUE in South Australia for observed Australian and Japanese fleets, which may be interpreted as circumstantial evidence for a recovery after high fishing mortality from driftnets in the albacore driftnet fisheries in the late 1980s. In practice, we set this initial F to 150% of the initial F used under the base assumption.

### 2.5.5 Other parameters

Growth was set to von Bertalanffy growth, with fixed CVs reflecting growth variation found in Manning and Francis (2005). Natural mortality was assumed fixed at 0.2 (Manning & Francis 2005), with a sensitivity run at 0.16 (i.e., -20%). We chose not to apply estimates used in the North Pacific (Semba & Yokoia 2016), as these were derived in the North Pacific based on regional growth studies (e.g., Fujinami et al. 2019).

### 2.5.6 Diagnostic model runs

Diagnostic model runs were established on the basis of CPUE series that we found to be the most robust and representative:

1. The New Zealand logsheet CPUE was used to represent relative biomass trends in high latitudes;
2. EU-Spain CPUE based on reported catches in weight; and,
3. Japanese logsheet CPUE to represent distant water and low-latitude fisheries.

Equal weight was given to all CPUE series. Other parameters and settings for the diagnostic case are given in Table 2.

## 2.6 Structural uncertainty grid

To adequately represent major uncertainties in assessment inputs, we constructed an uncertainty grid that incorporated nine axes of uncertainty and 3885 models along these axes. The grid considered:

1. **Catch scenarios:** (Table 1) - posterior mean catch (base) and $90^{th}$ percentile of the posterior distribution of predicted catches.
2. **Discard scenario:** (Table 1) - low ($25^{th}$ percentile), mean (base) and high ($75^{th}$ percentile) estimated discard rates.
3. **Initial F:** initial fishing mortality associated with equilibrium catch - assuming baseline $F$ or high (50% higher) initial exploitation.
4. **High latitude CPUE:** using the New Zealand CPUE series with (base) or without pre-2004 years (i.e., removing years when logsheet and observer CPUE differ - *RM early New Zealand*), or down-weighting both Australia and EU-Spain index to 25% of their original weight in favour of low latitude/high seas indices.
5. **Low latitude CPUE:** replacing the Japanese index (base) with the Australian low-latitude index, removing the EU-Spain index.
6. **Recruitment deviation:** low ($\sigma_R = 0.2$; base), forcing smaller recruitment deviations in the model (i.e., the model acts more like an age-structured production model; ISC 2018), or allowing greater variation in recruitment ($\sigma_R = 0.4$).
7. **Natural mortality:** base (0.2) or low (0.16) M.
8. **Survival fraction/density dependent recruitment:** $S_{frac} = 0.391, \beta = 2$ vs. scenarios described in ISC 2018: $S_{frac} = 0.378, \beta = 1$ (low) or $S_{frac} = 0.467, \beta = 3$ (high). Higher $\beta$ indicates increased over-compensation.
9. **Growth:** replacing Manning and Francis (2005) (base) with Joung et al. (2018) growth equations.

### 2.7 Dynamic surplus production sensitivities for individual CPUE series

As length frequency data are highly temporally variable, and spatio-temporal coverage is highly skewed over time, we sought to check trends found with the integrated assessment model against simpler models, namely dynamic surplus production models. The latter can be straightforwardly fitted to CPUE time series, and we applied the Schaefer surplus production model implemented in the *bdm* R package (Edwards 2017) to catch and CPUE indices from individual CPUE time series considered in the sensitivity grid for the integrated assessment model.

Neubauer et al. (2019) provided context for the application of dynamic surplus production models (DSPM) to sharks in the WCPFC. DSPM are fitted based on state-space equations (McAllister & Edwards 2016, Froese et al. 2017) and do not require equilibrium assumptions that make traditional approaches to surplus production assessments difficult to justify (Bonfil 2005). Examples of packages that implement DSPMs are JABBA ("Just Another Bayesian Biomass Assessment"; Winker et al. 2018) and BDM ("Bayesian biomass dynamics model" Edwards 2017). As such, the DSPM operates similarly to integrated assessments, where recruitment essentially functions as a process error term. The DSPMs tend to use an index of abundance (usually CPUE) to constrain the time series of abundance. Although productivity is usually estimated within DSPMs, it is useful to also constrain productivity via an informative prior (Edwards 2017).

We used a classic Schaefer production model (although other hybrid production functions can be used with this R package). The population dynamics are parametrised in terms of the relative depletion ($x_t = N_t/K$), with relative harvest $H_t$ also expressed in relative terms ($H_t = C_t/K$):

$$x_{t+1} = x_t + g(x_t) - H_t \tag{1}$$
$$g(x_t) = R_{max} x_t \left(1 - x_t\right). \tag{2}$$

#### 2.7.1 Priors for dynamic surplus production models

Population growth $R_{max}$ was calculated from methods in Pardo et al. (2018) based on the Euler-Lotka equation (see also Zhou et al. 2018), adjusted for survival to age at first maturity (Pardo et al. 2016). Estimating $R_{max}$ serves a dual purpose here: it can act as a reference point for depletion-based catch-only and SRA methods that cannot estimate stock productivity independently, but can also act as a prior for a DSPM for which $R_{max}$ is the productivity parameter.

Life history input values for the Euler-Lotka equation were compiled from ranges and point estimates reported in Clarke et al. (2015), with some adjustments to accommodate recent growth studies (Joung et al. 2018). Specifically, growth rate $K$ was taken as 0.1 with sufficient variability to encompass estimates from Southwest Pacific studies (i.e., 0.0885–0.164; see Figure 14 for the simulated inputs, and Figure 15 for the resulting value of $R_{max}$). When only ranges were reported, the distributions were constructed to encompass those ranges as extreme quantiles (i.e., near the 5th and 95th percentile).

We also integrated over methods to derive natural mortality in the simulation procedure. Specifically, we used methods described in Jensen (1996) (age-at-maturity based), Hewitt and Hoenig (2005) (maximum age based), and Pardo et al. (2016) (expected life-span derived), by simulating $R_{max}$ from the inputs under these mortality assumptions and combining the

outputs. This led to a broader distribution for $R_{max}$ than would be obtained if one considered a single method to estimate natural mortality. Note that the value for $M$ of 0.2 used for the integrated assessment is near the median value estimated here across methods, and the sensitivity at 0.16 is near the $25^{th}$ percentile of the distribution.

Priors for the carrying capacity, $K$, and initial population depletion in 1995 were formulated as vague log-normal distributions, encompassing scenarios of high initial depletion as well as high initial biomass (i.e., $> B_0$; Figure 16). All estimation was done within the bdm package, with Markov Chain Monte Carlo (MCMC) in the underlying Bayesian estimation software Stan (Stan Development Team 2018) used to estimate parameters. We ran the MCMC for 100 000 iterations, discarding the first 10 000 iterations as burn-in, and keeping 100 samples from each of 4 chains. The package allows for efficient set-up of surplus production models, and the sampler was fast, taking about 4 minutes for 100 000 iterations.

#### 2.7.2 Reference points

Clarke and Hoyle (2014) and Zhou et al. (2018) evaluated methods to derive reference points for elasmobranchs in the Western and Central Pacific Ocean. However, to date, there are no formally agreed reference points for sharks in the Western and Central Pacific Ocean. Recent shark assessments of oceanic whitetip shark, for example, compared fishing mortality to $F_{lim}$ as a tentative limit reference point for sharks, and to $F_{crash}$, the fishing mortality that would lead to extinction in the long-term. If one assumes a simple Schaefer surplus production model, then $F_{crash} = R_{max}$, the maximum population growth rate (intuitively, a population cannot be sustained if fishing removes more individuals than the population can maximally produce), and $F_{lim} = 0.75R_{max}$.

For blue shark, which have higher productivity than many other shark species, we also applied alternative reference points used for target fisheries. These include MSY based reference points (i.e., $F_{\text{MSY}}$ and $SB_{\text{MSY}}$), as well as spawning biomass relative to spawning biomass under $F = 0$ and average recruitment levels ($SB_0$).

## 3. RESULTS

### 3.1 Diagnostic model runs

#### 3.1.1 Model fits

The diagnostic run provided reasonable fits to recent CPUE for the New Zealand CPUE series (Figure 17). However, fits to the early CPUE for the New Zealand series did not fit to the initial peak in the late 1990s. EU-Spain CPUE was fitted reasonably, while the low latitude/high seas CPUE fit indicated more extreme fluctuations than the time series suggested. Aggregated length-frequencies fit reasonably well, although the model struggled to fit the peak in mature individuals near 200 cm in New Zealand/High latitude fisheries (Figures 18, 19). The fits were often not aligned temporally with LF samples; the latter showing large jumps in mean length that the model could not reproduce. As LF data are down-weighted to avoid undue impacts on biomass trends, modeled trends in LFs are largely driven by combinations of trends fitted to the CPUE indices and biological assumptions, as well as selectivity specification (Figure 20).

### 3.1.2 Model population trajectory

The model suggested an over-all increase in fishing mortality up to the early-mid 2000's (Figure 21), driven largely by the capture of large individuals in high-seas/low-latitude fisheries (Figure 22). Although the New Zealand fleet accounts for a large number of captures, the fishing mortality from those captures is estimated to be substantially lower than that inflicted by the low-latitude and high seas fisheries, including EU-Spain effort in the 2000s. Trends in $F$ led to an estimated decline in the biomass in the early 2000s which, along with high density dependent recruitment during the time, drove a 50% decline in stock status from levels near $SB_0$ (Figure 23). Subsequent declines in fishing mortality, due to discarding and declines in high latitude effort, led to a subsequent recovery that resulted in an estimated stock-size well above initial (1995) stock-size and $SB_0$ in recent years. Double-normal selectivity assumptions did not substantially impact population trajectories (Figure 24).

### 3.1.3 $R_0$ profile

Negative log-Likelihood profiles of $R_0$ (the only free parameter other then recruitment deviations), suggested that the estimate of $R_0$ was largely driven by the CPUE index data, which had a clear minimum for the negative log-likelihood (Figure 25). Nevertheless, splitting the CPUE likelihood into its components revealed a clear conflict between indices, notably between the EU-Spain series and the low-latitude/high seas series, with the estimated $R_0$ falling at the intersection of the negative log-likelihood profiles for these two CPUE series. The length-frequencies from the New Zealand samples were in agreement with the estimated $R_0$, while the EU-Spain samples did not provide much information. Low-latitude/high seas samples were aligned with the CPUE series, showing lower log-likelihoods at larger stock size. Conflicts were addressed by down-weighting the New Zealand/high latitude and EU-Spain CPUE in favour of the low-latitude/high-seas CPUE (with weights of 0.25 for both series to obtain a ratio of 2:1 in weight favouring the low-latitude/high-seas CPUE), dropping the EU-Spain series, and providing an alternative CPUE time-series for low-latitude/high-seas CPUE in the sensitivity grid.

## 3.2 Sensitivity grid

Grid models showed high consistency in overall population trajectories (Figure 27), with a median initial spawning biomass ($SB$) near $SB_0$, and a mean current stock status near $SB_0$, with an 80% range from $0.58 - 1.49SB_0$. Model runs with low current $SB$ were associated with high initial $F$ and the removal of EU-Spain or early New Zealand CPUE points (Figures 28, 26, 30, 29). Decision trees showed that absolute $SB_0$ was associated with the removal of these CPUE series, as well as growth and the low latitude CPUE, whereas life-history uncertainty only changed the absolute biomass estimate within the CPUE sensitivities (Figure 29). Relative stock status was largely influenced by the same CPUE assumptions in conjunction with productivity assumptions and initial $F$ (Figures 29, 30, 31). CPUE assumptions, therefore, are the most influential variable on stock status outcomes. Across all model runs, the mean current depletion was equivalent to $SB_0$, while the mean for series excluding the EU-Spain CPUE was $0.64SB_0$ vs $1.2SB_0$ for runs including this series. Similarly, after removing the EU-Spain series, models that also removed early years of the New Zealand CPUE series had a lower average status ($0.92SB_0$) than those including this part of the CPUE ($1.4SB_0$). Nearly all (96%) of the grid models had a final year biomass above $SB_{\text{MSY}}$.

Reference points were determined by a combination of factors in the grid models. $F_{\text{MSY}}$ was largely driven by the applied growth function, with very limited differences among

productivity scenarios (Figures 32). For runs with the Joung et al. (2018) growth, $F_{\text{MSY}}$ was around 0.16, while for runs with the Manning and Francis (2005) growth function, $F_{\text{MSY}}$ was around 0.14, with slightly different estimates depending on assumptions about M.

Current $F$ relative to $F_{\text{MSY}}$ was largely determined by the inclusion (or not) of EU-Spain and early New Zealand CPUE (Figure 32). While including the EU-Spain CPUE series lead to estimates of low $F$ relative to $F_{\text{MSY}}$ (mean 0.28), dropping this CPUE series led to a fishing mortality ratio around 0.87, but with large variance, depending on the discard scenario (Figures 32, 33, 34): Crucially, estimates where $F > F_{\text{MSY}}$ were associated with a low discard scenario and higher-allowed recruitment variation ($\sigma_R$). Similarly, when only the NZ series is excluded, mortality rates were largely determined by assumed discard rates. Given relatively low estimated fishing mortality rates compared to $F_{\text{MSY}}$, no models were estimated to exceed other potential reference points ($F_{lim,\text{AS}}$, $F_{crash,\text{AS}}$; Figures A-1, A-2, A-3, A-4, A-5)

Along similar lines, MSY varied between a mean of 8 700 mt for scenarios without EU-Spain CPUE (Figure 32), but varied around 42 000 mt for scenarios when including both EU-Spain and early New Zealand CPUE data. The distribution of MSY had a long tail depending on discard and productivity assumptions, with 95% of grid runs showing a $MSY$ below 55 000 mt.

### 3.3 Dynamic surplus production models

Dynamic surplus production models were largely in agreement with the integrated assessment in terms of recent stock trajectories as well as fishing mortality rates (Figure 37). Although the model fitted all CPUE series well, the estimates from the model using New Zealand CPUE for carrying capacity and fishing mortality rates did not appear credible (Figure 38), whereas models fitted to alternative indices were in agreement, indicating high fishing mortality rates (potentially near $F_{crash,\text{AS}} = 4F_{\text{MSY}}$ in the early 2000s), with recent $F$ likely below $F_{\text{MSY}}$ (Figure 38).

## 4. DISCUSSION

The outcomes of this assessment indicate a recent increasing trend in the biomass of Southwest Pacific blue shark. Although all CPUE indices are in agreement on the trajectory of the stock, the scale of the increase, as well as early CPUE trends, are far less certain. We aimed to address key uncertainties in relative biomass trends, as well as biological knowledge, through extensive sensitivity model-runs.

To address conflicts in CPUE, we produced models with alternate CPUE series and weights. The biggest impacts on model outcomes resulted from the removal of either the EU-Spain series, or early CPUE data from the New Zealand series. In both cases, stock trajectories and recent stock status were lower, with some model runs for the no-EU-Spain scenario showing current spawning biomass below $SB_{\text{MSY}}$ and exploitation above $F_{\text{MSY}}$. These scenarios were associated with low-productivity (low M, slow growth) and high exploitation (i.e., low discards, high initial F).

It is difficult to ascertain how much weight to apply to any one of the CPUE series - while the EU-Spain and New Zealand series may be over-optimistic due to targeting of sharks, they do align with the Chinese Taipei and New Zealand CPUE series derived from observer data, for example. Similarly, high latitude CPUE series may only index a small proportion of the total population, and availability may be affected by factors such as surface water productivity (Vedor et al. 2021). Our grid models show a large range of potential stock status outcomes, associated with affording high weight to a range of CPUE combinations. Despite this spread

in outcomes, our models mostly indicate that the biomass is above $SB_{\text{MSY}}$ and fishing mortality is below $F_{\text{MSY}}$, and therefore provide some certainty that fishing mortality is unlikely to be beyond $F_{lim,\text{AS}}$, $F_{crash,\text{AS}}$.

A range of the models, including our diagnostic case, estimated $SB$ values above $SB_0$, suggesting that high recent recruitment and low fishing mortality may have led to high stock size at or above biomass found under average recruitment in the absence of fishing. Dynamic surplus production models provided additional support for the conclusion that the stock has likely recovered from low levels to levels near or above those found in 1995, under $F = 0$ and average recruitment. Although we considered equilibrium reference points here, given the relatively late (with respect to initial fishery development) starting year of our assessment, and uncertain initial stock status, additional reference points such as $SB_{F=0}$ based reference points could be considered for blue shark. These reference points are used for some tuna stocks (e.g., Ducharme-Barth et al. 2020), where equilibrium reference points are not as practical.

The models in the sensitivity grid were still constrained by a range of uncertainties that are difficult to quantify, and there is no guarantee that they adequately included all relevant uncertainties. For instance, catch (especially early catch in driftnet fisheries) remains unknown and, due to observer coverage before the 2000s, even more recent catches (i.e., mid-1990s to early 2000s) are highly uncertain. Most driftnet fisheries were abandoned by the late 1980s and populations, if they were substantially affected, may have had sufficient time to recover by the time our assessment time-series commenced (i.e, 1995). This raises the possibility that the stock was only lightly fished before longline effort increased in the Southwest Pacific in the 1990s and early 2000s. This scenario would suggest that our initial $F$ estimates are high relative to actual $F$ in the early 1990s.

Actual catches may have been different or even outside of our prediction confidence bounds, and could, if they were known, lead to different conclusions about stock trajectories. However, there appears to be little to no data from early albacore driftnet fisheries, such that early exploitation may always remain a key uncertainty in the assessment of Southwest Pacific blue shark. Nevertheless, there are consistent signals in the data of relatively rapid increases in biomass in the face of recent reductions in fishing mortality. Such increases are evident from CPUE considered here, as well as in high latitude observer CPUE following cessation of driftnet fishing in high latitudes. Although individual data series may be questionable, taken together, these trends suggest a relatively productive stock, and provides some support for our model outcomes. In addition, model trajectories indicating decline and subsequent rapid rebuilding largely mirror those found in the north Pacific (ISC 2018), albeit at lower absolute biomass.

Although we included a range of the uncertainties raised in the previous attempt at assessing blue shark (Takeuchi et al. 2016), some of the patterns in the data (e.g., data from early Australian and Japanese observer data) suggest more local depletion and recovery dynamics, and recent tagging in New Zealand raises the possibility that some spawning-site fidelity may occur in blue shark (Elliott 2020). The stock structure of blue shark may, therefore, be substantially different from current assumptions that blue-shark consist of a single stock on ecological time-scales, even if substantial mixing occurs away from spawning grounds. In the absence of more long-term tagging data from a range of locations across the South Pacific, however, it is unclear what assumptions may be reasonable to make within the assessment regarding spatial stock structure. This is especially so given the paucity of reliable data at smaller strata; sparse observer effort between late 1990s and late 2000s mean that local trends in south Tasman and southern Australian waters are poorly resolved.

### 4.1 Main Assessment Conclusions

- The most influential axes of uncertainty was the weighting and inclusion of CPUE indices; high uncertainty remains in many model outputs across the sensitivity grid.
- The stock biomass was low throughout the region through the early 2000s following the expansion of longline fishing effort in the region.
- Estimates across the uncertainty grid largely indicated that the stock has recovered from lower biomass levels.
- 90% of model runs indicate that fishing mortality at the end of the assessment period was below $F_{\text{MSY}}$ and 96% of model runs show that the biomass is above $SB_{\text{MSY}}$, with high estimated spawning biomass near unfished levels near those expected under $F = 0$ and average recruitment across model runs, and minimum estimated $SB$ of $0.3SB_0$.
- Fishing mortality has declined over the last decade and is currently relatively low. This is largely as a result of most sharks being released upon capture from by the majority of longline fleets.
- Finally, considered against all conventional reference points the stock on average does not appear to be overfished and overfishing is not occurring.

Given some of the fundamental uncertainties highlighted above, we recommend:

- Increased effort to re-construct catch histories for sharks (and other bycatch species) from a range of sources. Our catch reconstruction models showed that model assumptions and formulation can have important implications for reconstructed catches. Additional data sources, such as log-sheet reported captures from reliably reporting vessels, may be incorporated into integrated catch-reconstruction models to fill gaps in observer coverage.
- Dynamic/non-equilibrium reference points, such as $SB_{F=0}$ be investigated for shark stock status, as they may be more appropriate for fisheries with uncertain early exploitation history and strong environmental influences.
- Additional tagging be carried out using satellite tags in a range of locations, especially known nursery grounds in South-East Australia and New Zealand, as well as high seas areas to the north and east of New Zealand, where catch-rates are high. Such tagging may help to resolve questions about the degree of natal homing and mixing of the stock.
- Tagging may also help to obtain better estimates of natural mortality, if carried out in sufficient numbers. This could be taken up as part of the WCPFC Shark Research Plan to assess the feasibility and scale of such an analysis.
- Additional growth studies from a range of locations could help build a better understanding of typical growth, as well as regional growth differences. Current growth data are conflicting, despite evidence that populations at locations of current tagging studies are likely connected or represent individuals from the same population.
- Genetic/genomic studies could be undertaken to augment the tagging work to help resolve these stock/sub-stock structure patterns.

## 5. ACKNOWLEDGEMENTS

We would like to thank Paul Hamer and Nicholas Ducharme-Barth for their constructive input throughout the assessment. We would also like to thank Paul Hamer, Graham Pilling and Sam McKechnie for helpful comments on earlier drafts of this manuscript. Finally, we acknowledge the funding of this work this work from the WCPFC Scientific Committee Project 107.

## 6. REFERENCES

Bonfil, R. (2005). Fishery stock assessment models and their application to sharks. In R. Bonfil & J. A. Musick (Eds.), *Management Techniques for Elasmobranch Fisheries* (p. 154). Rome: FAO.

Brouwer, S. & Hamer, P. (2020). *2021-2025 Shark Research Plan* (tech. rep. No. EB-IP-01 Rev1). WCPFC.

Brouwer, S.; Large, K., & Neubauer, P. (2021). *Characterisation of the fisheries catching South Pacific blue sharks (*Prionace glauca*) in the Western and Central Pacific Ocean* (tech. rep. No. SC17-2021/SA-IP-06). WCPFC.

Clarke, S.; Coelho, R.; Francis, M.; Kai, M.; Kohin, S.; Liu, K. M.; Simpfendorfer, C.; Tovar-Avila, J.; Rigby, C., & Smart, J. (2015). *Report of the Pacific shark life history expert panel workshop, 28-30 April 2015* (tech. rep. No. SC11-EB-IP-13). WCPFC.

Clarke, S. & Hoyle, S. (2014). *Development of limit reference points for elasmobranchs* (tech. rep. No. SC10-MI-WP-07). WCPFC.

Coelho, R.; Mejuto, J.; Domingo, A.; Yokawa, K.; Liu, K.-M.; Cortés, E.; Romanov, E. V.; da Silva, C.; Hazin, F.; Arocha, F., et al. (2018). Distribution patterns and population structure of the blue shark (*Prionace glauca*) in the Atlantic and Indian Oceans. *Fish and Fisheries*, *19*(1), 90–106.

Ducharme-Barth, N.; Vincent, M.; Hampton, J.; Hamer, P., & Pilling, G. (2020). *Stock assessment of bigeye tuna in the western and central Pacic Ocean* (tech. rep. No. WCPFC-SC16-2020/SA-WP-03). WCPFC.

Edwards, C. T. T. (2017). *Bdm: Bayesian biomass dynamics model*. R package version 0.0.0.9022.

Elliott, R. (2020). *Spatio-temporal patterns in movement, behaviour and habitat use by a pelagic predator, the blue shark (Prionace glauca), assessed using satellite tags* (Doctoral dissertation, University of Auckland).

Francis, M. P. & Duffy, C. (2005). Length at maturity in three pelagic sharks (*Lamna nasus*, *Isurus oxyrinchus*, and *Prionace glauca*) from New Zealand. *Fishery Bulletin*, *103*(3), 489–500.

Francis, R. C. (2011). Data weighting in statistical fisheries stock assessment models. *Canadian Journal of Fisheries and Aquatic Sciences*, *68*(6), 1124–1138.

Froese, R.; Demirel, N.; Coro, G.; Kleisner, K. M., & Winker, H. (2017). Estimating fisheries reference points from catch and resilience. *Fish and Fisheries*, *18*(3), 506–526.

Fujinami, Y.; Semba, Y., & Tanaka, S. (2019). Age determination and growth of the blue shark (*Prionace glauca*) in the western North Pacific Ocean. *Fishery Bulletin*, *117*.

Hewitt, D. A. & Hoenig, J. M. (2005). Comparison of two approaches for estimating natural mortality based on longevity. *Fishery Bulletin*, *103*(2), 433.

ISC (2018). *Stock assessment and future projections of blue shark in the North Pacific Ocean through 2015* (tech. rep. No. SC14-SA-IP-13). WCPFC.

Jensen, A. (1996). Beverton and holt life history invariants result from optimal trade-off of reproduction and survival. *Canadian Journal of Fisheries and Aquatic Sciences*, *53*(4), 820–822.

Joung, S. J.; Lyu, T., G; Hsu, H. H.; Liu, K. M., & Wang, S. B. (2018). Age and growth estimates of the blue shark (*Prionace glauca*) in the central South Pacific Ocean. *Marine and Freshwater Research*. doi:10.1071/MF17098

Kai, M. & Fujinami, Y. (2020). Estimation of mean movement rates for blue sharks in the northwestern Pacific Ocean. *Animal Biotelemetry*, *8*(35). doi:https://doi.org/10.1186/s40317-020-00223-x

Kai, M. & Fujinami, Y. (2018). Stock-recruitment relationships in elasmobranchs: Application to the North Pacific blue shark. *Fisheries Research*, *200*, 104–115.

Manning, M. J. & Francis, M. P. (2005). Age and growth of blue shark (*Prionace glauca*) from the New Zealand Economic Exclusive Zone. *New Zealand Fisheries Assessment Report 2005/26*. 52 p.

McAllister, M. & Edwards, C. (2016). Applications of a Bayesian surplus production model to New Zealand fish stocks. *New Zealand Fisheries Assessment Report*, *52*, 79.

Methot Jr, R. & Wetzel, C. R. (2013). Stock synthesis: A biological and statistical framework for fish stock assessment and fishery management. *Fisheries Research*, *142*, 86–99.

Murray, T. (1990). Review of research and of recent developments in South Pacific albacore fisheries with emphasis on large-scale pelagic driftnet fishing. Information Paper 2. In *Third South Pacific Albacore Research Workshop* (pp. 9–12).

Neubauer, P.; Large, K.; Brouwer, M., S.and Kai; Tsai, W.-P., & Liu, K.-M. (2021). *Input data for the 2021 South Pacific Blue Shark stock assessment* (tech. rep. No. WCPFC-SC17-2021/SA-IP-18). WCPFC.

Neubauer, P.; Richards, Y., & Tremblay-Boyer, L. (2019). *Alternative assessment methods for oceanic white-tip shark* (tech. rep. No. WCPFC-SC15-2019/SA-IP-13). WCPFC.

Northridge, S. P. (1991). Driftnet fisheries and their impacts on non-target species: A world wide review. *FAO Fisheries Technical Paper*, *320*. 115 p.

Pardo, S. A.; Kindsvater, H. K.; Reynolds, J. D., & Dulvy, N. K. (2016, August). Maximum intrinsic rate of population increase in sharks, rays, and chimaeras: The importance of survival to maturity. *Canadian Journal of Fisheries and Aquatic Sciences*, *73*(8), 1159–1163. doi:10.1139/cjfas-2016-0069

Pardo, S. A.; Cooper, A. B.; Reynolds, J. D., & Dulvy, N. K. (2018, January 5). Quantifying the known unknowns: Estimating maximum intrinsic rate of population increase in the face of uncertainty. *ICES Journal of Marine Science*. doi:10.1093/icesjms/fsx220

Richards, A. H. (1994). Problems of drift-net fisheries in the South Pacific. *Marine Pollution Bulletin*, *29*(1-3), 106–111.

Semba, Y. & Yokoia, H. (2016). *Update of age and sex specific natural mortality of the blue shark (Prionace glauca) in the North Pacific Ocean*. ISC/16/SHARKWG-1/06.

Sippel, T.; Wraith, J.; Kohin, S.; Taylor, V.; Holdsworth, J.; Taguchi, M.; Matsunaga, H., & Yokawa, K. (2016). *A summary of blue shark (Prionace glauca) and shortfin mako shark (Isurus oxyrinchus) tagging data available from the North and Southwest Pacific Ocean* (tech. rep. No. SC12-SA-IP-16). WCPFC.

Stan Development Team (2018). RStan: the R interface to Stan. R package version 2.17.3. Retrieved from http://mc-stan.org/

Takeuchi, Y.; Tremblay-Boyer, L.; Pilling, G. M., & Hampton, J. (2016). *Assessment of blue shark in the southwestern Pacific* (tech. rep. No. SC12-SA-WP-08). WCPFC.

Taylor, I. G.; Gertseva, V.; Methot Jr, R. D., & Maunder, M. N. (2013). A stock–recruitment relationship based on pre-recruit survival, illustrated with application to spiny dogfish shark. *Fisheries Research*, *142*, 15–21.

Tremblay-Boyer, L.; Carvalho, F.; Neubauer, P., & Pilling, G. (2019). *Stock assessment for oceanic whitetip shark in the Western and Central Pacific Ocean* (tech. rep. No. WCPFC-SC15-2019/SA-WP-06). WCPFC.

Vedor, M.; Mucientes, G.; Hernández-Chan, S.; Rosa, R.; Humphries, N.; Sims, D. W., & Queiroz, N. (2021). Oceanic diel vertical movement patterns of blue sharks vary with water temperature and productivity to change vulnerability to fishing. *Frontiers in Marine Science*, *8*, 891.

WCPFC (2016). *Twelfth Regular Session of the Scientific Committee: Summary Report*. WCPFC.
West, G.; Stevens, J. D., & Basson, M. (2004). *Assessment of blue shark population status in the western South Pacific* (tech. rep. No. AFMA Project R01/1157).
Williams, P.; Panizza, A.; Falasi, c.; Loganimoce, E., & Schneiter, E. (2020). *Status of Observer Data Management* (tech. rep. No. SC16-2020/ST-IP-02). WCPFC.
Winker, H.; Carvalho, F., & Kapur, M. (2018). Jabba: Just another bayesian biomass assessment. *Fisheries Research*, *204*, 275–288.
Zhou, S.; Deng, R.; Hoyle, S., & Dunn, M. (2018). *Identifying appropriate reference points for elasmobranchs within the WCPFC*. WCPFC-SC14-2018/MI-WP-07. Report to the Western and Central Pacific Fisheries Commission Scientific Committee. Fourteenth Regular Session, 8–16 August 2018, Busan, Korea.

# 7. TABLES

**Table 1:** Description of the 8 catch scenarios used in the stock assessment. The scenario used for the diagnostic case is highlighted in bold. The total mortality is the cumulative mortality assumed for individuals from the time they are hooked to after they are released back to the water. Further information, see Neubauer et al. (2021).

| Catch scenario | Catch levels | Discard and post-release-mortality |
|---|---|---|
| *Catch (Post exp)* | Mean | 100% mortality on all catches, independently of discard status |
| *Low Disc. (Post exp)* | Mean | 25% quantile of posterior distribution of annual discard rates; 17% post-release mortality |
| ***Mean Disc. (Post exp)*** | **Mean** | **Posterior mean of annual discard rates; 17% post-release mortality** |
| *High Disc. (Post exp)* | Mean | 75% quantile of posterior distribution of annual discard rates; 17% post-release mortality |
| *High Catch (90%)* | $90^{\text{th}}$ quantile | 100% mortality on all catches, independently of discard status |
| *Low Disc (90%)* | $90^{\text{th}}$ quantile | 25% quantile of posterior distribution of annual discard rates; 17% post-release mortality |
| *Mean Disc (90%)* | $90^{\text{th}}$ quantile | Posterior mean of annual discard rates; 17% post-release mortality |
| *High Disc (90%)* | $90^{\text{th}}$ quantile | 75% quantile of posterior distribution of annual discard rates; 17% post-release mortality |

**Table 2:** Description of the nine axes for the structural uncertainty grid. Settings used under the diagnostic case are highlighted in bold.

| Axis | Description |
|---|---|
| Catch scenario | **Base**, high |
| Discard scenario | Low, **base**, high |
| Initial F | Low, **base**, high |
| Recruitment deviation ($\sigma_R$) | **Low (0.2)**, high (0.4) |
| High latitude CPUE | **Base**, low weight, remove (RM) early New Zealand |
| Low latitude CPUE | **Japan**, Australia |
| Natural mortality | **Base (0.2)**, low (0.16) |
| Survival fraction | **Base**, low, high |
| Growth | **Manning and Francis (2005)**, Joung et al. (2018) |

**Table 3:** Description of the symbols used in the yield and stock status analyses. In this assessment, 'recent' is the average of the metric over the period 2016–2019, and 'latest' is 2020.

| Symbol | Description |
|---|---|
| $C_{latest}$ | Catch in the last year of the assessment (2020) |
| $C_{recent}$ | Catch in a recent period of the assessment (2016–2019) |
| $MSY$ | Equilibrium yield at $MSY$ |
| $SB_0$ | Equilibrium unfished spawning biomass under average recruitment |
| $SB_{MSY}$ | Spawning biomass that will produce $MSY$ |
| $SB_{latest}$ | Spawning biomass in the last year of the assessment (2020) |
| $SB_{recent}$ | Spawning biomass in a recent period of the assessment (2016–2019) |
| $SB_{latest}/SB_0$ | Spawning biomass in the latest time period (2020) relative to the equilibrium spawning biomass under $F = 0$ and average recruitment |
| $SB_{recent}/SB_0$ | Spawning biomass in the recent time period (2016–2019) relative to the equilibrium spawning biomass under $F = 0$ and average recruitment |
| $SB_{latest}/SB_{MSY}$ | Spawning biomass in the latest time period (2020) relative to that which will produce the maximum sustainable yield ($MSY$) |
| $SB_{recent}/SB_{MSY}$ | Spawning biomass in the recent time period (2016–2019) relative to that which will produce the maximum sustainable yield ($MSY$) |
| $F_{MSY}$ | Fishing mortality producing the maximum sustainable yield ($MSY$) |
| $F_{limAS}$, | Fishing mortality resulting in 0.5 of $SB_{MSY}$ |
| $F_{crashAS}$ | Fishing mortality resulting in population extinction when sustained on the long-term |
| $F_{latest}/F_{MSY}$ | Average fishing mortality-at-age for the last year of the assessment (2020) |
| $F_{recent}/F_{MSY}$ | Average fishing mortality-at-age for a recent period (2016–2019) |
| $F_{latest}$ | Latest fishing mortality (2020) compared to that producing maximum sustainable yield ($MSY$) |
| $F_{recent}$ | Recent fishing mortality (2016–2019) compared to that producing maximum sustainable yield ($MSY$) |
| $F_{latest}/F_{limAS}$ | Latest fishing mortality (2020) compared to that resulting in 0.5 of $SB_{MSY}$ |
| $F_{recent}/F_{limAS}$ | Recent fishing mortality (2016–2019) compared to that resulting in 0.5 of $SB_{MSY}$ |
| $F_{latest}/F_{crashAS}$ | Latest fishing mortality (2020) compared to that resulting in population extinction |
| $F_{recent}/F_{crashAS}$ | Recent fishing mortality (2016–2019) compared to that resulting in population extinction |

**Table 4:** Summary of reference points for 3885 grid models in the structural uncertainty grid

| | Mean | Median | Min | 10% | 90% | Max |
|---|---|---|---|---|---|---|
| $C_{latest}$ | 6010 | 6188 | 3219 | 3580 | 8454 | 10349 |
| $C_{recent}$ | 6815 | 7234 | 4007 | 4263 | 9135 | 9788 |
| MSY | 23902 | 13234 | 5462 | 7451 | 50727 | 311628 |
| $SB_0$ | 45150 | 27894 | 10148 | 13508 | 91763 | 455076 |
| $SB_{\text{MSY}}$ | 21202 | 13201 | 4686 | 6303 | 42881 | 210296 |
| $SB_{recent}/SB_0$ | 54566 | 22758 | 6774 | 8599 | 119091 | 605252 |
| $SB_{recent}$ | 47464 | 18385 | 5800 | 7638 | 106751 | 560768 |
| $SB_{latest}/SB_0$ | 1.03 | 1.08 | 0.30 | 0.58 | 1.49 | 1.66 |
| $SB_{recent}/SB_0$ | 0.88 | 0.87 | 0.27 | 0.49 | 1.21 | 1.29 |
| $SB_{latest}/SB_{\text{MSY}}$ | 2.19 | 2.28 | 0.64 | 1.23 | 3.15 | 3.61 |
| $SB_{recent}/SB_{\text{MSY}}$ | 1.88 | 1.84 | 0.57 | 1.06 | 2.57 | 2.80 |
| $F_{\text{MSY}}$ | 0.153 | 0.152 | 0.132 | 0.135 | 0.168 | 0.182 |
| $F_{lim,\text{AS}}$ | 0.231 | 0.228 | 0.199 | 0.205 | 0.253 | 0.274 |
| $F_{crash,\text{AS}}$ | 0.318 | 0.312 | 0.274 | 0.282 | 0.346 | 0.377 |
| $F_{latest}$ | 0.073 | 0.066 | 0.002 | 0.013 | 0.153 | 0.216 |
| $F_{recent}$ | 0.089 | 0.075 | 0.002 | 0.015 | 0.191 | 0.282 |
| $F_{latest}/F_{\text{MSY}}$ | 0.48 | 0.43 | 0.01 | 0.08 | 1.00 | 1.29 |
| $F_{recent}/F_{\text{MSY}}$ | 0.58 | 0.48 | 0.01 | 0.10 | 1.24 | 1.68 |
| $F_{latest}/F_{lim,\text{AS}}$ | 0.32 | 0.28 | 0.01 | 0.06 | 0.66 | 0.87 |
| $F_{recent}/F_{lim,\text{AS}}$ | 0.38 | 0.32 | 0.01 | 0.06 | 0.82 | 1.13 |
| $F_{latest}/F_{crash,\text{AS}}$ | 0.23 | 0.21 | 0.01 | 0.04 | 0.48 | 0.63 |
| $F_{recent}/F_{crash,\text{AS}}$ | 0.28 | 0.23 | 0.01 | 0.05 | 0.59 | 0.83 |

**Table 5:** Summary of reference points for the subset of 1944 grid models in the structural uncertainty grid using the median catch scenario and median discards estimates.

| | Mean | Median | Min | 10% | 90% | Max |
|---|---|---|---|---|---|---|
| $C_{latest}$ | 5441 | 5350 | 3219 | 3580 | 7449 | 8402 |
| $C_{recent}$ | 6441 | 6346 | 4007 | 4263 | 8597 | 9527 |
| MSY | 22243 | 11723 | 5462 | 7104 | 46279 | 311628 |
| $SB_0$ | 41916 | 24791 | 10148 | 13107 | 80364 | 455076 |
| $SB_{\text{MSY}}$ | 19686 | 11785 | 4686 | 6147 | 37524 | 210296 |
| $SB_{recent}/SB_0$ | 50650 | 20888 | 6774 | 8233 | 104014 | 605252 |
| $SB_{recent}$ | 44098 | 16290 | 5800 | 7214 | 94314 | 560768 |
| $SB_{latest}/SB_0$ | 1.03 | 1.08 | 0.30 | 0.58 | 1.49 | 1.66 |
| $SB_{recent}/SB_0$ | 0.88 | 0.87 | 0.27 | 0.50 | 1.21 | 1.29 |
| $SB_{latest}/SB_{\text{MSY}}$ | 2.19 | 2.27 | 0.64 | 1.23 | 3.15 | 3.61 |
| $SB_{recent}/SB_{\text{MSY}}$ | 1.88 | 1.83 | 0.57 | 1.06 | 2.57 | 2.80 |
| $F_{\text{MSY}}$ | 0.153 | 0.152 | 0.132 | 0.135 | 0.168 | 0.182 |
| $F_{lim,\text{AS}}$ | 0.231 | 0.228 | 0.199 | 0.205 | 0.252 | 0.274 |
| $F_{crash,\text{AS}}$ | 0.317 | 0.312 | 0.274 | 0.282 | 0.346 | 0.377 |
| $F_{latest}$ | 0.072 | 0.065 | 0.002 | 0.012 | 0.151 | 0.216 |
| $F_{recent}$ | 0.090 | 0.076 | 0.002 | 0.015 | 0.195 | 0.282 |
| $F_{latest}/F_{\text{MSY}}$ | 0.47 | 0.42 | 0.01 | 0.08 | 0.98 | 1.29 |
| $F_{recent}/F_{\text{MSY}}$ | 0.59 | 0.49 | 0.01 | 0.10 | 1.25 | 1.68 |
| $F_{latest}/F_{lim,\text{AS}}$ | 0.31 | 0.28 | 0.01 | 0.06 | 0.64 | 0.87 |
| $F_{recent}/F_{lim,\text{AS}}$ | 0.39 | 0.33 | 0.01 | 0.06 | 0.83 | 1.13 |
| $F_{latest}/F_{crash,\text{AS}}$ | 0.23 | 0.20 | 0.01 | 0.04 | 0.47 | 0.63 |
| $F_{recent}/F_{crash,\text{AS}}$ | 0.28 | 0.24 | 0.01 | 0.05 | 0.60 | 0.83 |

**Table 6:** Summary of reference points for the subset of 1941 grid models in the structural uncertainty grid using the high catch scenario and median discards estimates.

| | Mean | Median | Min | 10% | 90% | Max |
|---|---|---|---|---|---|---|
| $C_{latest}$ | 6580 | 7119 | 3219 | 3580 | 9157 | 10349 |
| $C_{recent}$ | 7190 | 8149 | 4007 | 4263 | 9289 | 9788 |
| MSY | 25563 | 14626 | 5462 | 7652 | 56392 | 311628 |
| $SB_0$ | 48388 | 29855 | 10148 | 14108 | 95870 | 455076 |
| $SB_{\text{MSY}}$ | 22720 | 14154 | 4686 | 6640 | 44822 | 210296 |
| $SB_{recent}/SB_0$ | 58488 | 24088 | 6774 | 8913 | 130542 | 605252 |
| $SB_{recent}$ | 50836 | 21023 | 5800 | 7877 | 111206 | 560768 |
| $SB_{latest}/SB_0$ | 1.03 | 1.09 | 0.30 | 0.58 | 1.49 | 1.66 |
| $SB_{recent}/SB_0$ | 0.88 | 0.87 | 0.27 | 0.49 | 1.21 | 1.29 |
| $SB_{latest}/SB_{\text{MSY}}$ | 2.19 | 2.29 | 0.64 | 1.23 | 3.15 | 3.61 |
| $SB_{recent}/SB_{\text{MSY}}$ | 1.88 | 1.85 | 0.57 | 1.06 | 2.57 | 2.80 |
| $F_{\text{MSY}}$ | 0.153 | 0.152 | 0.132 | 0.136 | 0.169 | 0.182 |
| $F_{lim,\text{AS}}$ | 0.231 | 0.228 | 0.199 | 0.206 | 0.253 | 0.274 |
| $F_{crash,\text{AS}}$ | 0.318 | 0.313 | 0.274 | 0.282 | 0.346 | 0.377 |
| $F_{latest}$ | 0.074 | 0.067 | 0.002 | 0.013 | 0.155 | 0.216 |
| $F_{recent}$ | 0.088 | 0.073 | 0.002 | 0.015 | 0.188 | 0.282 |
| $F_{latest}/F_{\text{MSY}}$ | 0.48 | 0.43 | 0.01 | 0.08 | 1.01 | 1.29 |
| $F_{recent}/F_{\text{MSY}}$ | 0.57 | 0.47 | 0.01 | 0.10 | 1.21 | 1.68 |
| $F_{latest}/F_{lim,\text{AS}}$ | 0.32 | 0.28 | 0.01 | 0.06 | 0.66 | 0.87 |
| $F_{recent}/F_{lim,\text{AS}}$ | 0.38 | 0.31 | 0.01 | 0.06 | 0.80 | 1.13 |
| $F_{latest}/F_{crash,\text{AS}}$ | 0.23 | 0.21 | 0.01 | 0.04 | 0.48 | 0.63 |
| $F_{recent}/F_{crash,\text{AS}}$ | 0.27 | 0.23 | 0.01 | 0.05 | 0.58 | 0.83 |

**Table 7:** Summary of reference points for the subset of 1295 grid models in the structural uncertainty grid using the median catch scenario and low discards estimates.

| | Mean | Median | Min | 10% | 90% | Max |
|---|---|---|---|---|---|---|
| $C_{latest}$ | 7160 | 7122 | 6064 | 6416 | 8176 | 8402 |
| $C_{recent}$ | 8436 | 8302 | 7574 | 7820 | 9295 | 9527 |
| MSY | 19593 | 12402 | 6504 | 7763 | 39993 | 81200 |
| $SB_0$ | 37576 | 27716 | 11940 | 14546 | 71959 | 119017 |
| $SB_{\text{MSY}}$ | 17670 | 13166 | 5439 | 6821 | 33066 | 55849 |
| $SB_{recent}/SB_0$ | 43543 | 20770 | 7350 | 9104 | 87565 | 144809 |
| $SB_{recent}$ | 37729 | 16266 | 6580 | 8047 | 81212 | 137033 |
| $SB_{latest}/SB_0$ | 1.00 | 1.02 | 0.30 | 0.59 | 1.46 | 1.59 |
| $SB_{recent}/SB_0$ | 0.87 | 0.81 | 0.28 | 0.51 | 1.18 | 1.24 |
| $SB_{latest}/SB_{\text{MSY}}$ | 2.14 | 2.16 | 0.64 | 1.25 | 3.10 | 3.44 |
| $SB_{recent}/SB_{\text{MSY}}$ | 1.84 | 1.74 | 0.58 | 1.09 | 2.52 | 2.66 |
| $F_{\text{MSY}}$ | 0.152 | 0.151 | 0.132 | 0.135 | 0.167 | 0.179 |
| $F_{lim,\text{AS}}$ | 0.229 | 0.227 | 0.199 | 0.203 | 0.249 | 0.270 |
| $F_{crash,\text{AS}}$ | 0.315 | 0.309 | 0.274 | 0.280 | 0.342 | 0.371 |
| $F_{latest}$ | 0.092 | 0.086 | 0.017 | 0.025 | 0.174 | 0.216 |
| $F_{recent}$ | 0.112 | 0.108 | 0.018 | 0.029 | 0.226 | 0.282 |
| $F_{latest}/F_{\text{MSY}}$ | 0.60 | 0.61 | 0.10 | 0.16 | 1.12 | 1.29 |
| $F_{recent}/F_{\text{MSY}}$ | 0.74 | 0.77 | 0.10 | 0.19 | 1.43 | 1.68 |
| $F_{latest}/F_{lim,\text{AS}}$ | 0.40 | 0.40 | 0.06 | 0.11 | 0.74 | 0.87 |
| $F_{recent}/F_{lim,\text{AS}}$ | 0.49 | 0.51 | 0.07 | 0.12 | 0.95 | 1.13 |
| $F_{latest}/F_{crash,\text{AS}}$ | 0.29 | 0.29 | 0.05 | 0.08 | 0.54 | 0.63 |
| $F_{recent}/F_{crash,\text{AS}}$ | 0.35 | 0.37 | 0.05 | 0.09 | 0.69 | 0.83 |

**Table 8:** Summary of reference points for the subset of 1296 grid models in the structural uncertainty grid using the median catch scenario and high discards estimates.

| | Mean | Median | Min | 10% | 90% | Max |
|---|---|---|---|---|---|---|
| $C_{latest}$ | 3802 | 3782 | 3219 | 3401 | 4295 | 4422 |
| $C_{recent}$ | 4439 | 4376 | 4007 | 4128 | 4861 | 4955 |
| MSY | 26252 | 11254 | 5462 | 6540 | 58246 | 311628 |
| $SB_0$ | 48713 | 23562 | 10148 | 12169 | 103819 | 455076 |
| $SB_{\text{MSY}}$ | 22847 | 11116 | 4686 | 5768 | 48458 | 210296 |
| $SB_{recent}/SB_0$ | 60995 | 21274 | 6774 | 7746 | 137707 | 605252 |
| $SB_{recent}$ | 53397 | 16526 | 5800 | 6658 | 124992 | 560768 |
| $SB_{latest}/SB_0$ | 1.05 | 1.13 | 0.31 | 0.59 | 1.52 | 1.66 |
| $SB_{recent}/SB_0$ | 0.90 | 0.89 | 0.27 | 0.47 | 1.23 | 1.29 |
| $SB_{latest}/SB_{\text{MSY}}$ | 2.24 | 2.38 | 0.65 | 1.24 | 3.20 | 3.61 |
| $SB_{recent}/SB_{\text{MSY}}$ | 1.91 | 1.92 | 0.57 | 1.01 | 2.62 | 2.80 |
| $F_{\text{MSY}}$ | 0.154 | 0.153 | 0.134 | 0.136 | 0.170 | 0.182 |
| $F_{lim,\text{AS}}$ | 0.232 | 0.230 | 0.202 | 0.206 | 0.253 | 0.274 |
| $F_{crash,\text{AS}}$ | 0.319 | 0.314 | 0.278 | 0.283 | 0.348 | 0.377 |
| $F_{latest}$ | 0.052 | 0.047 | 0.002 | 0.010 | 0.110 | 0.127 |
| $F_{recent}$ | 0.067 | 0.058 | 0.002 | 0.011 | 0.150 | 0.177 |
| $F_{latest}/F_{\text{MSY}}$ | 0.34 | 0.33 | 0.01 | 0.06 | 0.70 | 0.80 |
| $F_{recent}/F_{\text{MSY}}$ | 0.43 | 0.41 | 0.01 | 0.07 | 0.93 | 1.06 |
| $F_{latest}/F_{lim,\text{AS}}$ | 0.22 | 0.22 | 0.01 | 0.04 | 0.46 | 0.53 |
| $F_{recent}/F_{lim,\text{AS}}$ | 0.29 | 0.27 | 0.01 | 0.05 | 0.61 | 0.70 |
| $F_{latest}/F_{crash,\text{AS}}$ | 0.16 | 0.16 | 0.01 | 0.03 | 0.33 | 0.38 |
| $F_{recent}/F_{crash,\text{AS}}$ | 0.21 | 0.20 | 0.01 | 0.03 | 0.44 | 0.51 |

**Table 9:** Summary of reference points for the subset of 1295 grid models in the structural uncertainty grid dropping the EU - Spain series from the model.

| | Mean | Median | Min | 10% | 90% | Max |
|---|---|---|---|---|---|---|
| $C_{latest}$ | 5464 | 5175 | 3219 | 3401 | 7881 | 8454 |
| $C_{recent}$ | 6512 | 6474 | 4007 | 4180 | 8372 | 8731 |
| MSY | 8716 | 8116 | 5462 | 6411 | 12029 | 18738 |
| $SB_0$ | 16795 | 15137 | 10148 | 11831 | 24779 | 44380 |
| $SB_{\text{MSY}}$ | 7909 | 7146 | 4686 | 5439 | 11732 | 21019 |
| $SB_{recent}/SB_0$ | 10211 | 9464 | 6774 | 7657 | 13783 | 19765 |
| $SB_{recent}$ | 8958 | 8319 | 5800 | 6554 | 12248 | 17213 |
| $SB_{latest}/SB_0$ | 0.64 | 0.65 | 0.30 | 0.36 | 0.79 | 0.87 |
| $SB_{recent}/SB_0$ | 0.56 | 0.58 | 0.27 | 0.31 | 0.69 | 0.77 |
| $SB_{latest}/SB_{\text{MSY}}$ | 1.36 | 1.41 | 0.64 | 0.75 | 1.65 | 1.86 |
| $SB_{recent}/SB_{\text{MSY}}$ | 1.19 | 1.24 | 0.57 | 0.66 | 1.46 | 1.65 |
| $F_{\text{MSY}}$ | 0.154 | 0.152 | 0.133 | 0.136 | 0.170 | 0.182 |
| $F_{lim,\text{AS}}$ | 0.233 | 0.230 | 0.201 | 0.206 | 0.253 | 0.274 |
| $F_{crash,\text{AS}}$ | 0.321 | 0.316 | 0.277 | 0.284 | 0.348 | 0.377 |
| $F_{latest}$ | 0.134 | 0.132 | 0.075 | 0.095 | 0.180 | 0.216 |
| $F_{recent}$ | 0.170 | 0.164 | 0.096 | 0.123 | 0.227 | 0.282 |
| $F_{latest}/F_{\text{MSY}}$ | 0.87 | 0.86 | 0.49 | 0.61 | 1.13 | 1.29 |
| $F_{recent}/F_{\text{MSY}}$ | 1.10 | 1.06 | 0.65 | 0.81 | 1.43 | 1.68 |
| $F_{latest}/F_{lim,\text{AS}}$ | 0.58 | 0.57 | 0.32 | 0.41 | 0.75 | 0.87 |
| $F_{recent}/F_{lim,\text{AS}}$ | 0.73 | 0.70 | 0.42 | 0.53 | 0.95 | 1.13 |
| $F_{latest}/F_{crash,\text{AS}}$ | 0.42 | 0.41 | 0.23 | 0.30 | 0.55 | 0.63 |
| $F_{recent}/F_{crash,\text{AS}}$ | 0.53 | 0.51 | 0.31 | 0.38 | 0.69 | 0.83 |

**Table 10:** Summary of reference points for the subset of 1296 grid models in the structural uncertainty grid removing early years (<2005) from the New Zealand CPUE

| | Mean | Median | Min | 10% | 90% | Max |
|---|---|---|---|---|---|---|
| $C_{latest}$ | 5778 | 5831 | 3219 | 3549 | 8327 | 9217 |
| $C_{recent}$ | 6662 | 7183 | 4007 | 4196 | 8736 | 9229 |
| MSY | 10358 | 9691 | 5462 | 7453 | 14233 | 23927 |
| $SB_0$ | 20158 | 18476 | 10148 | 13520 | 29676 | 57451 |
| $SB_{\text{MSY}}$ | 9493 | 8735 | 4686 | 6284 | 14081 | 27513 |
| $SB_{recent}/SB_0$ | 16437 | 15481 | 6774 | 8599 | 24066 | 39071 |
| $SB_{recent}$ | 13962 | 13897 | 5800 | 7638 | 20280 | 31503 |
| $SB_{latest}/SB_0$ | 0.83 | 0.84 | 0.30 | 0.52 | 1.13 | 1.25 |
| $SB_{recent}/SB_0$ | 0.71 | 0.77 | 0.27 | 0.43 | 0.89 | 0.97 |
| $SB_{latest}/SB_{\text{MSY}}$ | 1.76 | 1.80 | 0.64 | 1.10 | 2.38 | 2.68 |
| $SB_{recent}/SB_{\text{MSY}}$ | 1.51 | 1.64 | 0.57 | 0.90 | 1.90 | 2.07 |
| $F_{\text{MSY}}$ | 0.153 | 0.152 | 0.132 | 0.135 | 0.169 | 0.182 |
| $F_{lim,\text{AS}}$ | 0.231 | 0.228 | 0.199 | 0.205 | 0.253 | 0.274 |
| $F_{crash,\text{AS}}$ | 0.318 | 0.312 | 0.274 | 0.282 | 0.346 | 0.377 |
| $F_{latest}$ | 0.103 | 0.101 | 0.038 | 0.056 | 0.153 | 0.216 |
| $F_{recent}$ | 0.123 | 0.116 | 0.048 | 0.067 | 0.191 | 0.282 |
| $F_{latest}/F_{\text{MSY}}$ | 0.67 | 0.65 | 0.25 | 0.38 | 1.00 | 1.29 |
| $F_{recent}/F_{\text{MSY}}$ | 0.80 | 0.77 | 0.31 | 0.44 | 1.24 | 1.68 |
| $F_{latest}/F_{lim,\text{AS}}$ | 0.44 | 0.43 | 0.16 | 0.25 | 0.66 | 0.87 |
| $F_{recent}/F_{lim,\text{AS}}$ | 0.53 | 0.51 | 0.20 | 0.29 | 0.82 | 1.13 |
| $F_{latest}/F_{crash,\text{AS}}$ | 0.32 | 0.31 | 0.12 | 0.18 | 0.48 | 0.63 |
| $F_{recent}/F_{crash,\text{AS}}$ | 0.39 | 0.37 | 0.15 | 0.21 | 0.59 | 0.83 |

**Table 11:** Summary of reference points for the subset of 1296 grid models in the structural uncertainty grid with high initial fishing mortality.

| | Mean | Median | Min | 10% | 90% | Max |
|---|---|---|---|---|---|---|
| $C_{latest}$ | 5966 | 6147 | 3219 | 3542 | 8373 | 10349 |
| $C_{recent}$ | 6785 | 7397 | 4007 | 4248 | 9116 | 9770 |
| MSY | 23114 | 15008 | 7625 | 8526 | 47405 | 133549 |
| $SB_0$ | 44096 | 33538 | 10546 | 15019 | 84494 | 194425 |
| $SB_{\text{MSY}}$ | 20726 | 16008 | 4870 | 7027 | 39086 | 90148 |
| $SB_{recent}/SB_0$ | 49923 | 19325 | 6774 | 8030 | 113312 | 262686 |
| $SB_{recent}$ | 43309 | 15566 | 5800 | 7118 | 98806 | 242084 |
| $SB_{latest}/SB_0$ | 0.95 | 0.94 | 0.30 | 0.36 | 1.50 | 1.66 |
| $SB_{recent}/SB_0$ | 0.81 | 0.82 | 0.27 | 0.31 | 1.22 | 1.29 |
| $SB_{latest}/SB_{\text{MSY}}$ | 2.03 | 2.01 | 0.64 | 0.75 | 3.17 | 3.61 |
| $SB_{recent}/SB_{\text{MSY}}$ | 1.73 | 1.77 | 0.57 | 0.66 | 2.60 | 2.80 |
| $F_{\text{MSY}}$ | 0.153 | 0.152 | 0.133 | 0.136 | 0.168 | 0.182 |
| $F_{lim,\text{AS}}$ | 0.231 | 0.228 | 0.201 | 0.206 | 0.252 | 0.274 |
| $F_{crash,\text{AS}}$ | 0.318 | 0.312 | 0.276 | 0.283 | 0.346 | 0.377 |
| $F_{latest}$ | 0.077 | 0.070 | 0.005 | 0.014 | 0.159 | 0.215 |
| $F_{recent}$ | 0.095 | 0.079 | 0.005 | 0.016 | 0.200 | 0.282 |
| $F_{latest}/F_{\text{MSY}}$ | 0.50 | 0.45 | 0.03 | 0.09 | 1.04 | 1.28 |
| $F_{recent}/F_{\text{MSY}}$ | 0.62 | 0.52 | 0.03 | 0.10 | 1.28 | 1.68 |
| $F_{latest}/F_{lim,\text{AS}}$ | 0.33 | 0.29 | 0.02 | 0.06 | 0.69 | 0.86 |
| $F_{recent}/F_{lim,\text{AS}}$ | 0.41 | 0.34 | 0.02 | 0.07 | 0.85 | 1.13 |
| $F_{latest}/F_{crash,\text{AS}}$ | 0.24 | 0.21 | 0.01 | 0.04 | 0.50 | 0.63 |
| $F_{recent}/F_{crash,\text{AS}}$ | 0.30 | 0.25 | 0.01 | 0.05 | 0.62 | 0.83 |

# 8. FIGURES

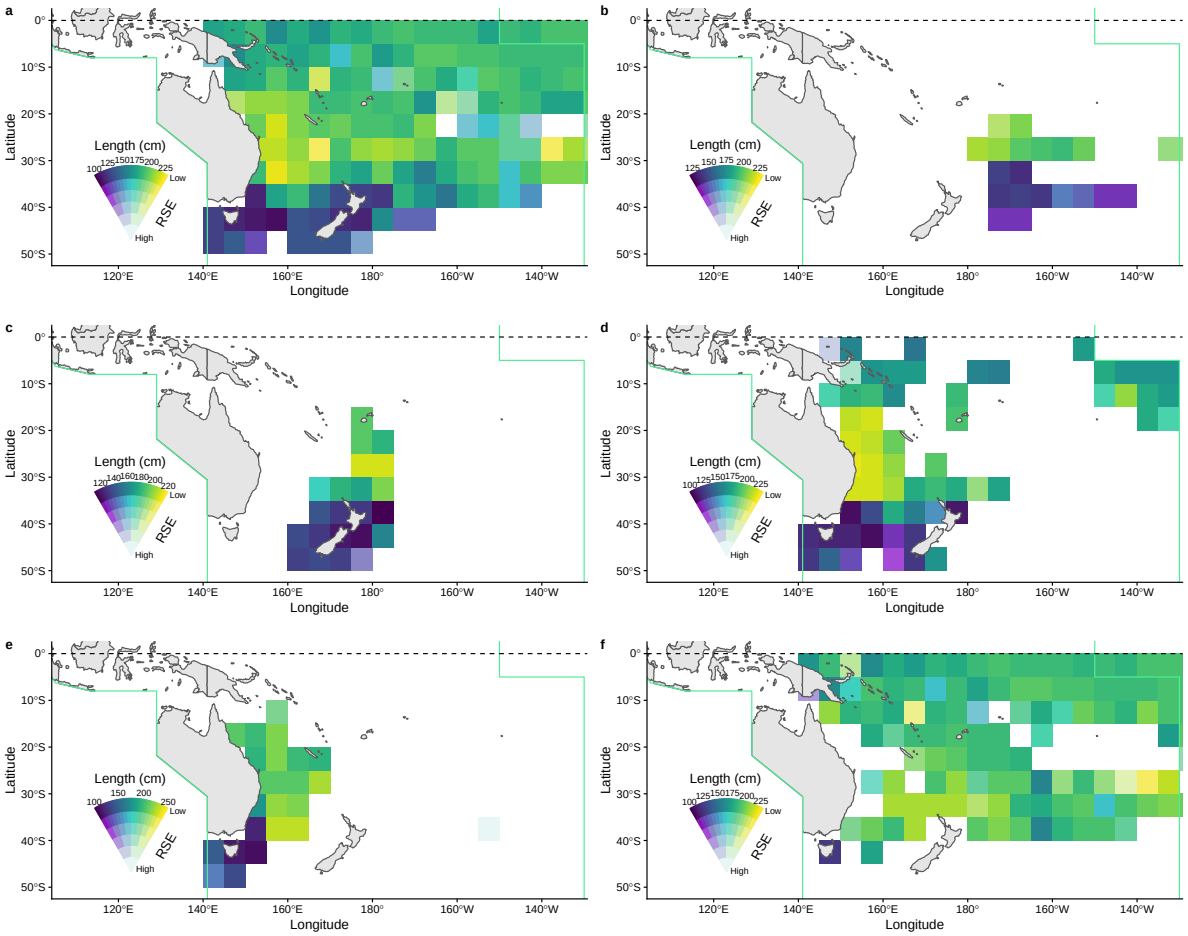


**Figure 1:** Maps of average length shaded by variability in lengths (SE of mean length). Samples are from a) Combined dataset, b) EU-Spain, c) New Zealand d) Japan, e) Australa and f) a group of prominent fishing nations (Chinese Taipei, Korea, Fiji, China, Vanuatu).

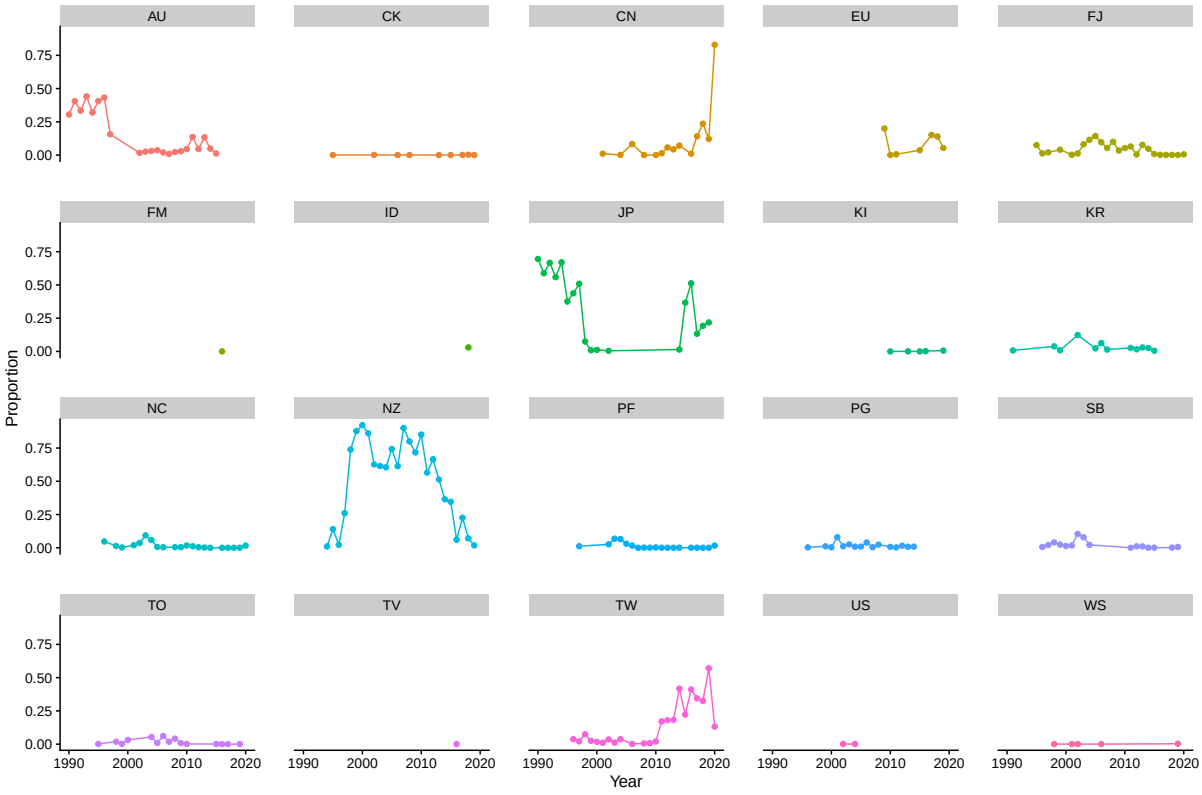


**Figure 2:** Proportion of length frequency samples across all flags over time by each CCM in the observer dataset.

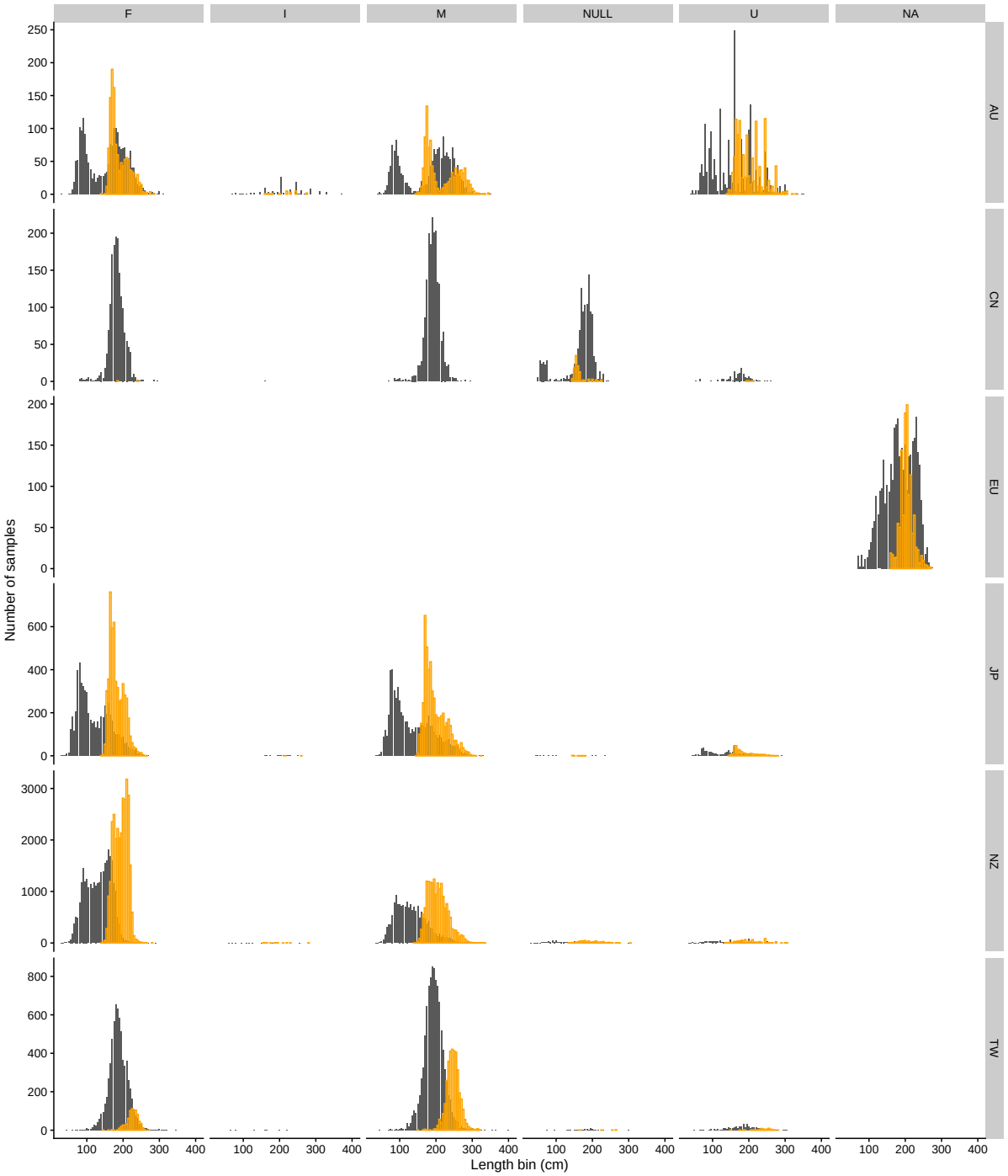


**Figure 3:** Length frequency by flag, for flags with reasonable numbers of samples. Orange histograms show high latitude samples with addition of five years growth according to Manning and Francis (2005).

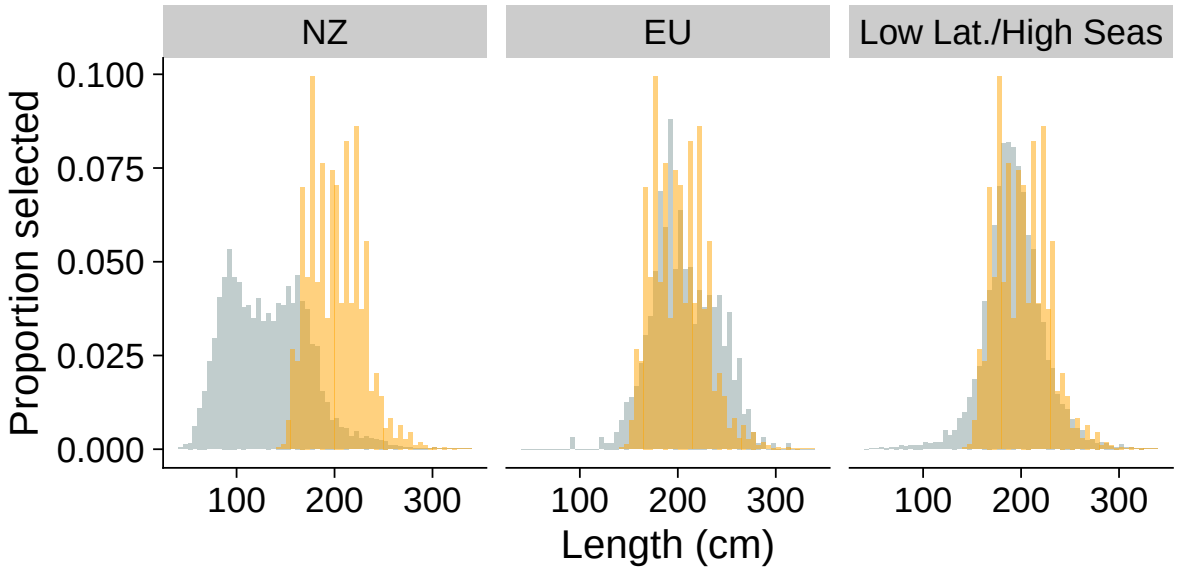


**Figure 4:** Length proportions by fleet definition in the stock assessment. Orange histograms show New Zealand fleet samples (including South Tasman samples from Japan and Australia) with addition of five years growth according to Manning and Francis (2005).

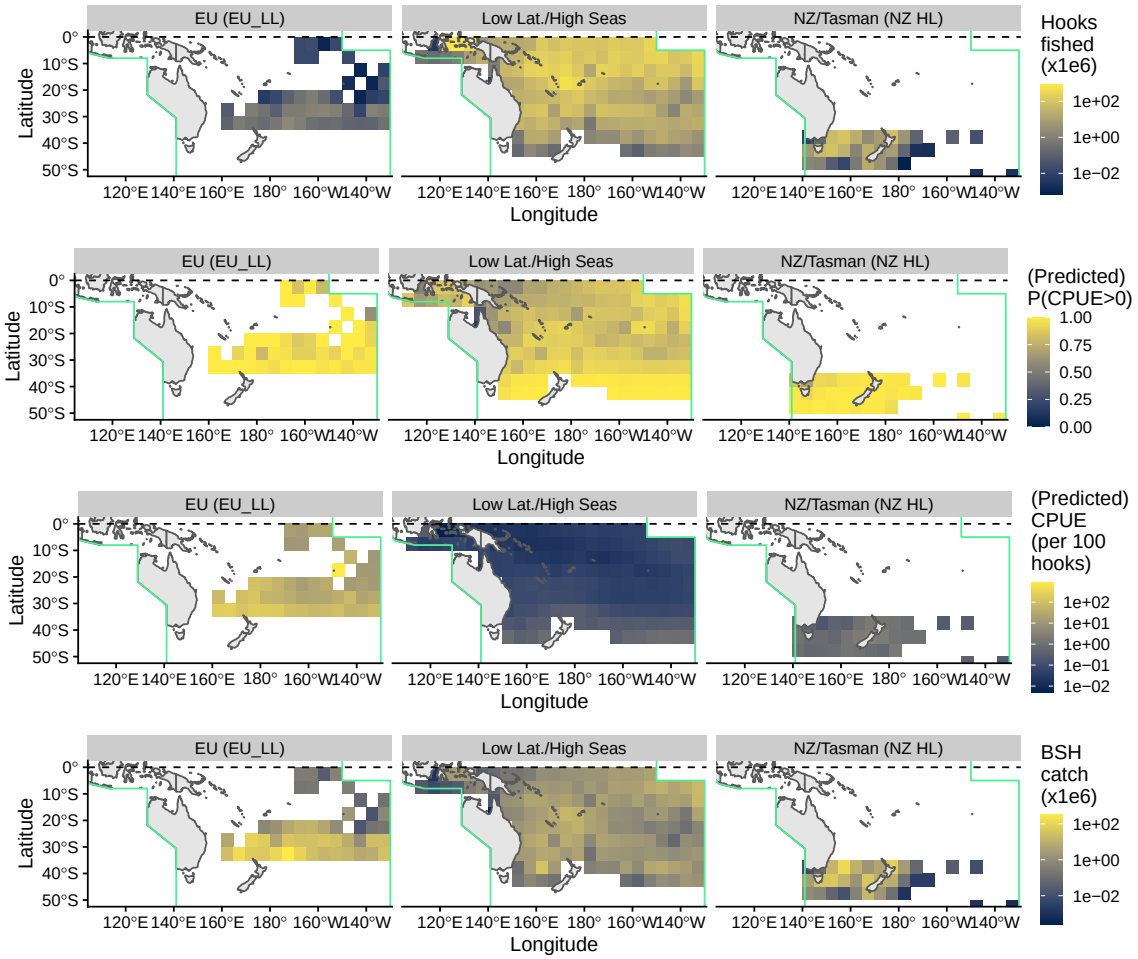


**Figure 5:** Areas as fleets - characteristics of fleets included in the model: Predicted (Low Latitude/High Seas, New Zealand/Tasman) and reported (EU-Spain) fleet characteristics by 5x5 spatial strata: (top row) Total number of hooks fished, (2nd row) Proportion of observed strata (5'x5', fleet, month) with non-zero blue shark catch; (3rd row) mean CPUE across observed strata (5'x5', fleet, month; - note that CPUE is in terms of weight for the EU-Spain fleet, and numbers for Low Latitude/High Seas, New Zealand/Tasman fleets); (bottom row) BSH catch, in numbers of BSH for Low Latitude/High Seas, New Zealand/Tasman fisheries, and kg for the EU-Spain fishery.

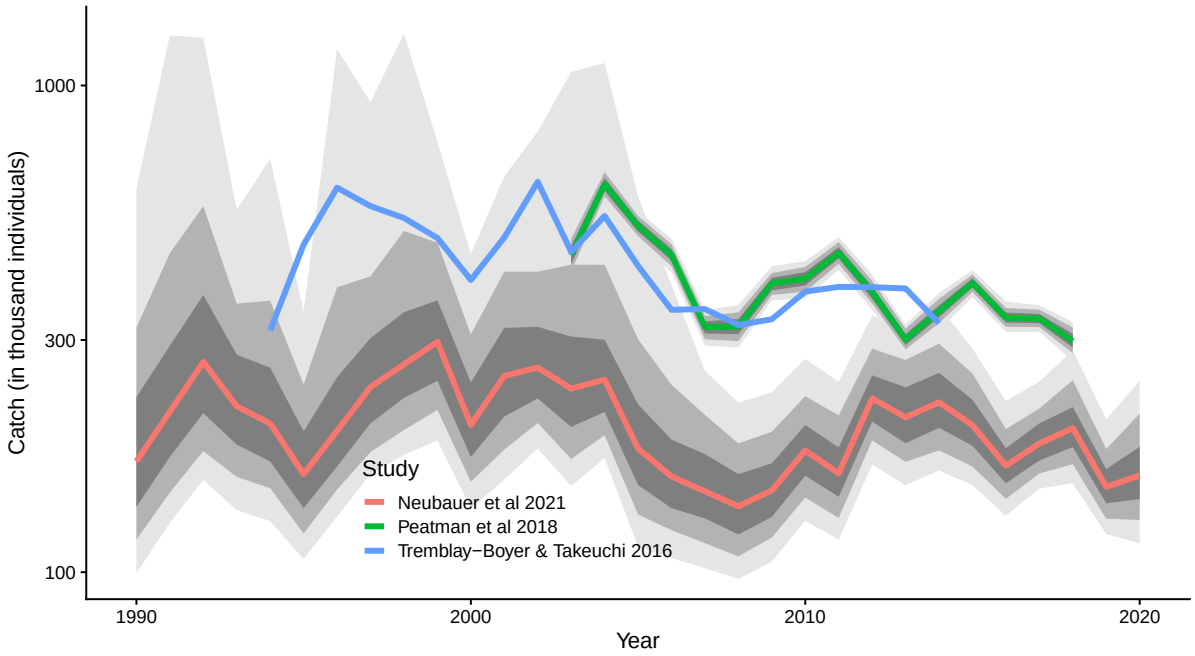


**Figure 6:** Predicted total blue shark captures (posterior median (red); 75% confidence (dark grey) and 80% confidence (light grey)) using the observer catch-rate GLMM in conjunction with L-BEST effort. 2016 values were corrected from initial published values post-SC12 and the re-calculated total captures from the 2016 analysis are shown for comparison.

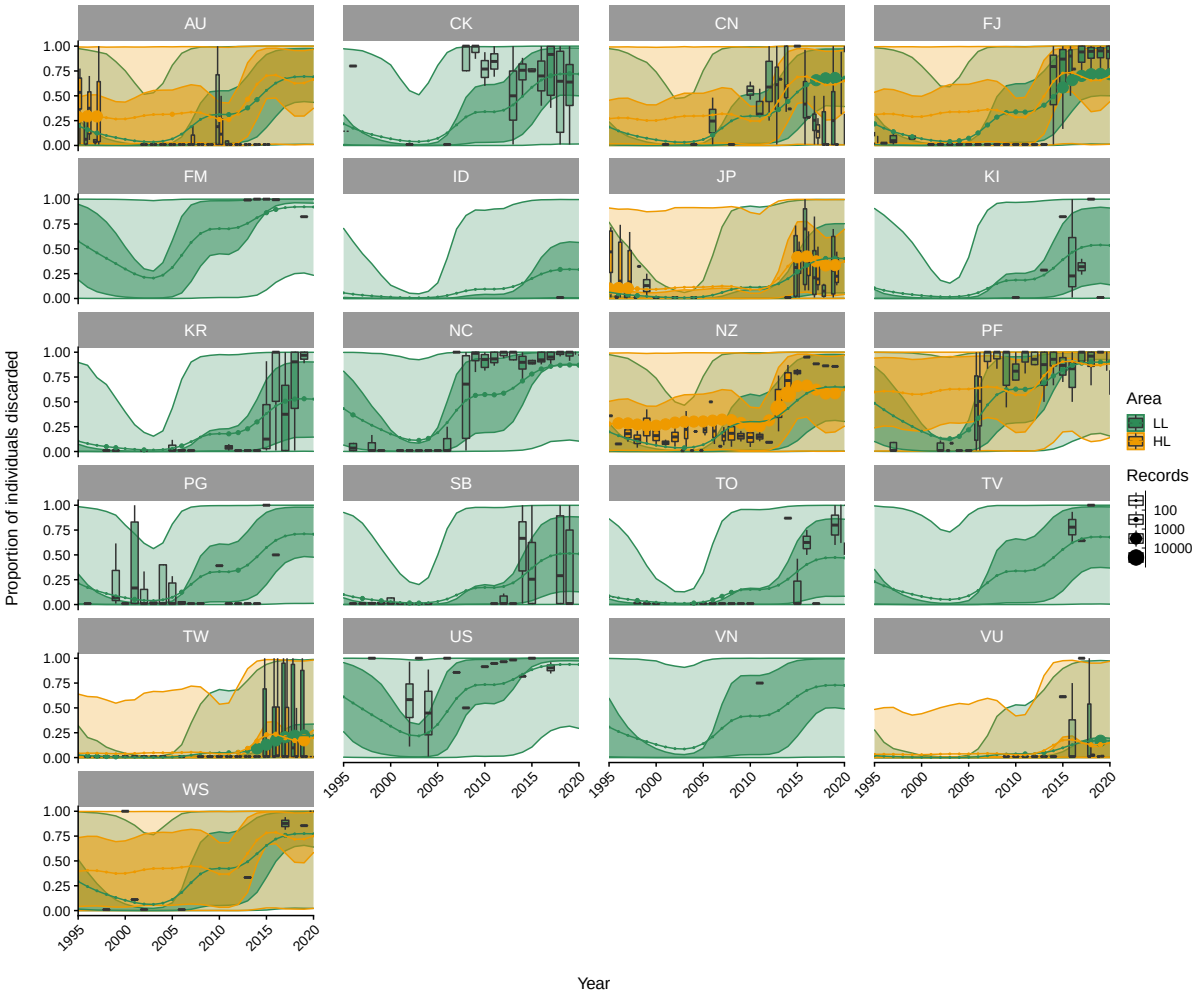


**Figure 7:** Estimated flag-year effects (expected proportion discarded) for flags in the observer dataset, split along low-latitude and high-latitude (>= 35 degree South), showing the posterior median, 75% (dark shade) and 95% (light shade) posterior confidence. The distribution of input data is shown by underlying boxplots.

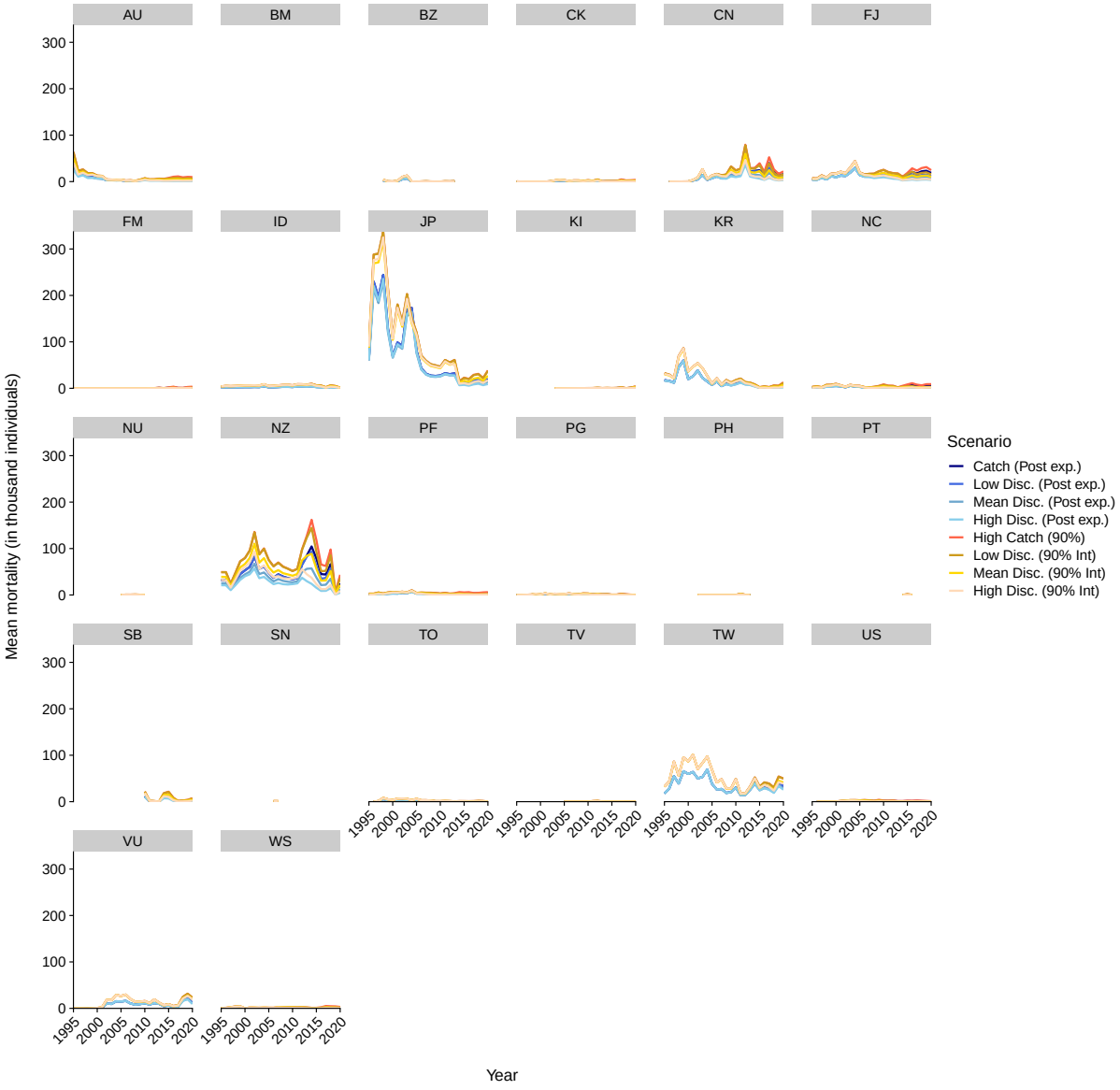


**Figure 8:** Predicted total fishing related mortality by flag, including 17% post release mortality for live-discarded blue sharks. Interactions refer to the posterior median (50%) and $90^{th}$ percentile (90%) of the predicted catch from the observer catch rate model. Low, median and high discard scenarios refer to the 25%, 50% (median) and 75% discard estimates.

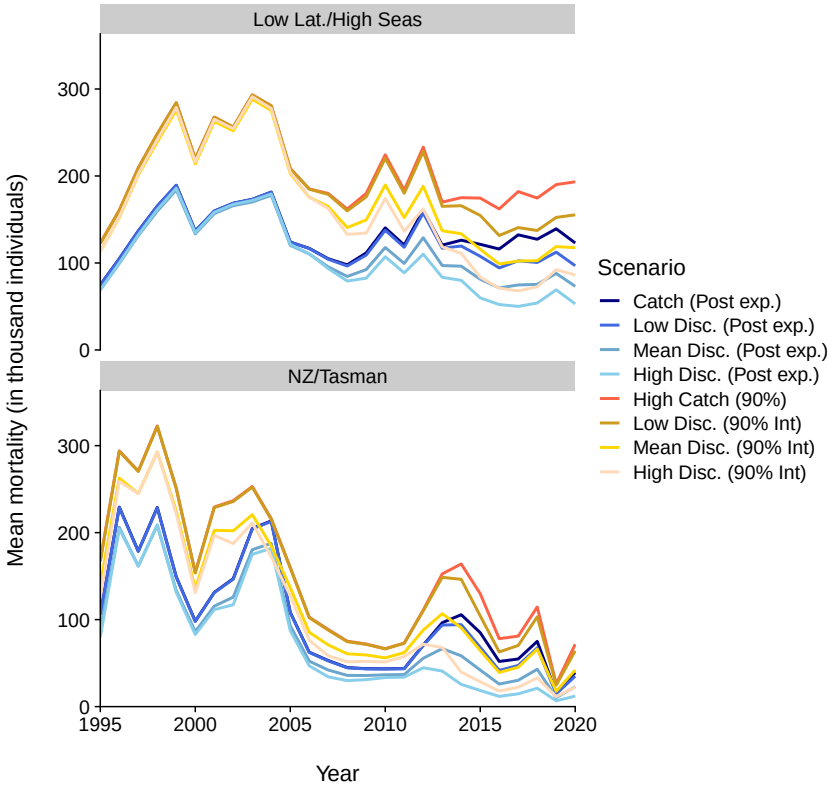


**Figure 9:** Predicted total fishing related mortality by latitudinal stratum (high [>= 35 degree South] and low latitude [< 35 degree South]), including 17% post release mortality for live-discarded blue sharks. Interactions refer to the posterior median (50%) and $90^{th}$ percentile (90%) of the predicted catch from the observer catch rate model. Low, median and high discard scenarios refer to the 25%, 50% (median) and 75% discard estimates. All discard estimates were applied at flag and latitudinal stratum level to overall interactions.

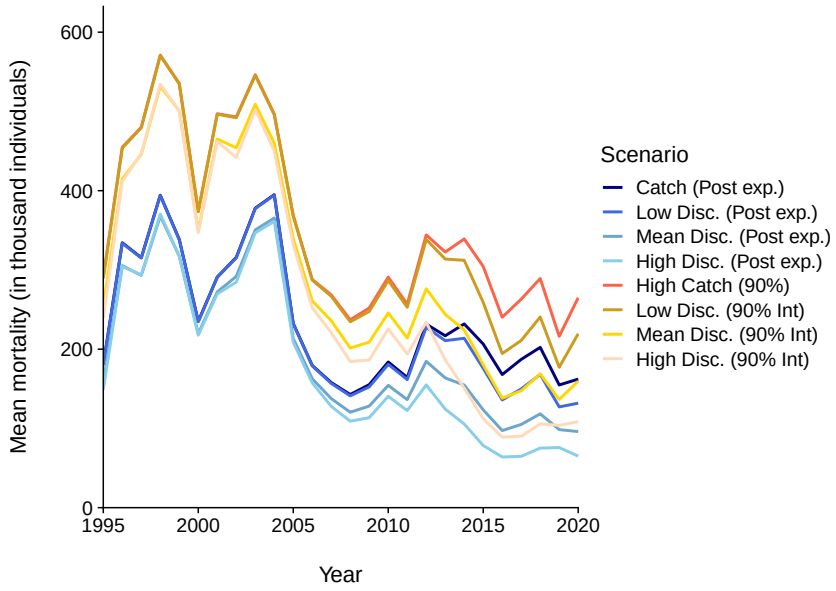


**Figure 10:** Predicted total fishing related mortality, including 17% post release mortality for live-discarded blue sharks. Interactions refer to the posterior median (50%) and $90^{th}$ percentile (90%) of the predicted catch from the observer catch rate model. Low, median and high discard scenarios refer to the 25%, 50% (median) and 75% discard estimates. All discard estimates were applied at flag and latitudinal stratum level to overall interactions.

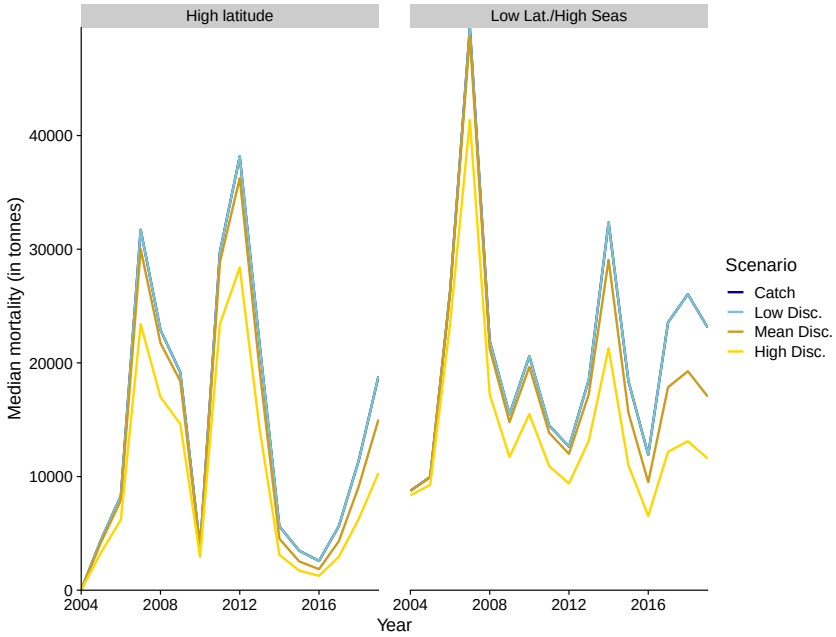


**Figure 11:** Predicted total fishing related mortality for the EU-Spain fleet, including 17% post release mortality for live-discarded blue sharks. Interactions refer to logsheet reported catches. Low, median and high discard scenarios refer to the 25%, 50% (median) and 75% discard estimates.

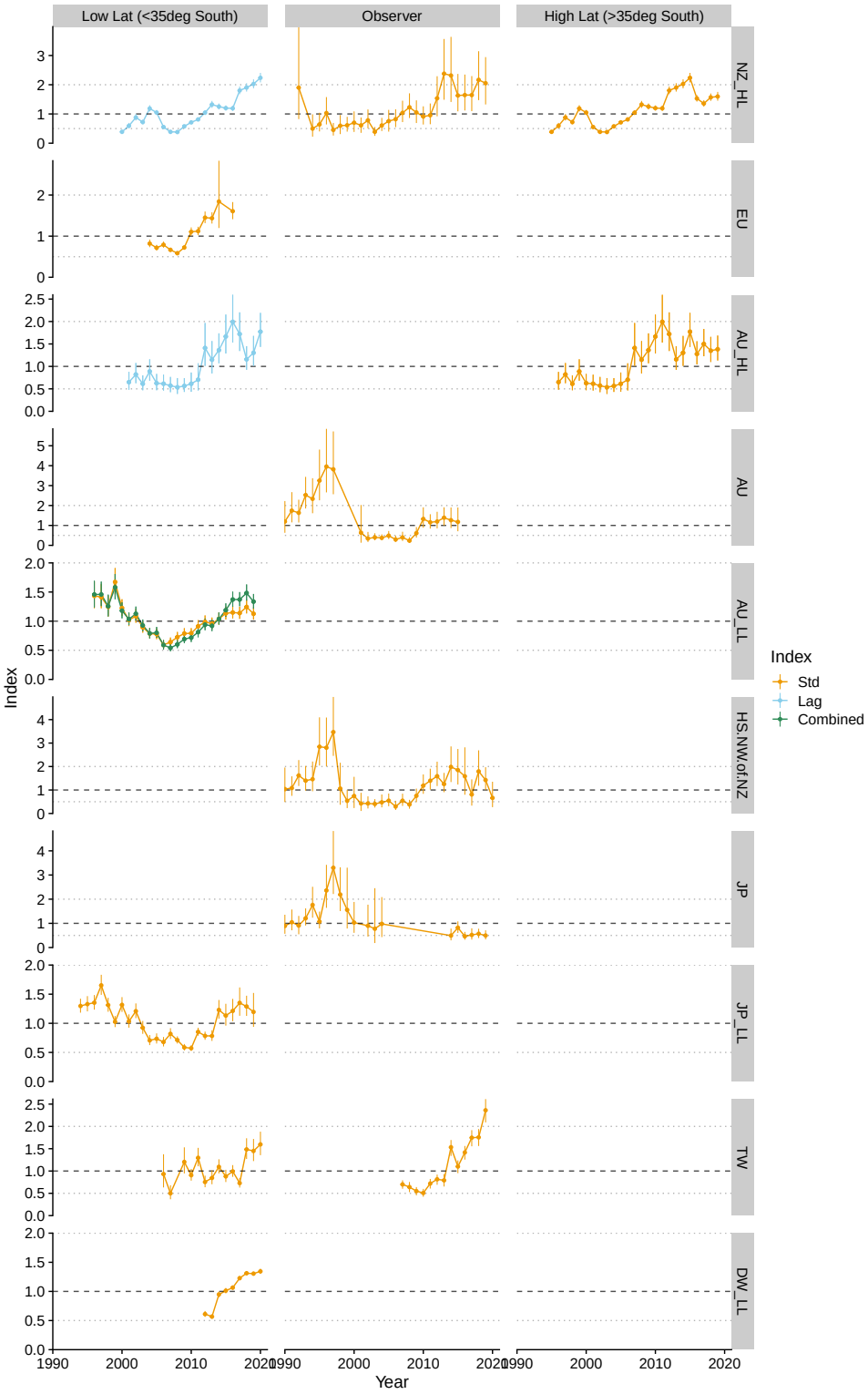


**Figure 12:** Standardised (circles with standard error) CPUE indices for CCMs included in the logsheet CPUE analyses. The Chinese–Taipei observer CPUE is included for comparison. To aid comparison between high- and low- latitude CPUE series, the high-latitude indices were lagged by 5 years and re-plotted (blue CPUE) with the low-latitude indices; 4-5 years is the apparent lag given length frequencies observed in the high latitude fisheries.

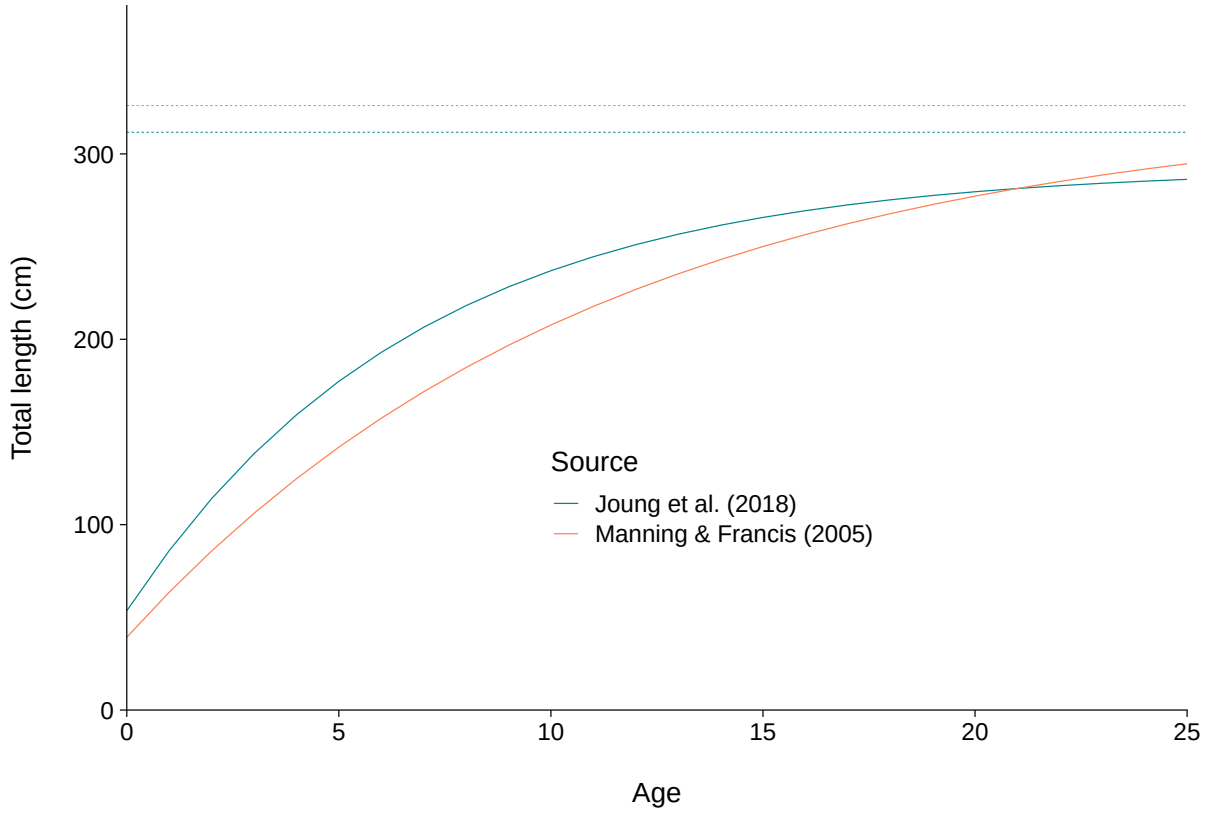


**Figure 13:** Comparison of growth curves for blue shark in the Southwest Pacific Ocean used in the current assessment. Dashed lines show $L_\infty$ for each growth curve.

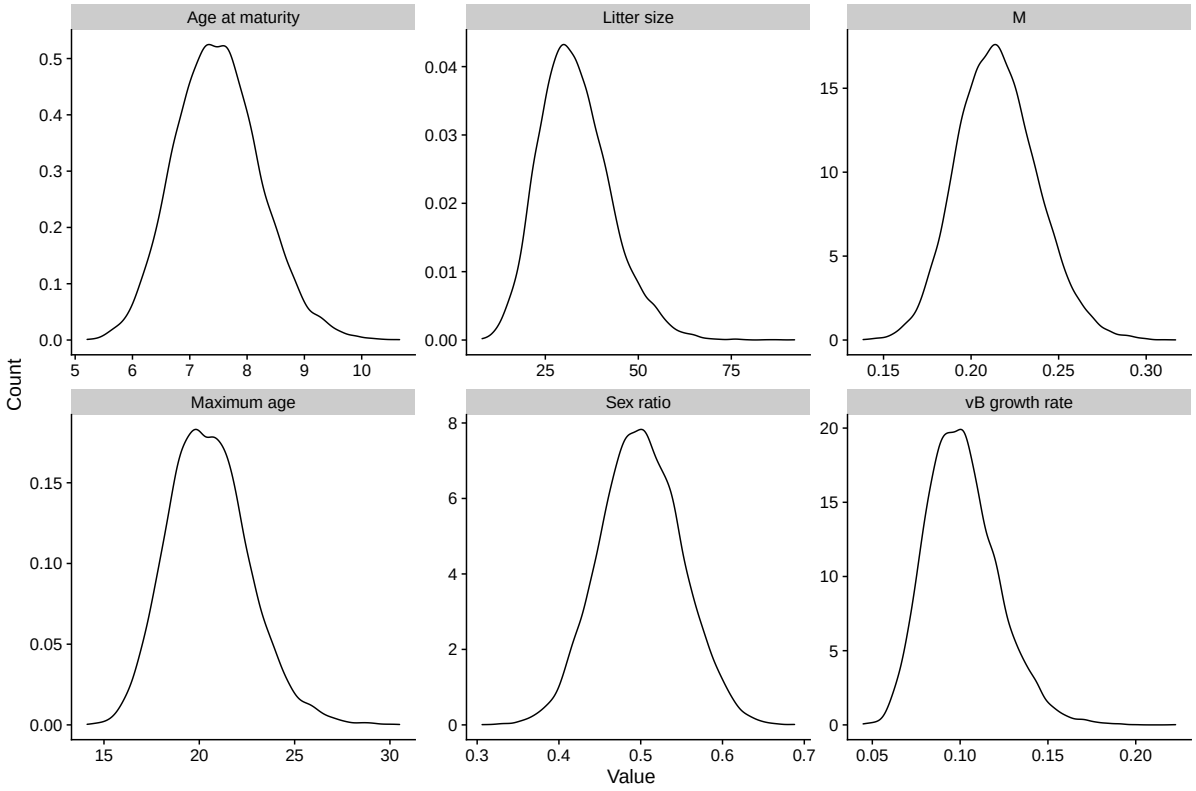


**Figure 14:** Input values for $R_{max}$ simulations for blue shark, based on parameter values reported in the literature (vB, von Bertalanffy).

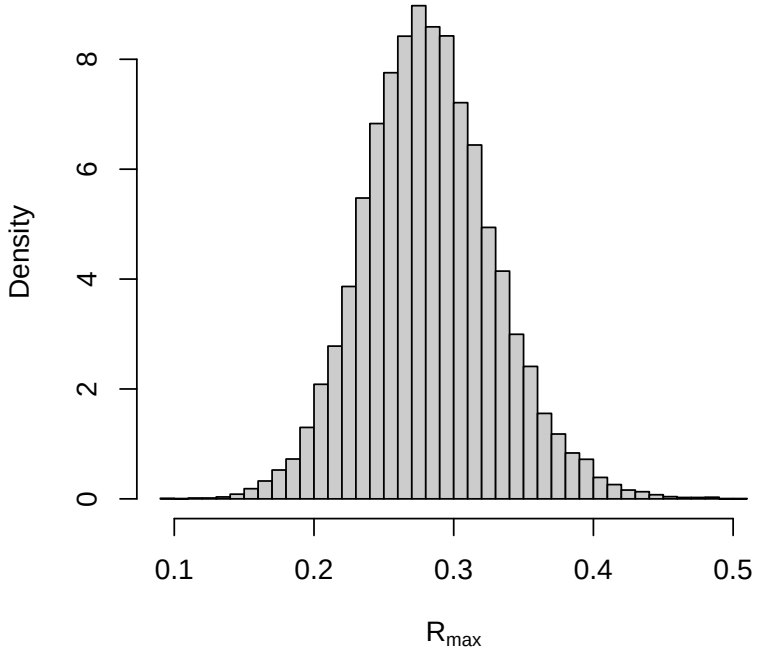


**Figure 15:** Simulated distribution over $R_{max}$ for blue shark using distributions over input parameters shown in Figure 14.

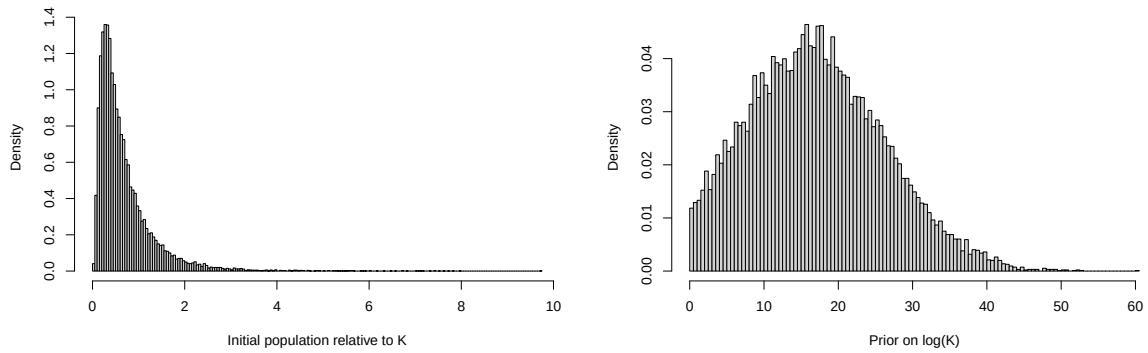


**Figure 16:** Prior distributions for initial depletion and (log) carrying capacity (K) for the dynamic surplus production model.

.

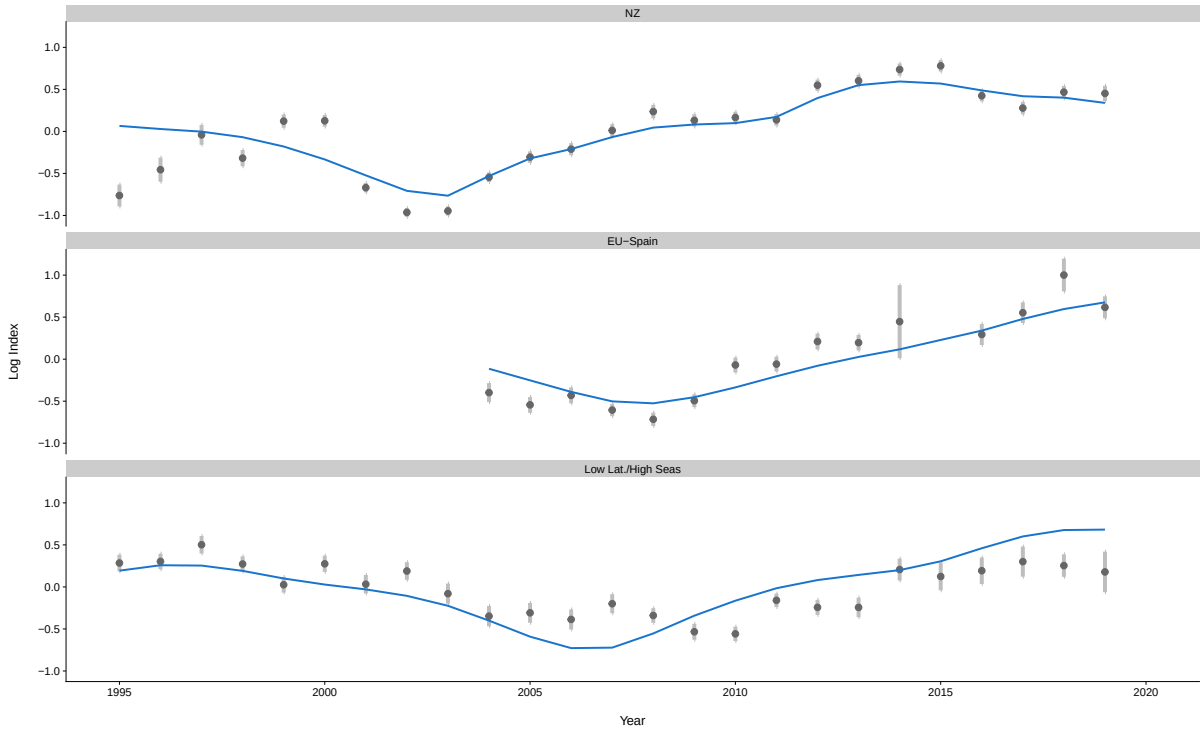


**Figure 17:** Observed (grey dots) vs. predicted (blue line) CPUE on the log-scale for index longline fleets under the diagnostic case, with vertical light grey bands showing the 95% confidence interval for each year index.

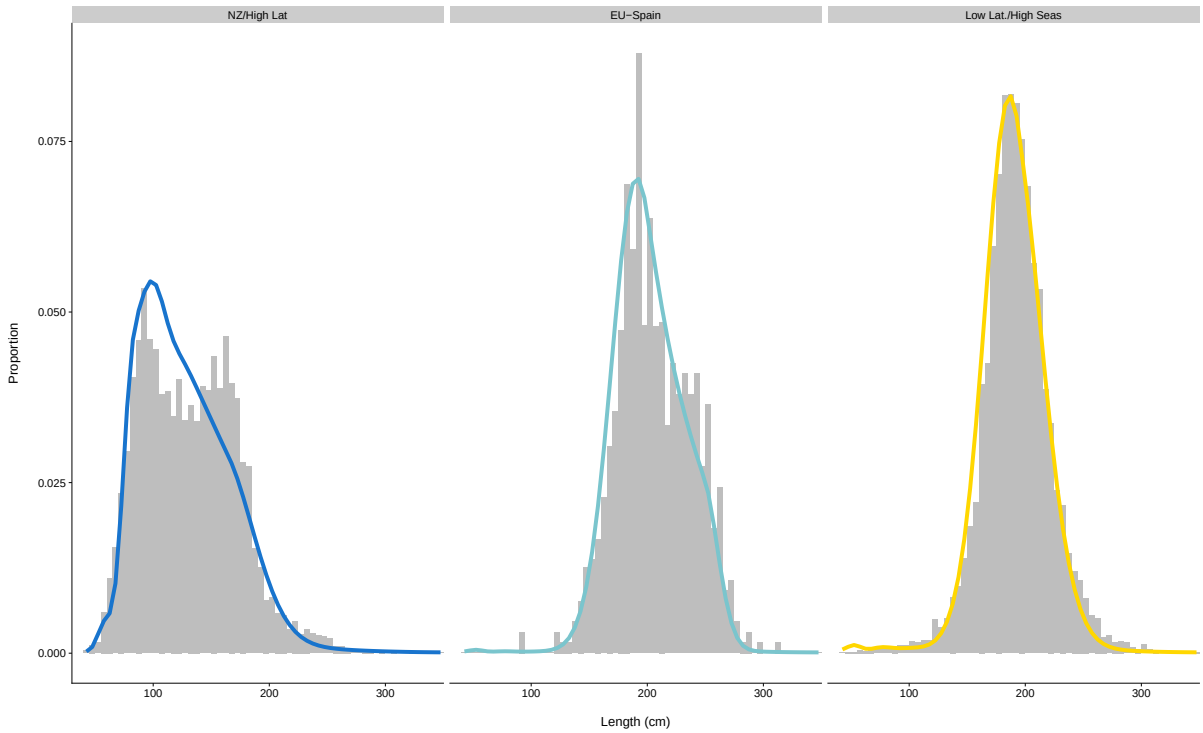


**Figure 18:** Observed (grey bars) vs. predicted (coloured line) catch-at-length for each fleet aggregated over all years for the diagnostic case.

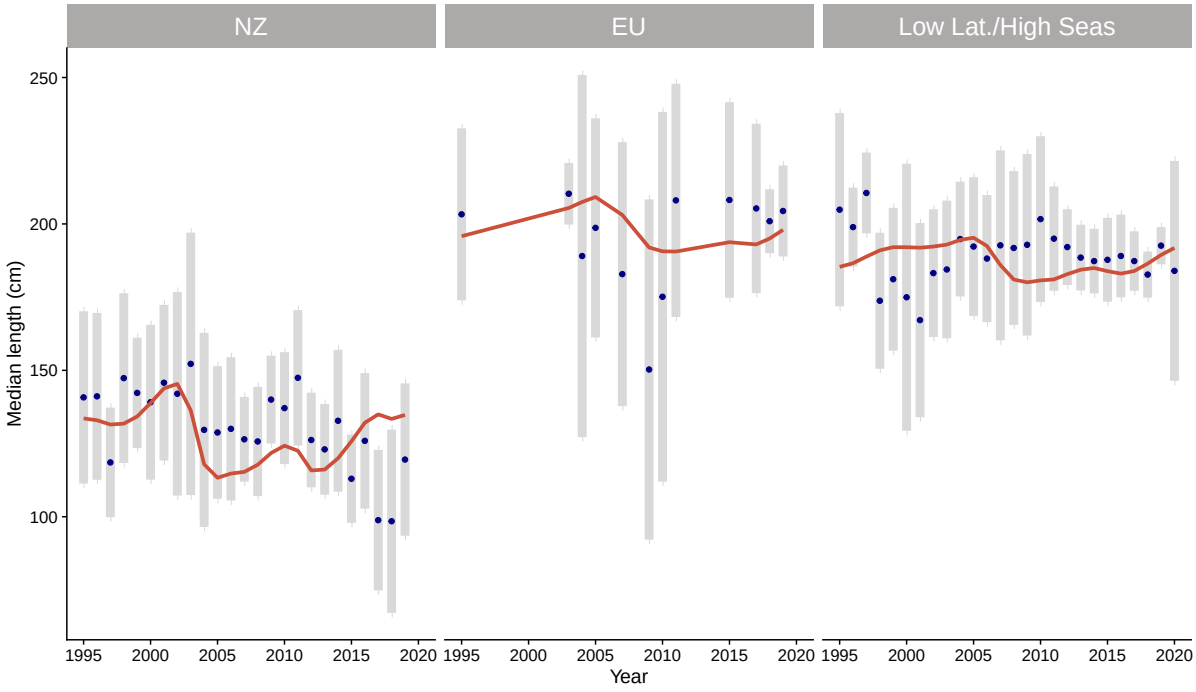


**Figure 19:** Temporal trend in the observed (navy points) vs. predicted (red line) catch-at-length for each fleet for the diagnostic case. The grey bands cover the 95% quantile range for the observations.

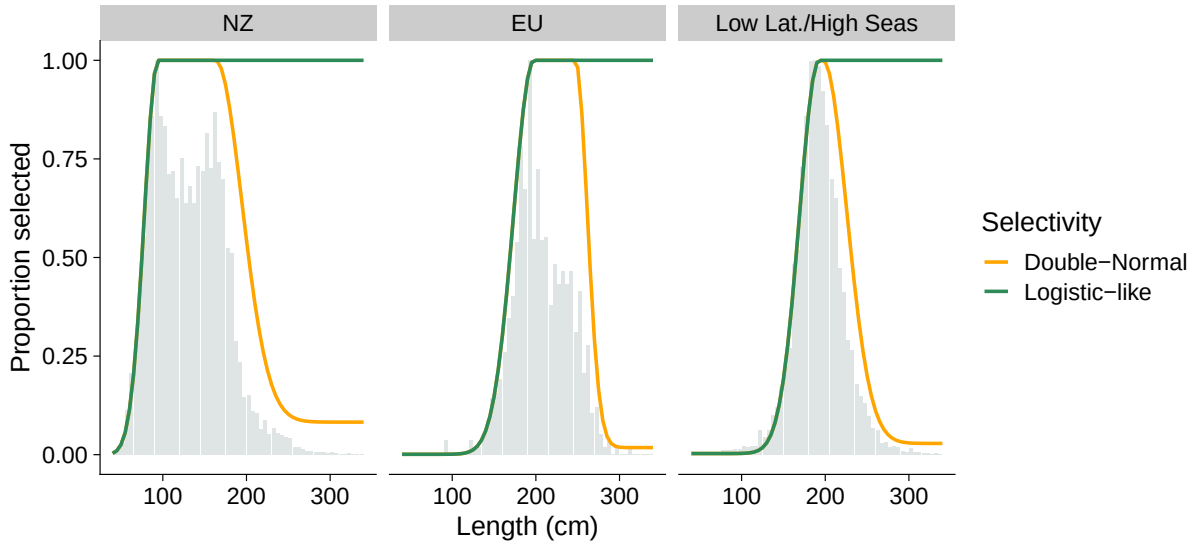


**Figure 20:** Observed (light blue bars) vs. predicted (coloured lines) catch-at-length for each fleet aggregated over all years under two size selectivity scenario.

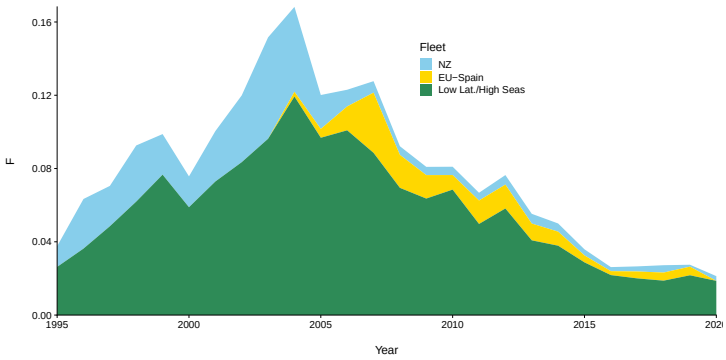


**Figure 21:** Fishing mortality by fleet estimated for the diagnostic case over the time-span of the assessment.

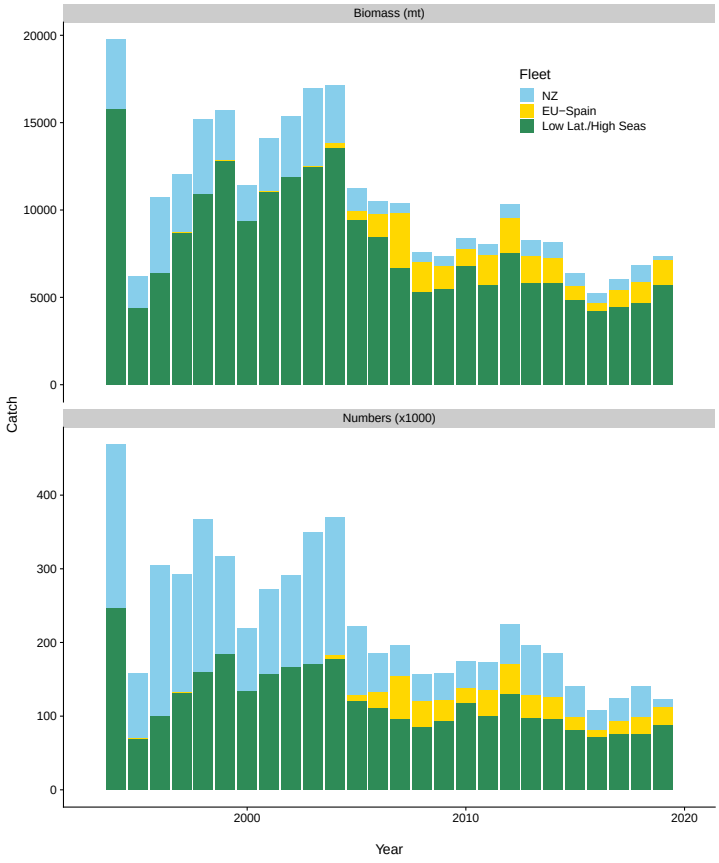


**Figure 22:** Catch by fleet in biomass and numbers.

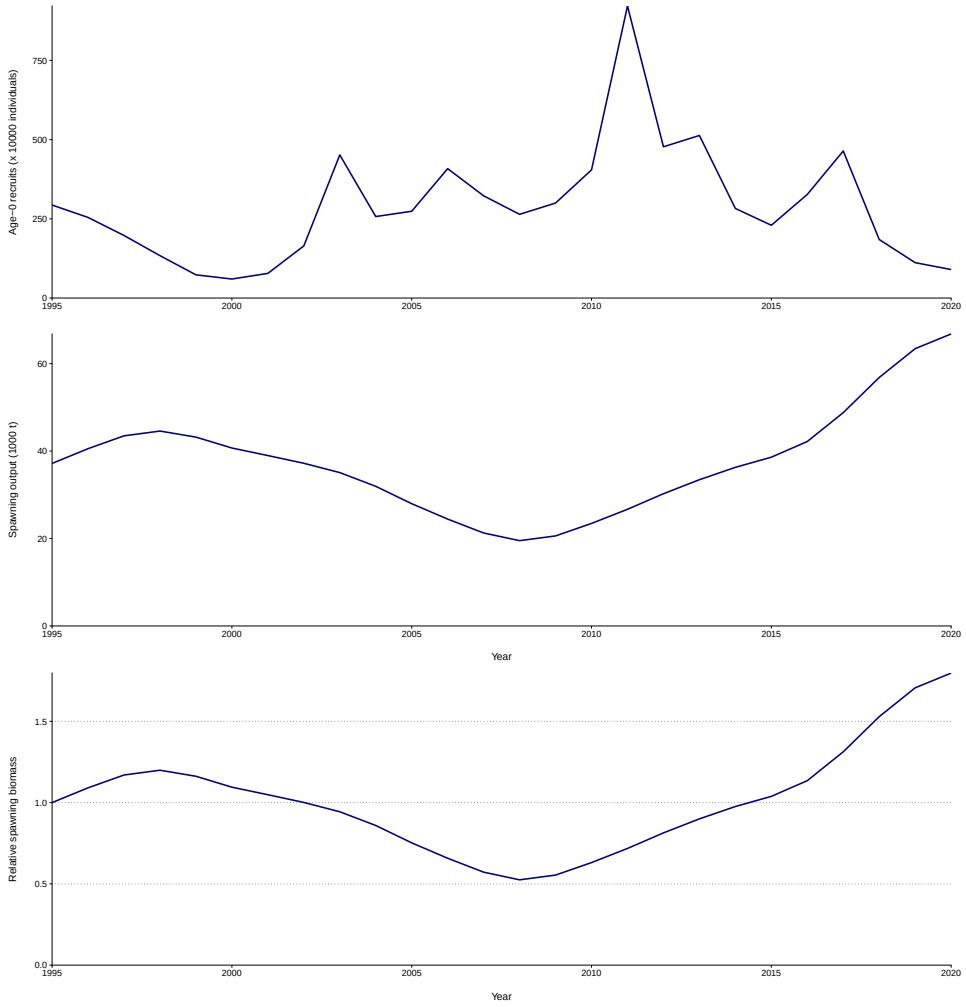


**Figure 23:** Total biomass, recruitment and spawning biomass for the diagnostic case estimated between 1995–2020.

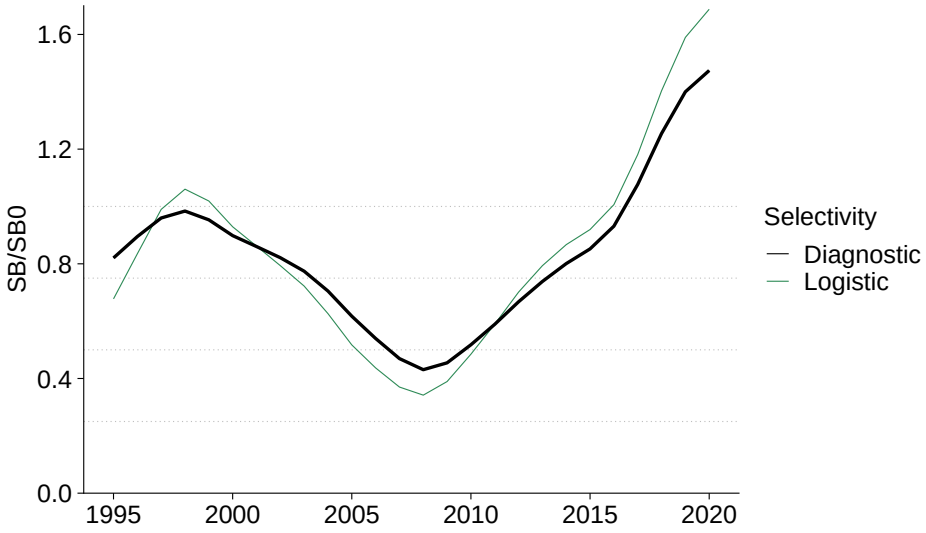


**Figure 24:** Relative spawning biomass for the diagnostic case (double normal) and logistic-like selectivity.

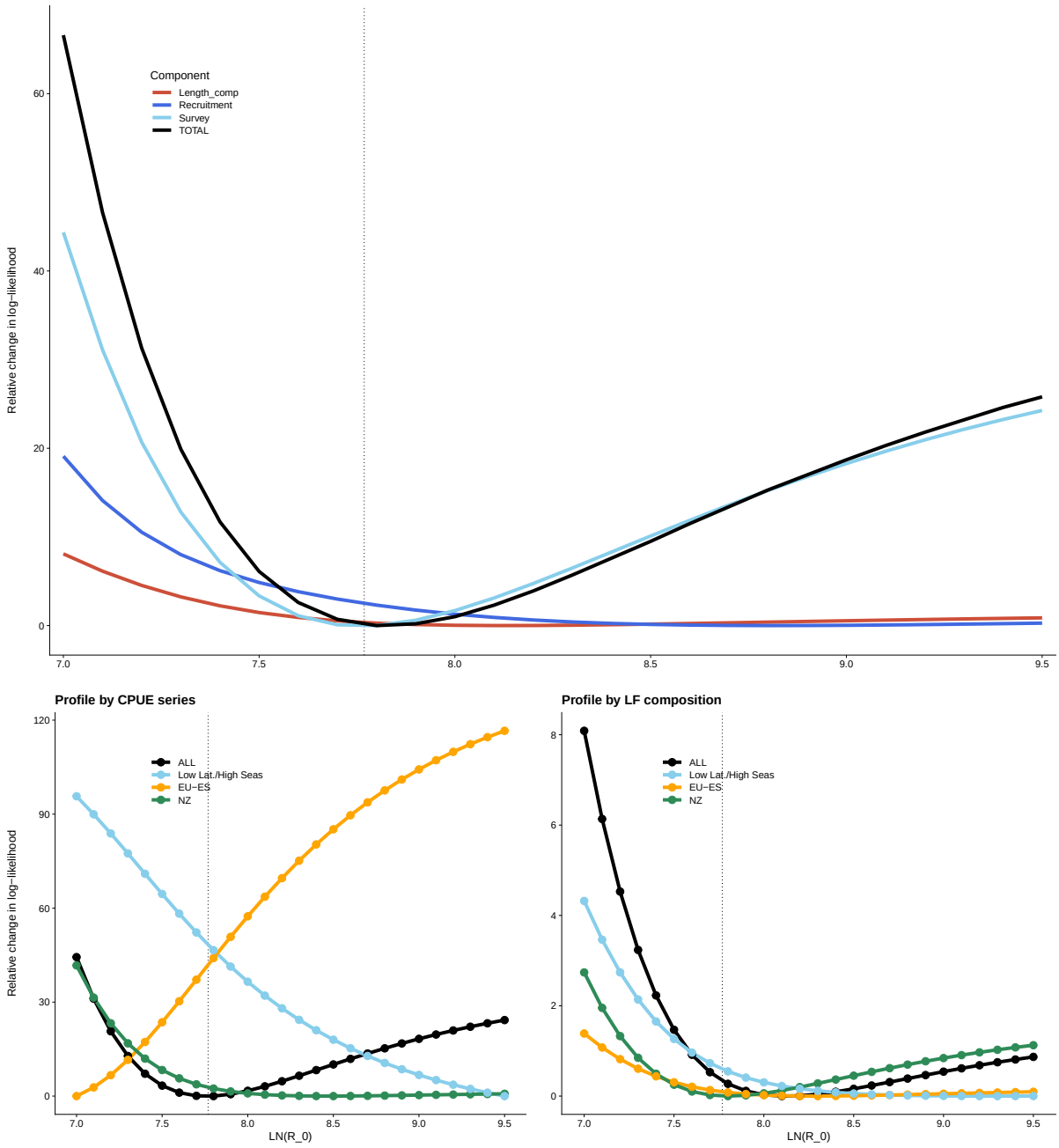


**Figure 25:** Relative change in log-likelihood for different values of $LN(R_0)$. The top panel shows the total likelihood and contribution by each component. The bottom panels show individual components by fleet for the CPUE (left) and catch-at-length data (right). The dotted line shows the value for $LN(R_0)$ estimated under the diagnostic case.

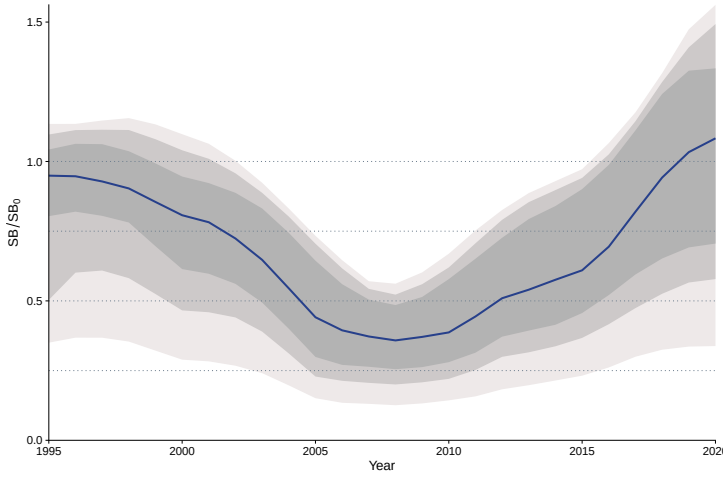


**Figure 26:** Median prediction of depletion in spawning biomass over all (unweighted) grid runs, with $0.025^{th}$-$0.975^{th}$, $0.10^{th}$-$0.90^{th}$ and $0.25^{th}$-$0.75^{th}$ quantile intervals. The horizontal grey lines are placed at intervals of 25% in the lower part of the graph to aid visualization.

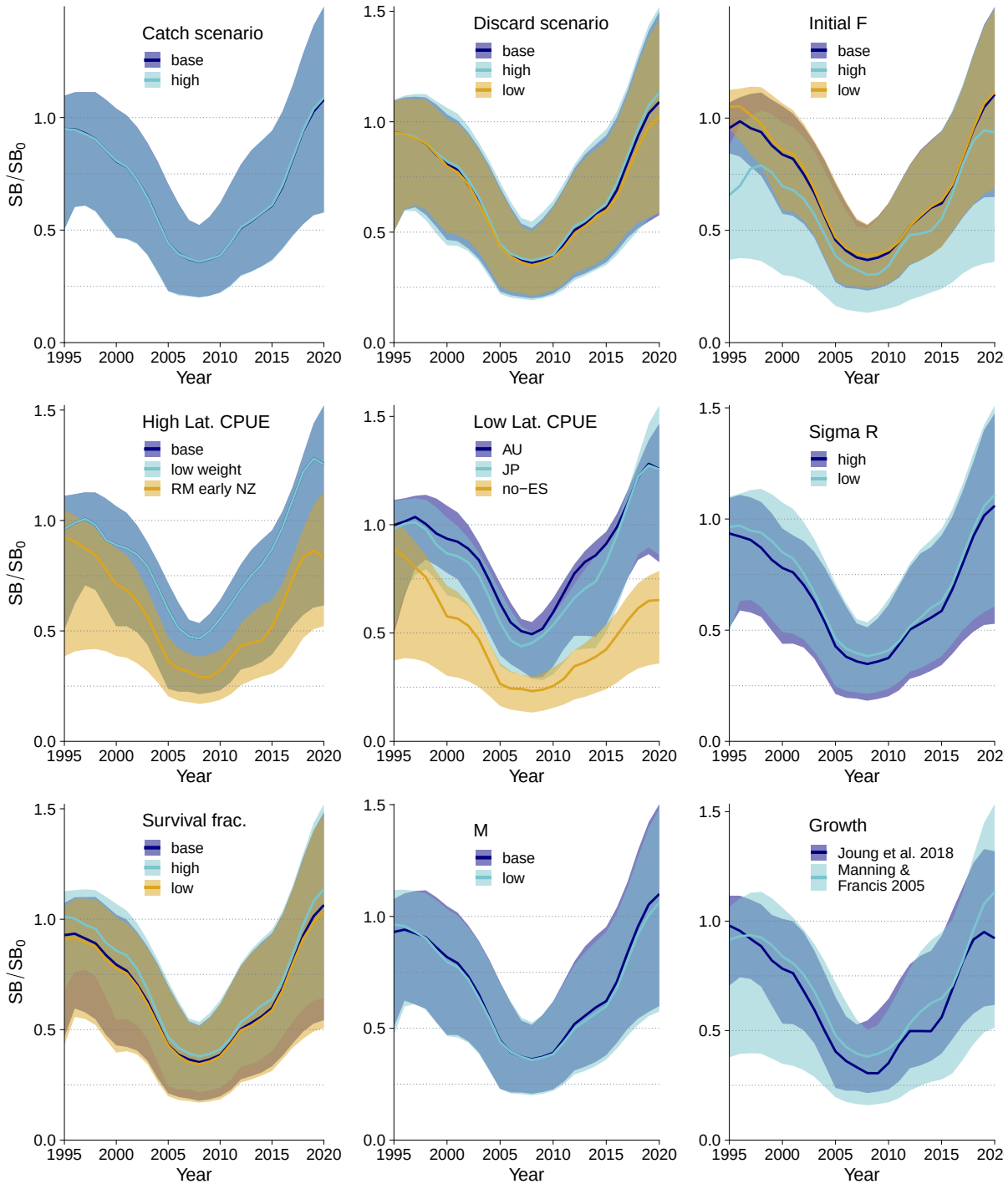


**Figure 27:** Median and inter-quartile bounds for depletion in spawning biomass for each structural uncertainty axis, colour-code by the level used for each axis. The horizontal grey lines are placed at intervals of 25% in the lower part of the graph to aid visualization.

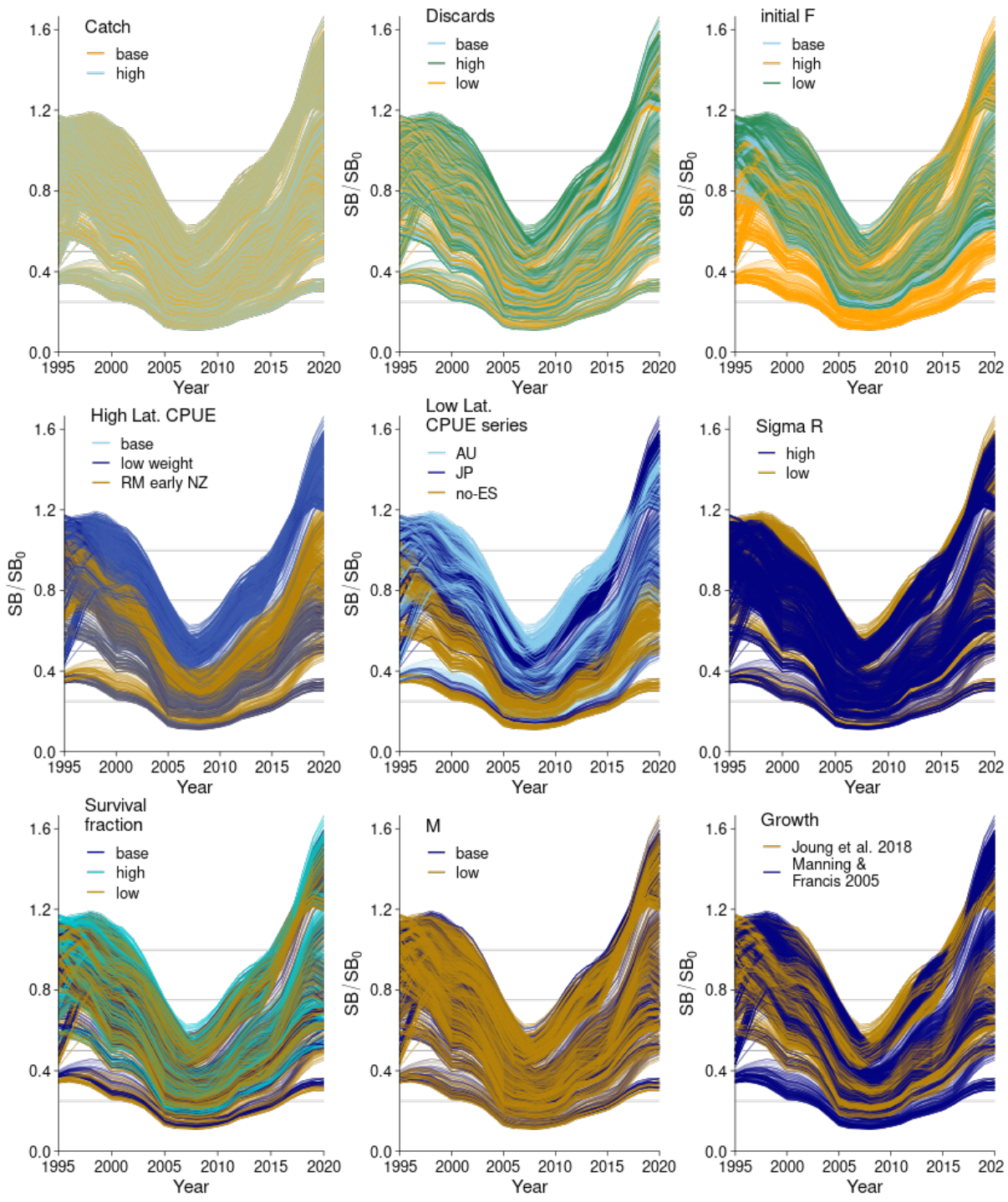


**Figure 28:** Prediction of depletion in spawning biomass for each structural uncertainty grid run, with panel for each grid axis highlighting the different levels within. The horizontal grey lines are placed at intervals of 25% in the lower part of the graph to aid visualization.

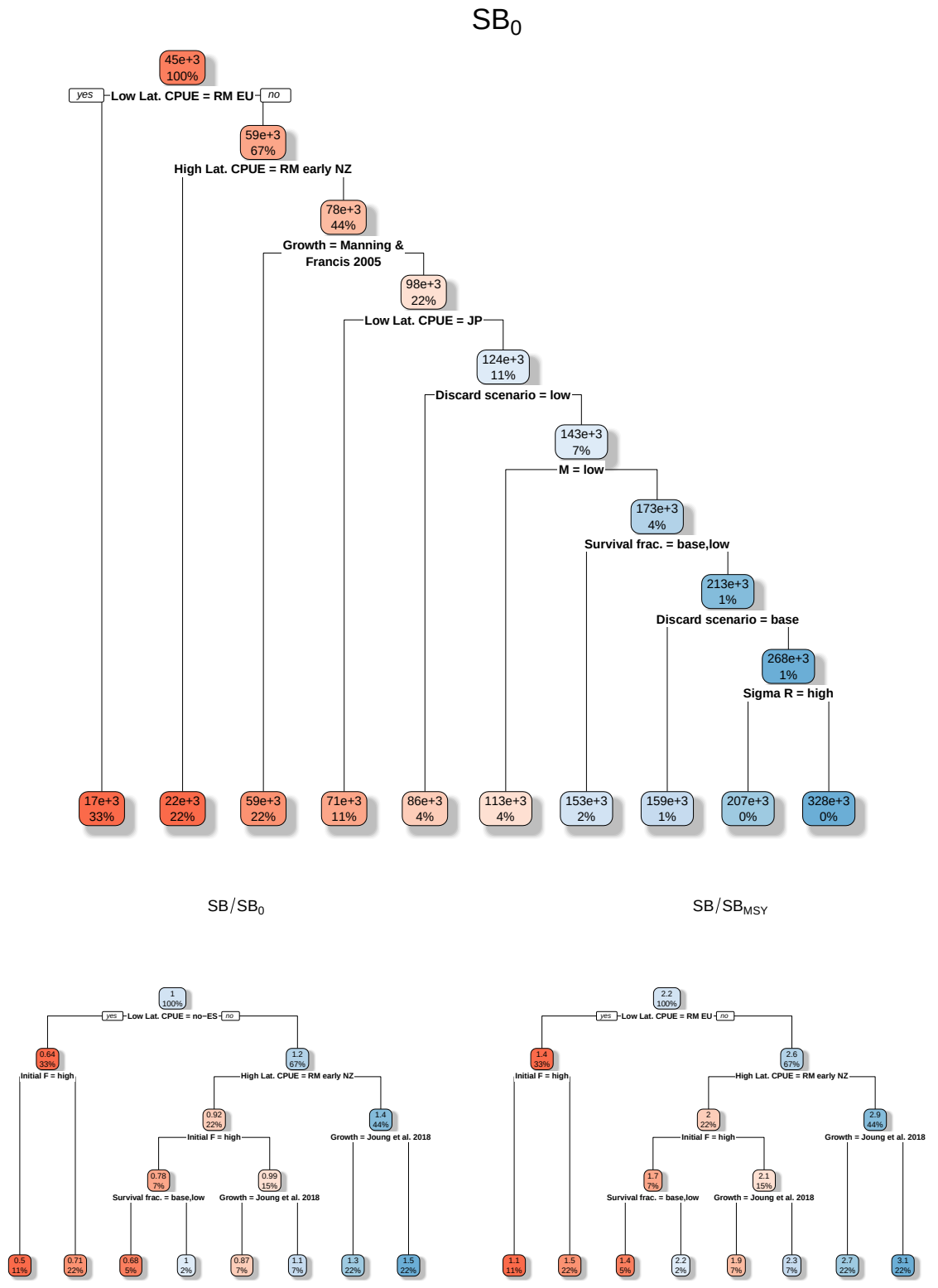


**Figure 29:** Decision trees: positive ('yes') values for each split are on the left, leafs on the decision tree show the mean value ($SB_0$ or $SB_{latest}/SB_0$ or $SB_{latest}/SB_{\text{MSY}}$) by leaf, as well as the percentage of records on that leaf. (RM=remove).

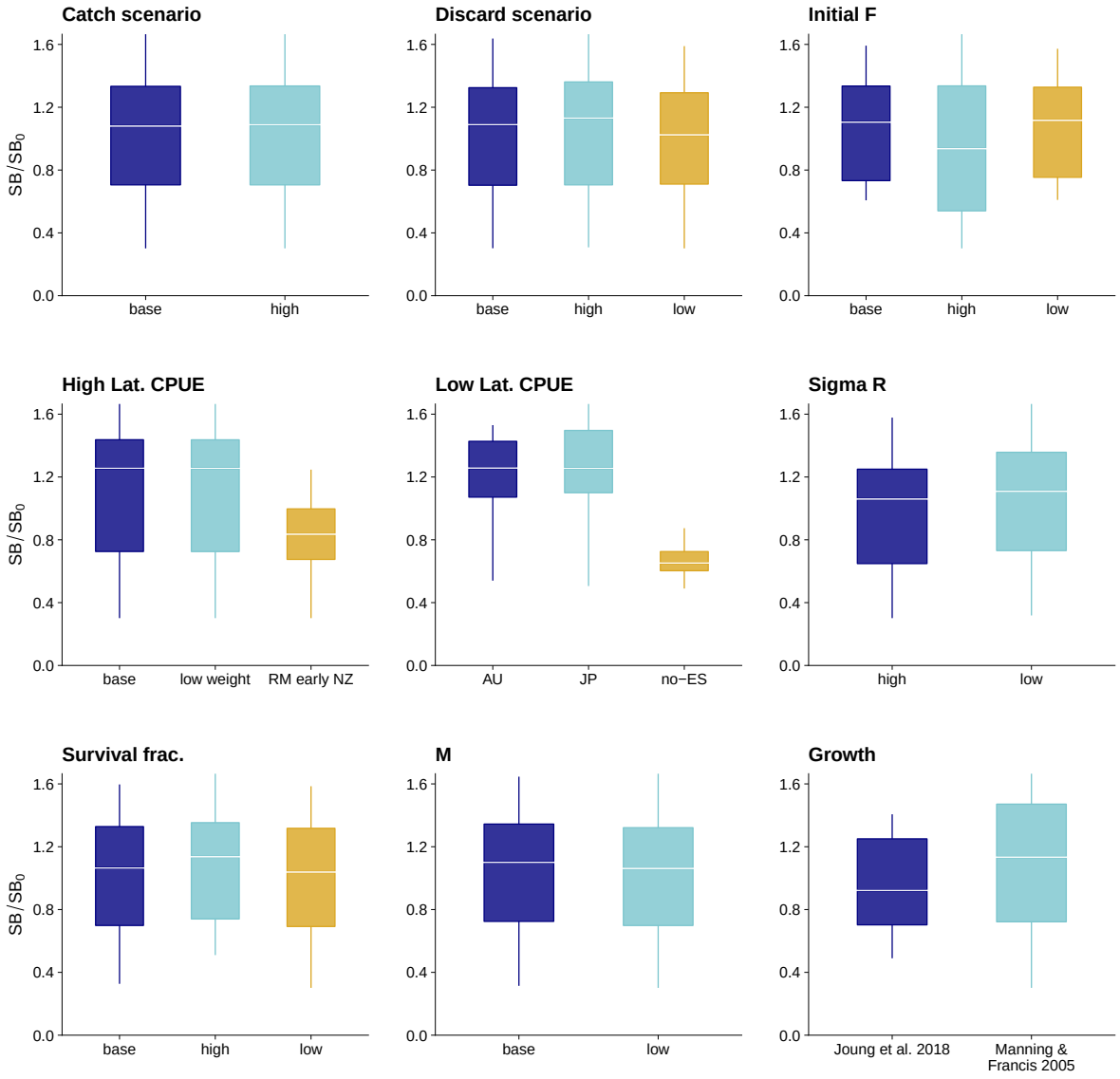


**Figure 30:** Median (white bar) and inter-quartile bounds (box) for $SB_{latest}/SB_0$ in the final year of the assessment for each structural uncertainty axis. The whiskers extend to 1.5× the interquartile range.

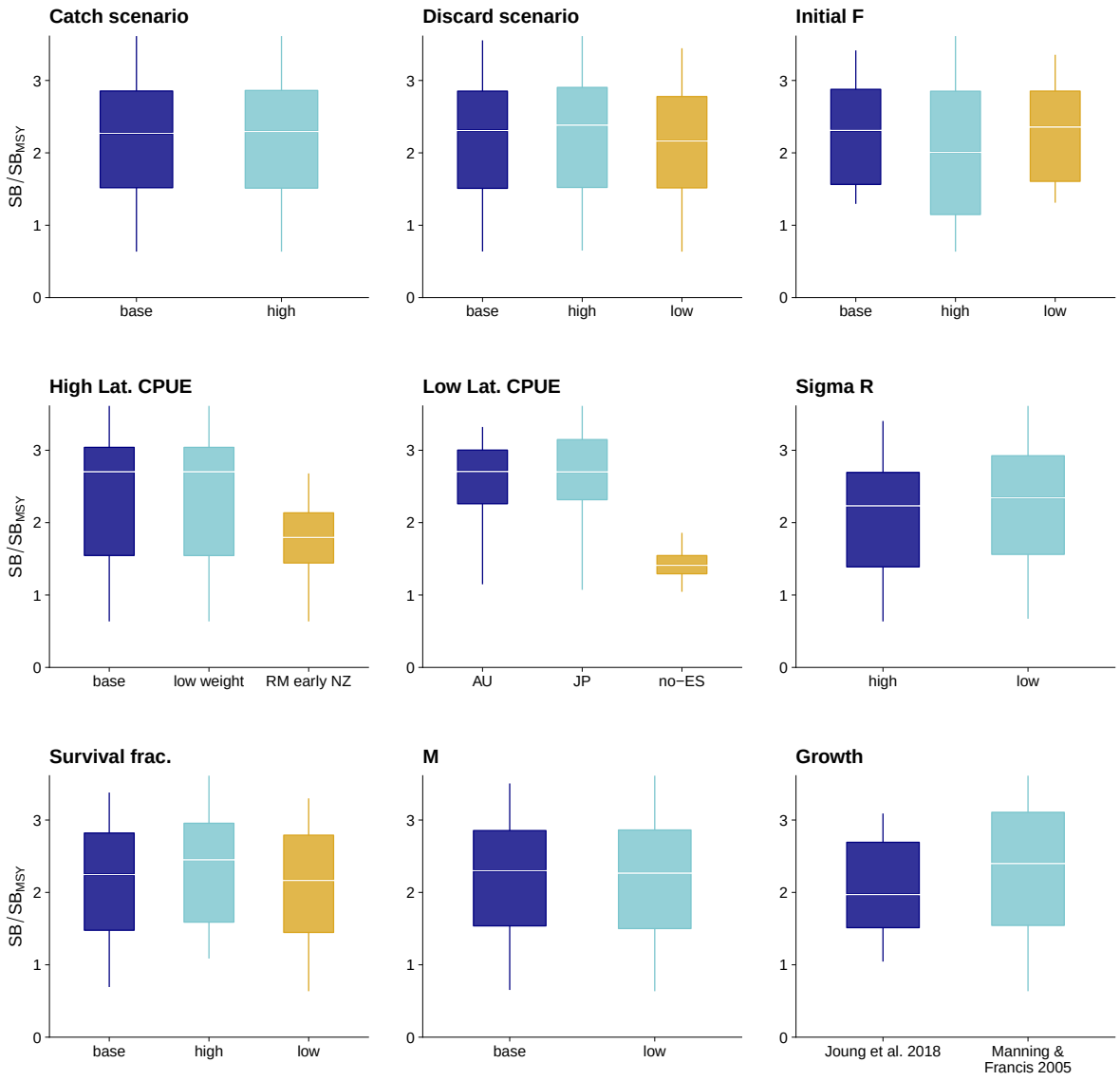


**Figure 31:** Median (white bar) and inter-quartile bounds (box) for $SB_{latest}/SB_{\text{MSY}}$ in the final year of the assessment for each structural uncertainty axis. The whiskers extend to 1.5× the interquartile range.

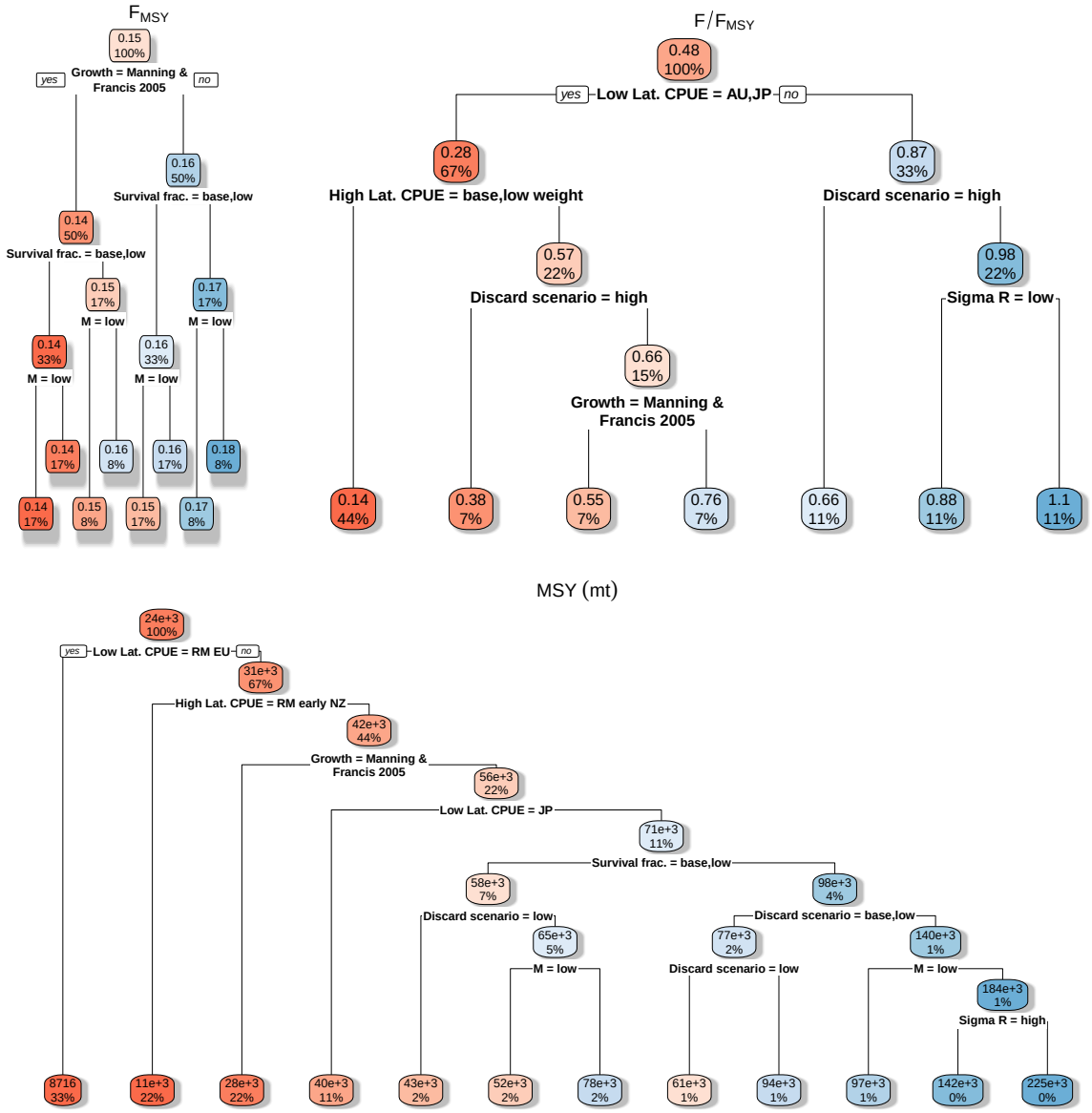


**Figure 32:** Decision trees: positive ('yes') values for each split are on the left, leafs on the decision tree show the mean value ($MSY$, $F_{\text{MSY}}$ and $F_{latest}/F_{\text{MSY}}$) by leaf, as well as the percentage of records on that leaf. Note that for $F_{latest}/F_{\text{MSY}}$ and $MSY$, 'yes' for Australia or Japan low latitude CPUE also includes EU - Spain; similarly, a 'base' or 'low weight' scenario for high latitude CPUE (New Zealand / EU - Spain) also includes early CPUE from New Zealand (RM=remove).

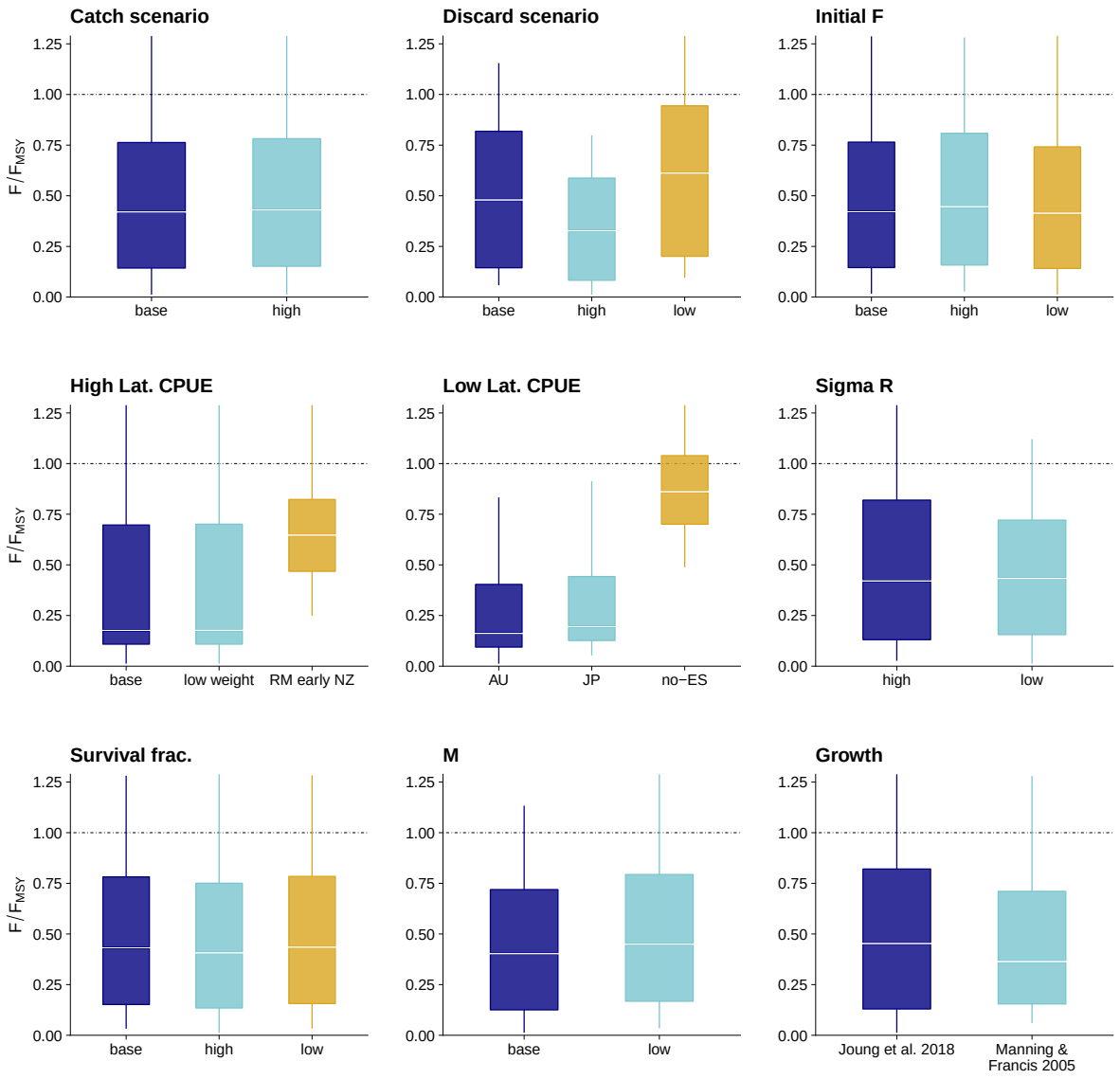


**Figure 33:** Median (white bar) and inter-quartile bounds (box) for $F_{latest}/F_{\text{MSY}}$ in the final year of the assessment for each structural uncertainty axis. The whiskers extend to 1.5× the interquartile range. The dashed line shows the level where $F = F_{\text{MSY}}$.

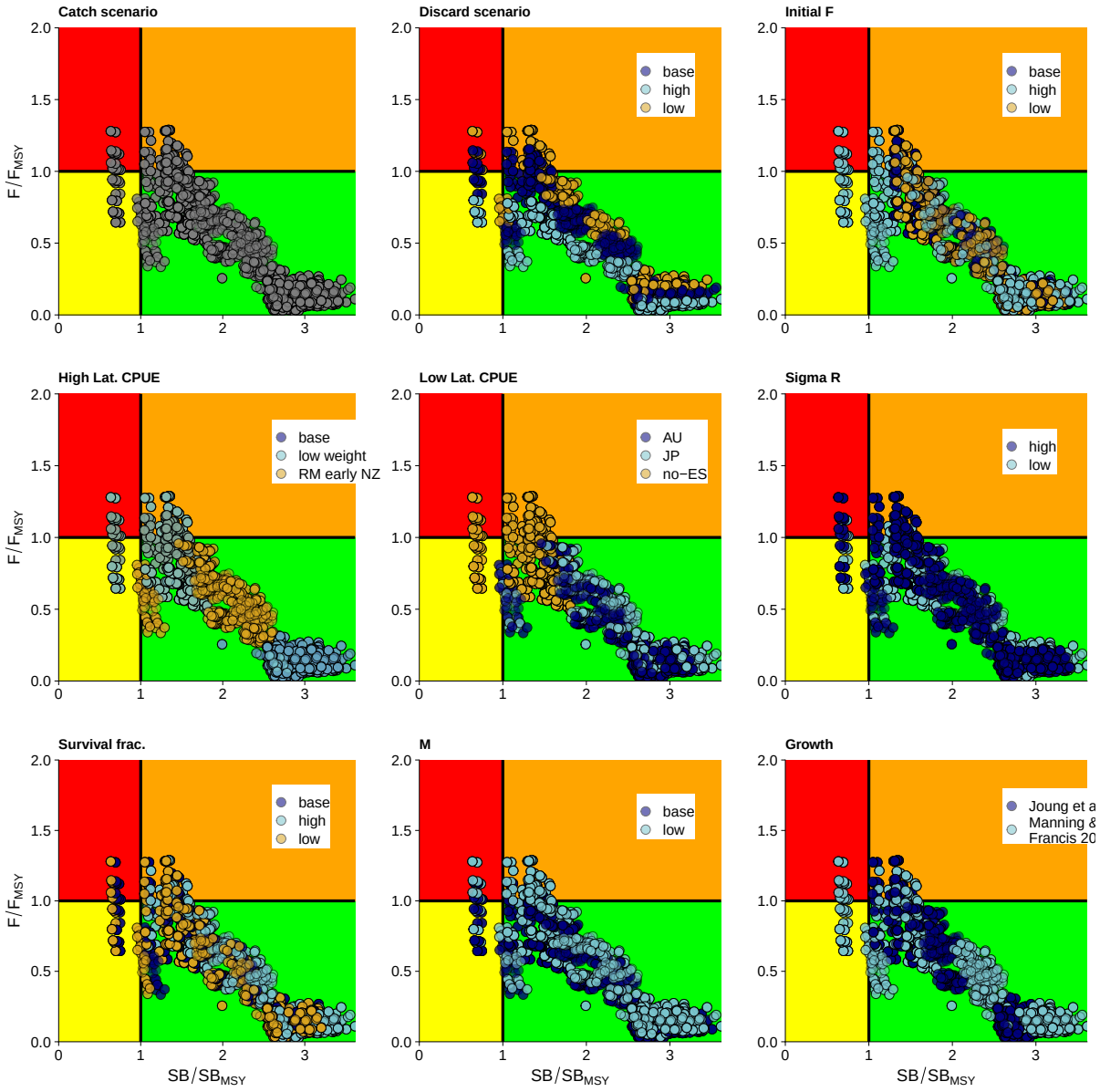


**Figure 34:** Kobe plots summarising status in the final year for each of the models in the structural uncertainty grid, based on $SB_{latest}/SB_{\text{MSY}}$ and $F_{latest}/F_{\text{MSY}}$. The stock is considered to be overfished when $SB_{latest}/SB_{\text{MSY}} < 1$ and undergoing overfishing when $F_{latest}/F_{\text{MSY}} > 1$.

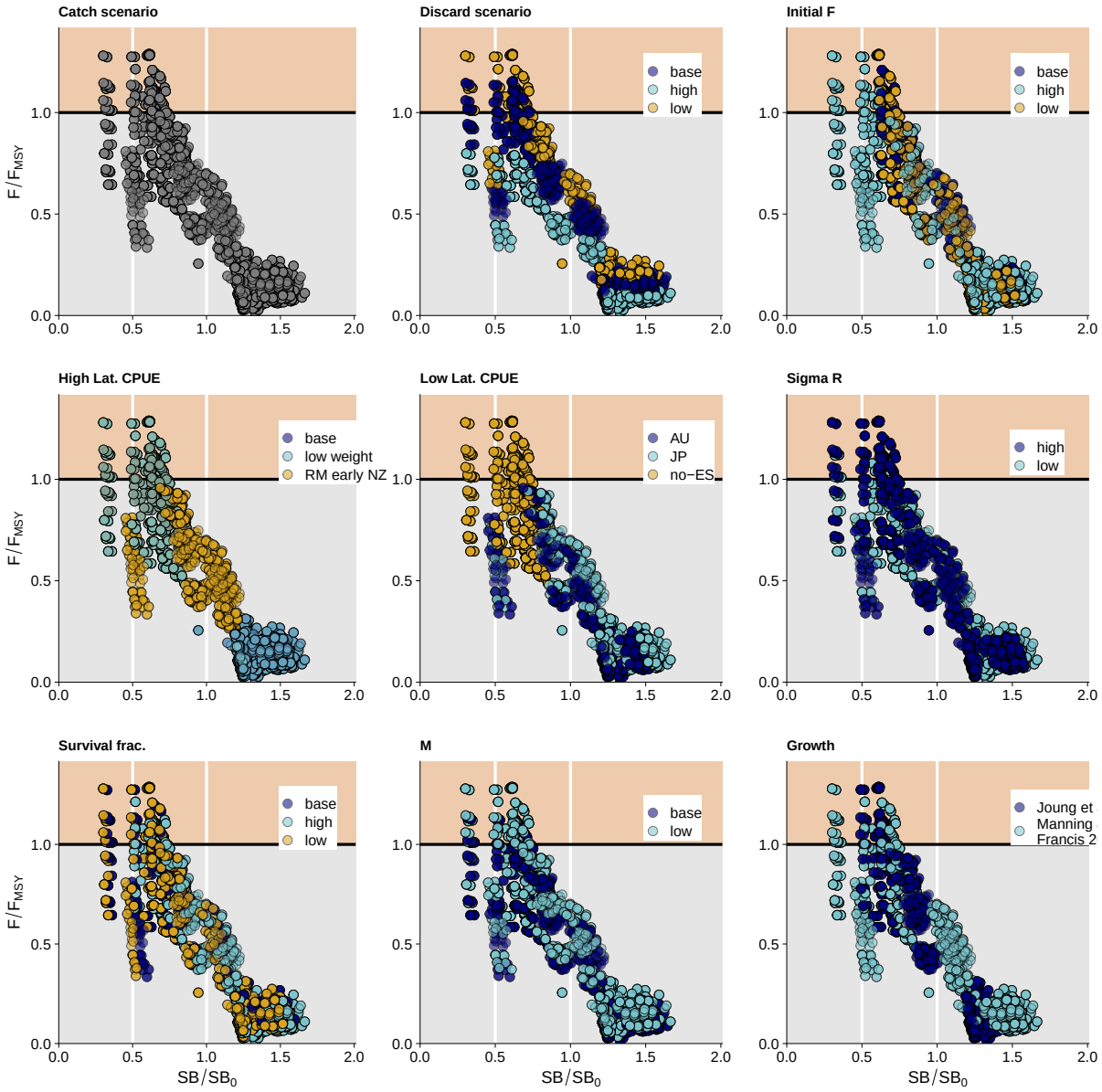


**Figure 35:** Panel plot summarising stock status in the final year for each of the models in the structural uncertainty grid for $SB_{latest}/SB_0$ and $F_{latest}/F_{\text{MSY}}$. The stock is considered to be undergoing overfishing when $F_{latest}/F_{\text{MSY}} > 1$ (beige zone). Guidelines were added in white at $0.5SB_{latest}/SB_0$ and $SB_{latest}/SB_0$.

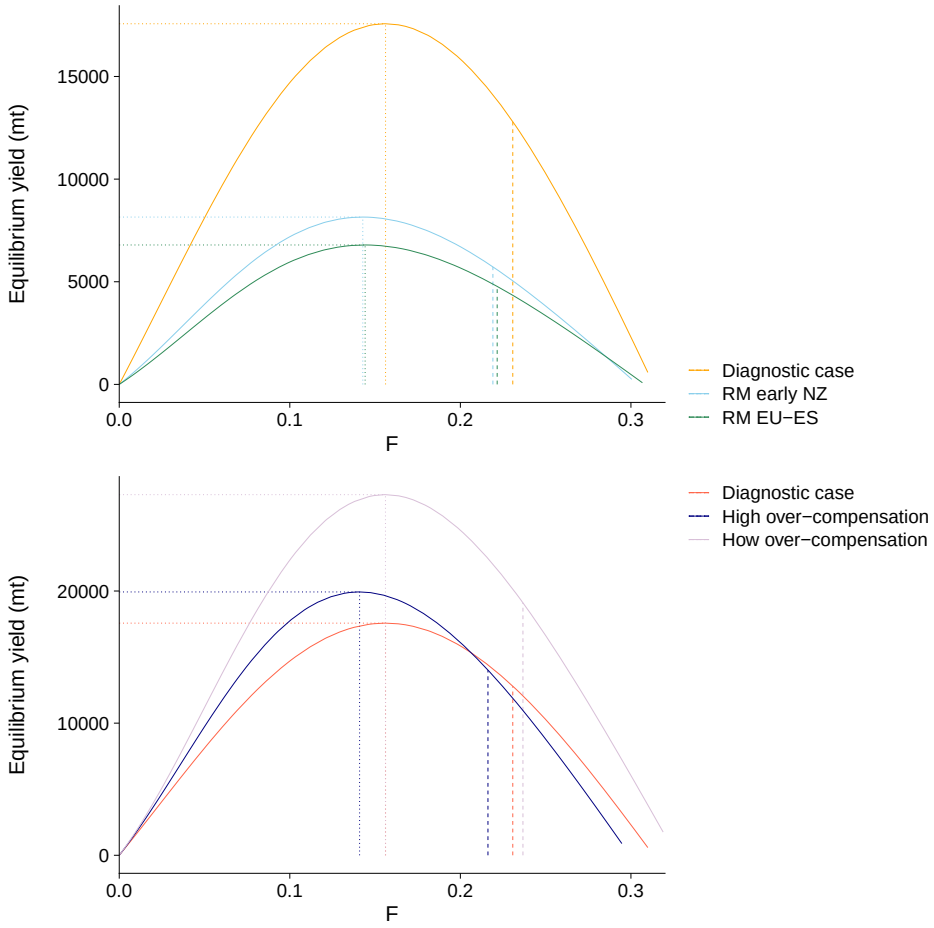


**Figure 36:** Yield profiles for Southwest Pacific blue shark under three CPUE scenarios, with $F_{\text{MSY}}$ indicated by dotted vertical lines, and $F_{lim,\text{AS}}$ shown as dashed lines.

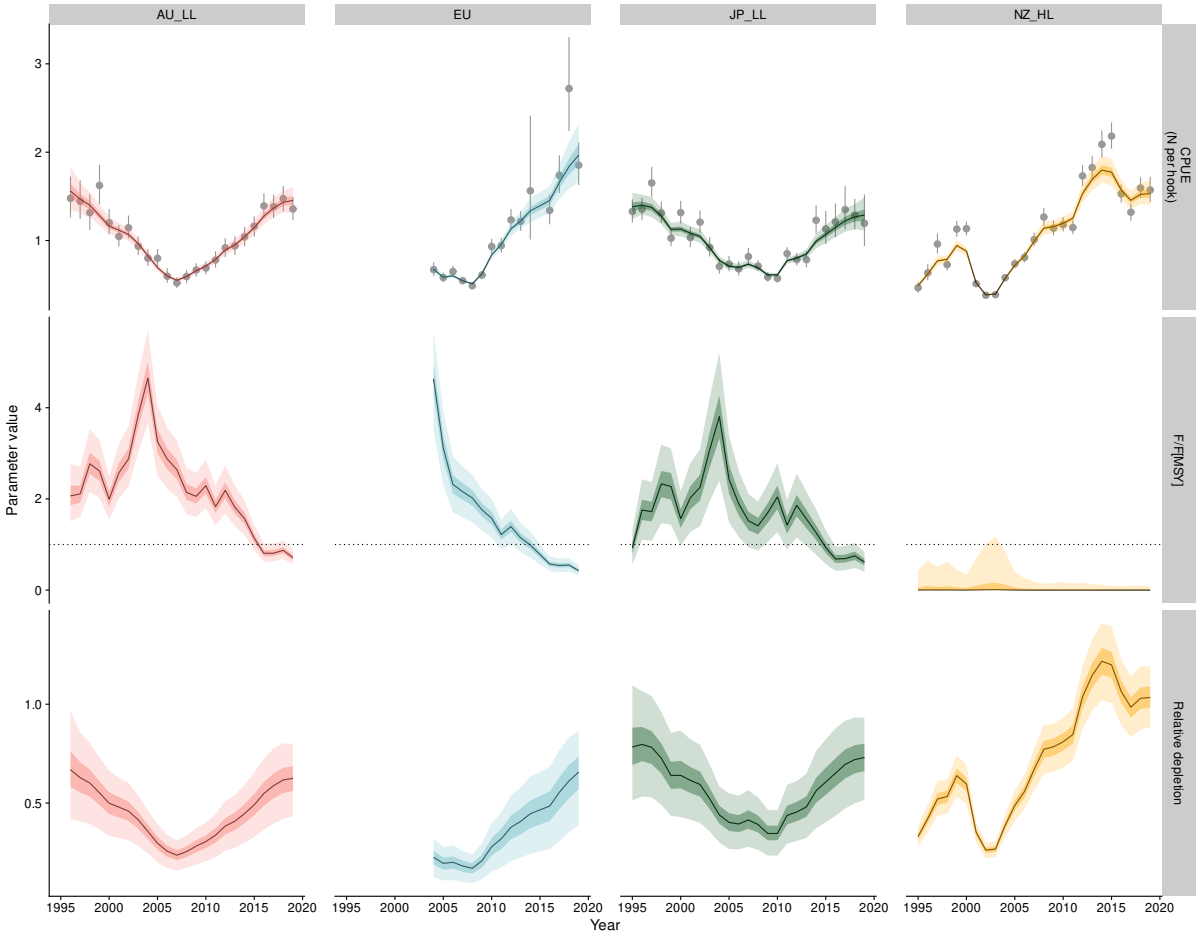


**Figure 37:** Fitting of catch-per-unit-effort (CPUE) data using a dynamic surplus production model with independent model runs for each CPUE indices (dark shading, inter-quartile; light shading, 95% confidence interval). Top row: Predicted CPUE with input CPUE (points) and observation error (inter-quartile range). Middle row: Time series of risk ratio of overfishing $F/F_{MSY}$ estimated in the dynamic surplus production model. Bottom row: Estimated relative depletion (relative to unfished abundance $K$). (Note that the stock was not unfished in the first year of the time-series.)

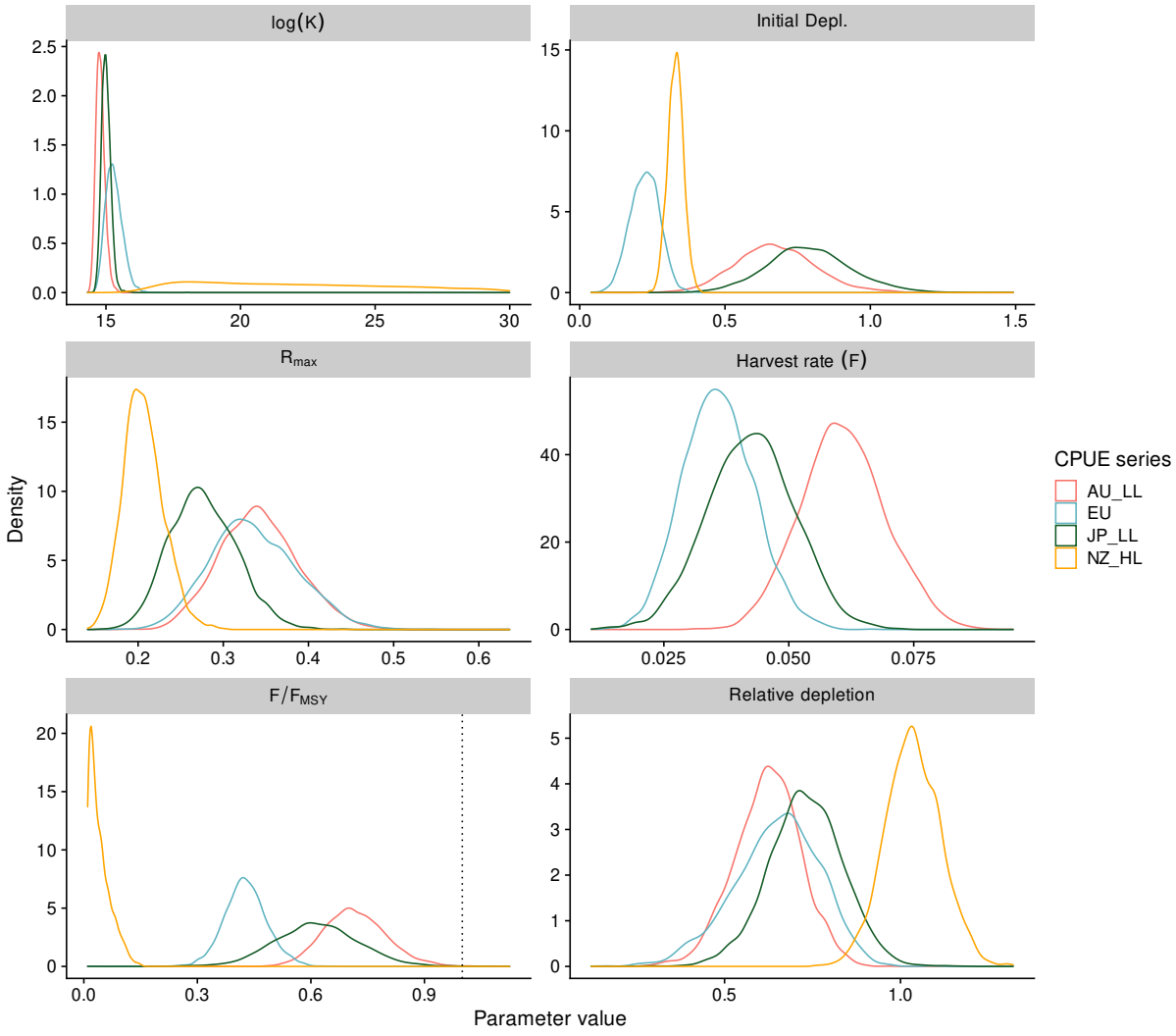


**Figure 38:** Marginal posterior densities for derived parameters (harvest rate, risk ratio of overfishing $F/F_{MSY}$) and selected estimated parameters (initial depletion, carrying capacity $K$, intrinsic population growth $R_{max}$ and relative depletion) for different model runs with alternative CPUE indices.

## APPENDIX A: Supplementary figures

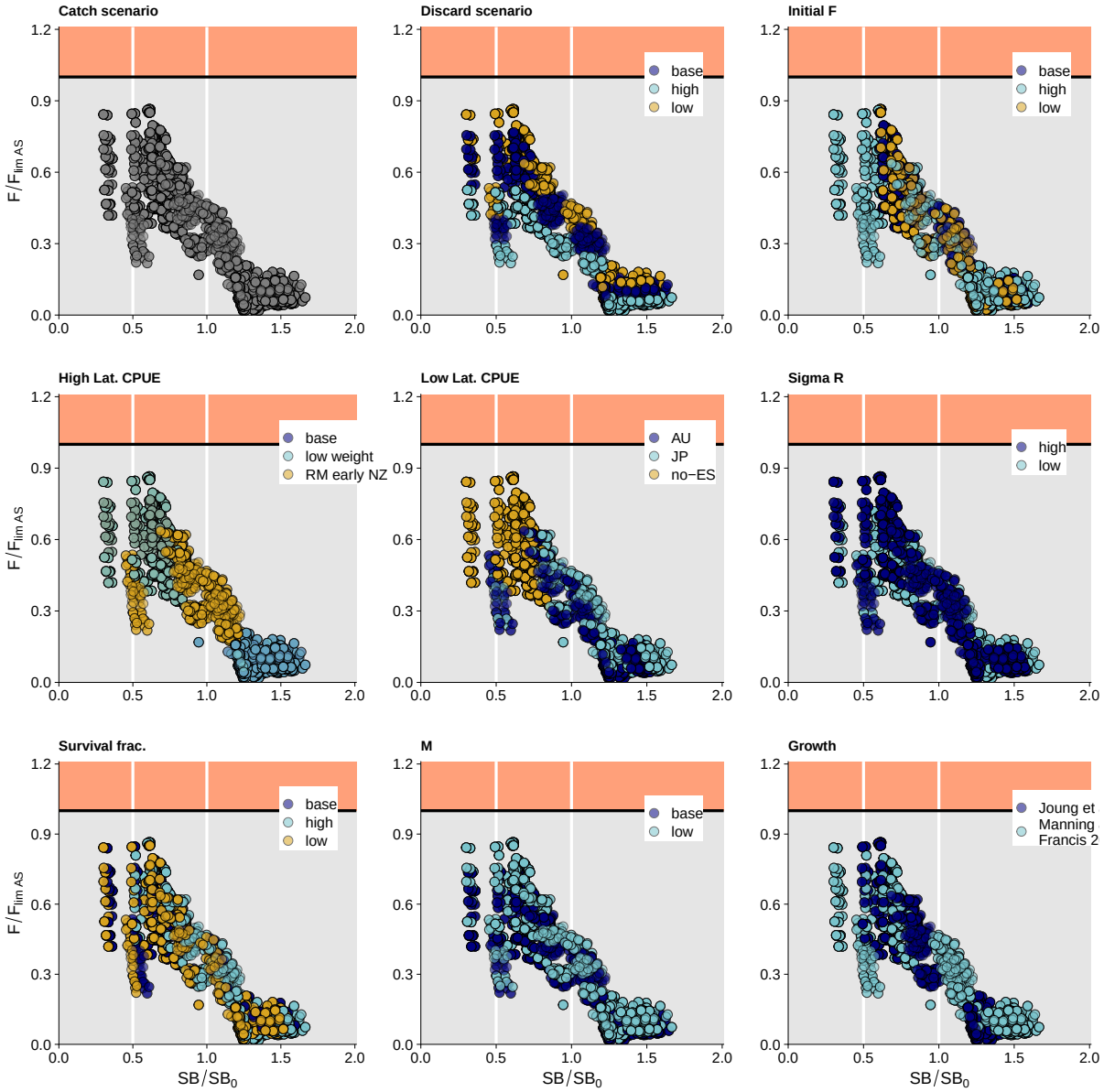


**Figure A-1:** Panel plot summarising stock status in the final year for each of the models in the structural uncertainty grid for $SB/SB_0$ and $F/F_{lim,\text{AS}}$. When $F/F_{lim,\text{AS}} > 1$ (orange zone), the spawning biomass has declined below $0.5SB_{MSY}$. Guidelines were added in white at $0.5SB/SB_0$ and $SB/SB_0$.

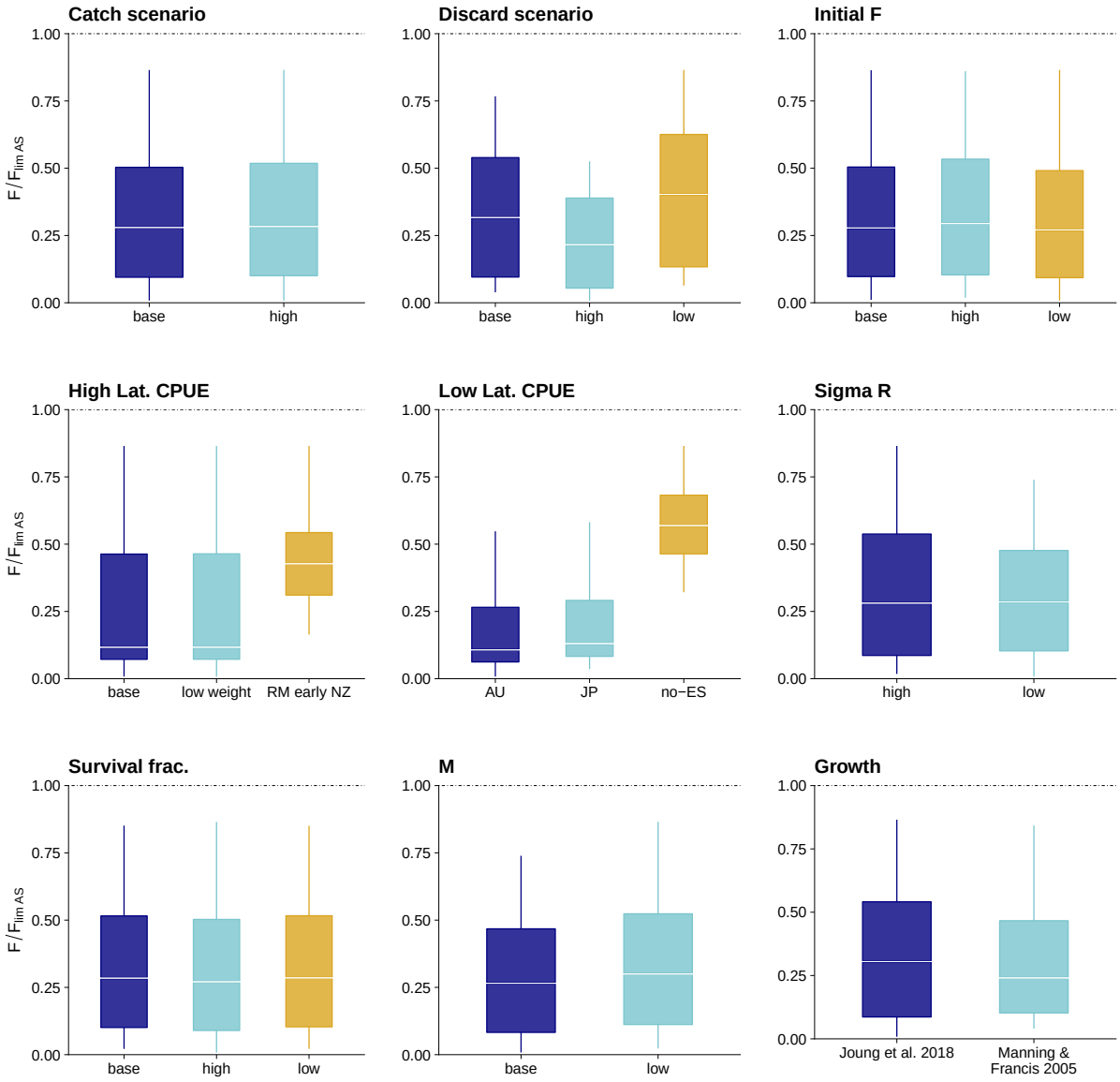


**Figure A-2:** Median (white bar) and inter-quartile bounds (box) for $F/F_{lim}$ in the final year of the assessment for each structural uncertainty axis. The whiskers extend to 1.5× the interquartile range. The dashed line shows the level where $F = F_{lim}$.

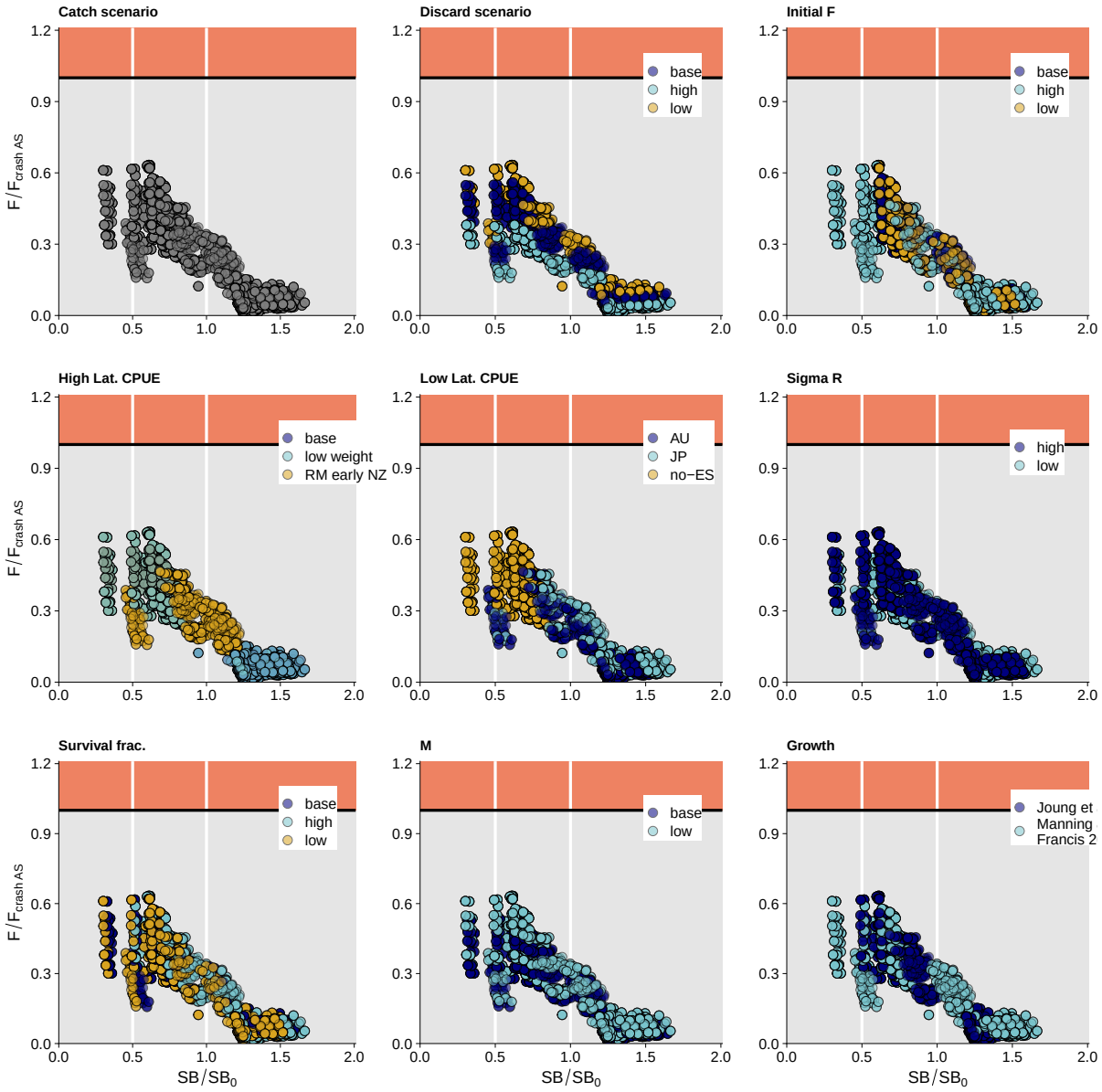


**Figure A-3:** Panel plot summarising stock status in the final year for each of the models in the structural uncertainty grid for $SB/SB_0$ and $F/F_{crash,\text{AS}}$. The population is expected to become extinct when levels of $F$ in excess of $F_{crash,\text{AS}}$ (i.e. $F/F_{crash,\text{AS}} > 1$; pink zone) are maintained on the long-term. Guidelines were added in white at $0.5SB/SB_0$ and $SB/SB_0$.

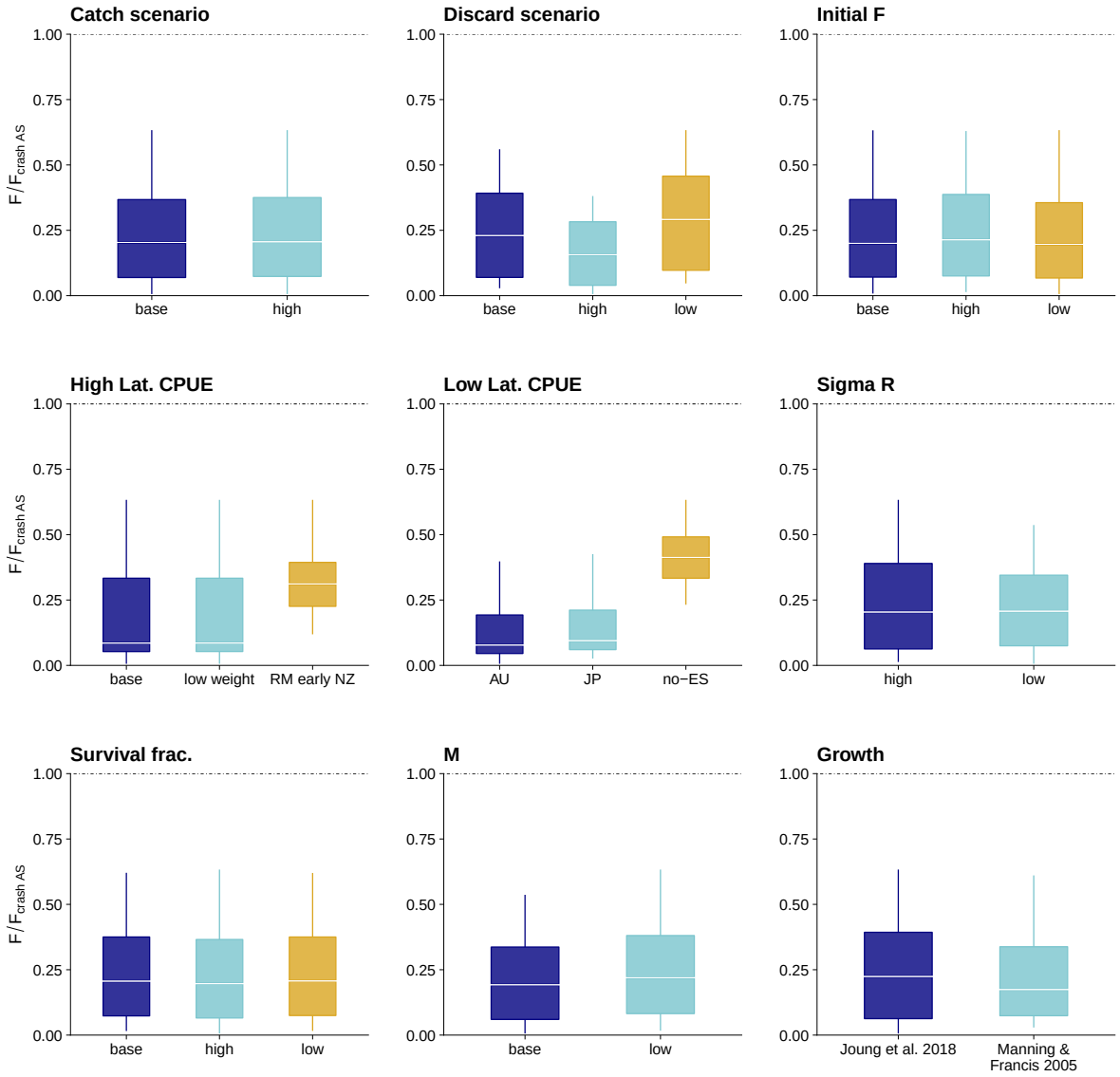


**Figure A-4:** Median (white bar) and inter-quartile bounds (box) for $F/F_{crash}$ in the final year of the assessment for each structural uncertainty axis. The whiskers extend to 1.5× the interquartile range. The dashed line shows the level where $F = F_{crash}$.

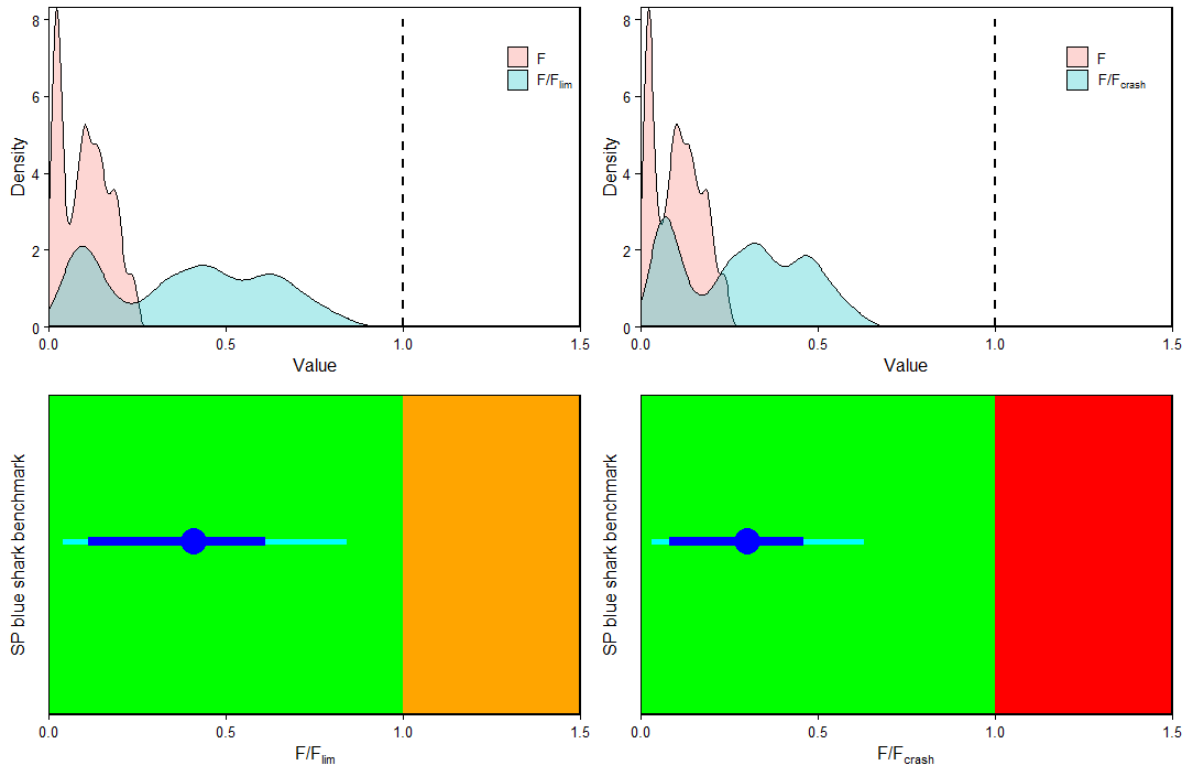


**Figure A-5:** Density distribution of 3006 model runs estimating $F_{latest}$, $F_{latest}/F_{lim}$ (top left) and $F_{latest}/F_{crash}$ (top right) as well as the status relative to risk-based fishing mortality benchmarks showing the median (blue point), $20^{th}$ and $80^{th}$ percentiles (thick blue line) and range (light blue line) for $F_{latest}/F_{lim}$ (bottom left) and $F_{latest}/F_{crash}$ (bottom right).